Alma Mater Studiorum – Università di Bologna

DOTTORATO DI RICERCA IN

BIOINGEGNERIA

Ciclo XXV

Settore Scientifico Disciplinare: ING-IND/34

Subject-specific musculoskeletal models of the lower limbs for the prediction of skeletal loads during motion

a dissertation by

Giordano Valente, Ph.D. Candidate

Supervisor

Prof. Luca Cristofolini

Co-supervisors

Fulvia Taddei, Ph.D.
Saulo Martelli, Ph.D.
Prof. Marco Viceconti

Reviewers

Prof. Ugo Della Croce
Prof. Harinderjit Singh Gill

Ph.D. Coordinator

Prof. Angelo Cappello

Bologna, March 2013

A mio nonno Tonino,
inconsapevole Maestro di vita

Abstract

An accurate knowledge of the physiological loading conditions on the skeletal system during human movements may have significant clinical implications in several orthopedic and neurological contexts. However, the determination of skeletal loading conditions in vivo and their relationship to the health of bone and cartilage tissues, still represent an open question. Computational modeling of the musculoskeletal system is the only practicable method providing a valuable approach to muscle and joint loading analyses in vivo, but the lack of a thorough validation of model predictions represents a crucial shortcoming limiting the translation process of computational methods into the orthopedic and neurological practice. A growing concern about the accuracy of scaled-generic models is focusing the attention on subject-specific modeling, particularly when pathological musculoskeletal conditions need to be studied. Nevertheless, subject-specific data cannot be always collected in the research and clinical practice, and there is a lack of valuable methods and

frameworks for building models and incorporating them in simulations of motion, still preventing the system to be practical, user friendly and effort effective.

The overall aim of the present PhD thesis was to introduce improvements to the state-of-the-art musculoskeletal modeling for the prediction of physiological skeletal loads (i.e. muscle and joint forces) during motion. To this aim, a threefold goal was articulated as follows: (i) develop state-of-the art subject-specific models and perform clinical and methodological analyses of skeletal load predictions; (ii) analyze the sensitivity of model predictions to relevant musculotendon model parameters and kinematic uncertainties; (iii) design an efficient software framework integrating and simplifying the effort-intensive phases of subject-specific modeling pre-processing.

The goals were successfully achieved with a four-part research project, presenting strengths and added values. The first part allowed to underline the relevance of subject-specific musculoskeletal modeling to determine physiological skeletal loads during gait, corroborating the choice of full subject-specific modeling for the analyses of pathological conditions. The second and third part allowed to characterize the sensitivity of skeletal load predictions to major musculotendon parameters and kinematic uncertainties, and to develop robust probabilistic methods applied for methodological and clinical purposes. The last part allowed to create an efficient software framework for subject-specific modeling and simulation, which is practical, user friendly and effort effective.

To overcome some modeling limitations, future research development aims at the implementation of more accurate models describing lower-limb joint mechanics and musculotendon paths, and the assessment of an overall scenario of the crucial model parameters affecting the skeletal load predictions through probabilistic modeling.

Contents

General Introduction

I.1 Research rationale

Human locomotion is constituted by a set of complex tasks to perform that, although natural, takes years to develop and is fundamental to the quality of life. The complex way in which the muscles coordinate allows to propel and support the body during movement that muscle action induces accelerating the body segments [1,2]. The study of the biomechanics of locomotion has a long history, where methods for human movement analysis can provide quantitative information on the kinematics and kinetics of motion as well as sequence and timing of muscle activity through electromyography (EMG) [3].

Muscle coordination is achieved by muscle excitation governed by the central nervous system (CNS) to enable body motion. This causes the generation

of individual muscle forces that, through tendon insertions into bones, are transmitted to the skeletal system. In addition, joint contact forces are exerted between articulating surfaces of two adjacent bone segments, representing the sum of joint intersegmental forces (or joint resultant forces) and joint compressive forces. Intersegmental forces are due to body inertial forces and external forces applied, compressive forces are due to muscle forces and forces in other soft tissues (e.g., ligaments) crossing the joint. Muscle and joint contact forces, assuming ligament forces negligible, constitute the physiological loading condition of a bone segment. They anatomically represent the internal loads balancing the external loads in the instantaneous equilibrium of a bone segment.

Tissue growth and maintenance of bone and cartilage are affected by the dynamic loading experienced during daily life, and altered skeletal loads contribute as co-factor in the onset and follow-up of several musculoskeletal disorders, e.g., bone fractures, bone deformities, cartilage degeneration, joint pain [4–6]. Much has been studied about the morphology and mechanical behavior of bone and cartilage, whose knowledge is fundamental for the improvement of diagnosis and treatment of joint and bone diseases. However, a large amount of questions still remain open, particularly about the determination of skeletal loading conditions in vivo and how they are related to the health of the tissues.

Therefore, an accurate knowledge of the physiological loading conditions on the skeletal system during human movements may have significant clinical implications, contributing in the improvement of clinical treatments in several orthopedics and neurological contexts. A summary of some relevant implications is provided as follows.

Overall, one of the most relevant clinical problem is represented by possible bone fractures, for instance in presence of osteopenia (low bone mineral density typical from osteoporosis), sarcopenia (loss of skeletal muscle mass) and neuromotor control degradation, conditions that are frequently present in elderly [7]. The instantaneous risk of bone fracture during movement is determined by the intrinsic properties of bone, related to its structural behavior, and by extrinsic properties due to the bone loading conditions. Individual bone properties and

physiological loads improve the accuracy in the prediction of the risk of bone fracture.

Joint osteoarthritis, a degenerative disease concerning degradation of the articular cartilage, can impair mobility and cause pain. The disease can be treated in several ways that may include or not surgery, based on clinical assessment of the patient. Excessive joint loading during normal daily activities and obesity, in conjunction with local joint vulnerabilities related to age, are confirmed risk factors in the etiopathogenesis of osteoarthritis [8,9], particularly at the knee and hip joints. In addition, weakness of some hip and knee muscle groups significantly correlates with radiographic signs of osteoarthritis [10,11]. Knowing the joint contact forces and cartilage stress during movement improves the treatment strategies for the disease.

Arthroplasty is an orthopedic surgical procedure in which joint surfaces are realigned by osteotomy, remodeled, or replaced by prostheses, and it is adopted as treatment for several pathologies, especially osteoarthritis. The long term success of total joint replacements, particularly at the hip, is determined by several factors such as surgical technique, design and material of the implant, loading conditions to which it is exposed. Consequently, for the prediction of clinical outcomes after surgery, it is fundamental to analyze parameters such as primary stability, bone remodeling and joint function [12–14]. All these parameters require the knowledge of subject-specific joint loading to be accurately studied. Therefore, an accurate knowledge of skeletal loads in vivo is essential in the prediction of the consequences of specific factors of the joint reconstruction.

Limb-salvage surgery is increasingly adopted in the treatment of bone tumors, that besides several advantages, still presents allograft and plate fractures as major complications [13,14]. Rehabilitation therapy is usually managed in such a way to prevent complete load bearing for long time to avoid the fracture risk. Therefore, understanding the biomechanics of the reconstructed limbs would contribute in analyzing alternative rehabilitation protocols and improving the surgical technique, accounting for the mechanical failure of the implant [17]. A first fundamental step is to accurately assess the loads acting on the reconstructed bone, to then evaluate how these loads influence the risk of fracture and how they

evolve during the follow-up period. Therefore, in this process, the evaluation of the loads acting on the reconstruction at the end of the rehabilitation protocol is essential.

Cerebral palsy is a neurological disease caused by a lesion to the brain, and results in impaired gait (i.e. crouch gait) that can lead to bone deformities and joint pain and deterioration [18,19]. To develop successful treatments for crouch gait, clinicians need to understand how joint loads change with abnormal knee flexion during gait, which is typical of the associated crouch gait. The risk of joint deterioration and bone fractures associated with altered joint loading could be reduced by a more upright posture, but it would be very helpful for clinicians to quantify the relationship between knee flexion and skeletal loads on the tibia.

In vivo experimental measurements of muscle and joint contact forces during motion are currently unfeasible with non-invasive devices. Otherwise, in vivo measurements can be conducted with different levels of invasiveness, representing an approach that is impracticable in most clinical and research contexts. For instance, force transducers can be placed on a tendon to then remove the devices after data collection; joint contact force measurements can be performed through telemetric joint prostheses, implanted for total joint replacements (e.g. [20,21]). A non-invasive ultrasonic technique has been recently developed for tendon force measurements, based on the relationship between the speed of sound in the tendon and the traction force applied [22]. However, it has been applied to in-vitro animal tendons only, and to assess in vivo reproducibility, non-invasive calibration tests have to be designed [23]. The experimental scenario is therefore limited to a small number of subjects and is representative only of specific post-operative situations, highlighting fundamental limitations of experimental techniques in providing an exhaustive description of the skeletal loading conditions in vivo.

Computational modeling of the musculoskeletal system is the only practicable method providing a valuable approach to muscle and joint loading analyses in vivo. Recent and accelerated advances in computer technology and performance are driving computational modeling towards important challenges in clinical scenarios. The development of new modeling methods and numerical

simulation algorithms, which are computationally efficient, are increasingly raising the interest in musculoskeletal modeling and simulation among the biomechanical and medical communities.

I.2 Lower-limb musculoskeletal modeling and simulation for skeletal load predictions

In general, a scientific model can be intended as an artifact used to idealize a portion of reality for specific scientific purposes. Since the 1970's, simple multibody mechanical models have been proposed to study human locomotion, to understand the overall mechanical energetics [24]. Typical examples are the inverted single and double pendulum, or other planar systems with few degrees of freedom. Simple non-muscle based models present the virtue of possessing few variables, which simplifies the understanding of the relationship between cause and effect. However, the fundamental limitation is represented by their inapplicability to study muscle coordination during motion [25]. Therefore, in a musculoskeletal system, what to idealize and include in a model, with a corresponding level of complexity, depends on the intended application of the model.

When muscle and joint loading during movement need to be investigated, a model ought to include a multibody system of bone and soft tissues, whose bodies are connected by ideal joints and actuated by musculotendon units (Figure 1). In the multibody system model, each body segment, made of bone and soft tissues, is assumed to be rigid. This allows to describe the inertial properties of each body through its mass, position of the center of mass and moments of inertia. The mechanical linkage representing the multibody system includes joint models defining kinematical constraints and location and orientation of joint reference frames. Musculotendon models require the definition of musculotendon paths based on geometric data, musculotendon dynamics to define force-generating capacities, excitation-contraction dynamics to consider the time course of muscle activation.

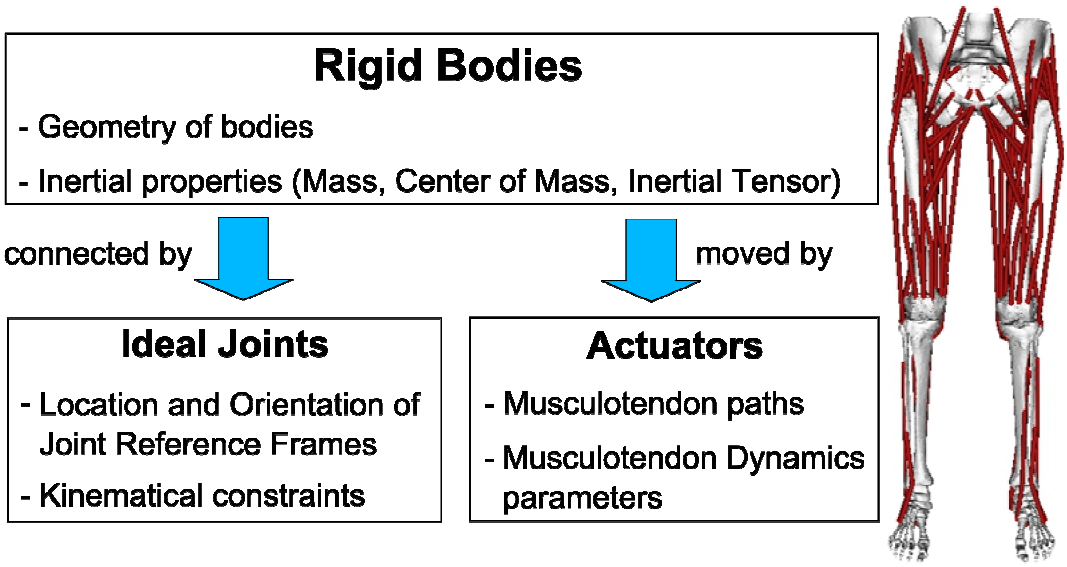

Figure 1 - Multibody model applied to the lower-limb musculoskeletal system: essential model parts suitable to perform skeletal load predictions in vivo

Defining $\mathbf{q},\dot{\mathbf{q}},\ddot{\mathbf{q}}$ the vectors of generalized coordinates, velocities and accelerations, the Newton - Euler equations of motion applied to a multibody system can be written as:

$$\mathbf{I}(\mathbf{q})\ddot{\mathbf{q}} + \mathbf{R}(\mathbf{q})\mathbf{f}_{mus} + \mathbf{g}(\mathbf{q}) + \mathbf{c}(\mathbf{q},\dot{\mathbf{q}}) + \mathbf{e}(\mathbf{q},\dot{\mathbf{q}}) = \mathbf{0}$$

where:

- $\mathbf{I}(\mathbf{q})\ddot{\mathbf{q}}$ = vector of generalized inertial forces, where $\mathbf{I}(\mathbf{q})$ is the system mass matrix
- $\mathbf{R}(\mathbf{q})\mathbf{f}_{mus}$ = vector of net joint moments, where $\mathbf{R}(\mathbf{q})$ is the matrix of muscle moment arms and $\mathbf{f}_{mus}$ is the vector of musculotendon forces
- $\mathbf{g}(\mathbf{q})$ = vector of gravity forces
- $\mathbf{c}(\mathbf{q},\dot{\mathbf{q}})$ = vector of Coriolis and centrifugal forces
- $\mathbf{e}(\mathbf{q},\dot{\mathbf{q}})$ = vector of non-muscle external forces applied by the environment

Considering a multibody system with *n* joints actuated by *m* muscles, the relationship between net joint moments ($\mathbf{M_j}$) and muscle forces is described by a set of linear algebraic equations:

$$\mathbf{M}_j = \mathbf{R}_{ji}(\mathbf{q})\mathbf{f}_i$$

with $0 < j < n$ and $0 < i < m$. To calculate muscle forces $\mathbf{f}_i$ corresponding to the prescribed net joint moments, the matrix of muscle moment arms ($\mathbf{R}_{ji}$) needs to be inverted. If $m > n$, i.e. the number of muscles spanning a joint is greater than the number of degrees of freedom specifying joint movement in the model, the system is indeterminate and a net joint moment can be produced by an infinite number of muscle force solutions. This is known as muscle-moment redundancy or muscle load sharing problem, which is one of the main challenges in musculoskeletal modeling since the 1970's [26]. Most muscle force solutions rely on the application of optimization theory, and they commonly fall in two conceptually different techniques: inverse dynamics and forward dynamics methods. Joint contact forces can then be calculated as sum of compressive forces, calculated from muscle forces and direction of muscle lines of action, and intersegmental forces, due to inertial and external forces (Figure 2). Muscle forces are demonstrated to be the primary contributors to joint contact forces.

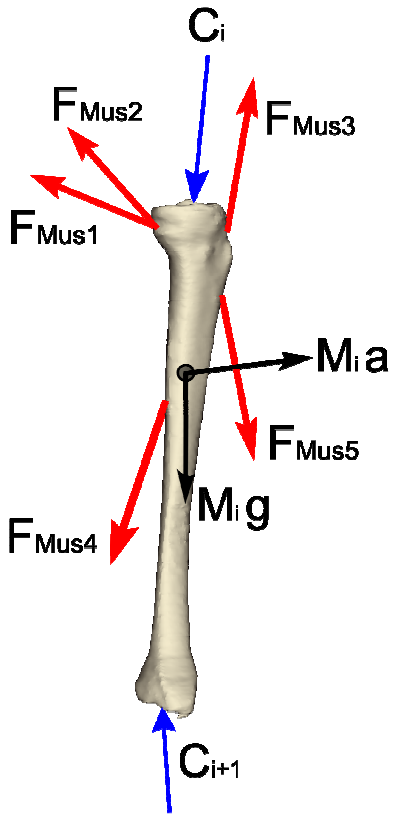

Figure 2 - Free body diagram of the i^{th} body segment of a multibody system in instantaneous equilibrium. Black arrows are gravity and inertial forces, red arrows are muscle forces, blue arrows are joint contact forces

The inverse dynamics method uses joint kinematics and ground reaction forces data as inputs to calculate the net joint moments applied about each joint: typically, Newton - Euler equations of motion of a single body segment are solved recursively from distal to proximal. Then, the muscle load sharing problem is solved at each time instant using static optimization to minimize a certain performance criterion [27]. Objective functions based on physiological criteria, are adopted for daily motion tasks under investigation, resulting in similar muscle force predictions [28].

Conversely, the forward dynamics method uses neural excitation signals as inputs to calculate the resulting joint kinematics, integrating simultaneously the equations of motion, activation and contraction dynamics. Dynamic optimization can be adopted to solve one single optimization problem in a movement cycle and predict all quantities simultaneously. Lower-limb muscle forces obtained from static and dynamic optimization solutions were compared for simulations of walking, leading to no significant differences between the two approaches [29]. The dynamic optimization approach is nowadays considered inefficient due to the vast computational time involved. Alternatively, EMG-driven methods can be used to calculate muscle forces using as inputs raw EMG approximating neural commands and joint kinematics [30–33]. These methods possess strengths, avoiding optimization theory, of accounting for individual muscle recruitment patterns and co-contraction strategies. Nevertheless, two major limitations are related to the inability of incorporating deep muscles for which EMG measurements cannot be made, and to the errors which EMG signals are prone to.

Recent approaches have been developed to use forward dynamics methods much more efficiently. Particularly, Computed Muscle Control (CMC) [34] and NeuroMusculoskeletal Tracking (NMT) [35] algorithms use feedback control theory to generate forward dynamics simulations including muscle activation dynamics, adopting two different approaches to solve the muscle load sharing problem: CMC uses static optimization at each time step, NMT uses a time-dependent performance criterion over the entire task period.

Recent research [36] showed that static optimization (SO), CMC and NMT methods do not produce significant different muscle force estimates in human

locomotion, concluding that muscle activation dynamics and time-dependent performance criteria need to be modeled only in ballistic motor tasks (e.g., jumping or sprinting), and therefore making static optimization the most attractive method for efficiency and robustness.

Excellent reviews on methods for musculoskeletal modeling and simulation can be found in [1,2,28,31].

Several commercial and open-source software packages are available that numerically solve equations of motion applied to multibody systems, inverse and forward dynamics problems with optimization theory. Among others, OpenSim [37] (https://simtk.org/home/opensim), a freely available package whose first version was released in 2007, is increasingly used by the biomechanical community with different background and for a wide variety of research and clinical purposes. The software represents a state-of-the art tool in multibody dynamics modeling and simulation for musculoskeletal systems, and is built on top of the Simbody (https://simtk.org/home/simbody) application programming interface (API), an open-source multibody dynamics engine.

Most analyses using musculoskeletal modeling for skeletal load estimates focused on methodological studies and healthy subject conditions. Few analyses focused on clinical questions, and none of the optimization methods adopted have been successfully translated into the clinical practice yet.

Important studies have been performed to understand the influence of femoral anteversion on femoral loading conditions in total hip replacement patients [38] and derive a femoral loading profile in post-operative situations [39]. Similarly, changes in hip loading were assessed after surgery, related to deviations in kinematics, kinetics and muscle force-generating capacity [40]. Cohorts of people with patellofemoral joint osteoarthritis and pain were studied, finding altered muscle forces, particularly: lower hip abductor muscle forces during walking [41], co-contraction of quadriceps and hamstring muscles and greater normalized muscle forces during walking and running [33]. Crouch gait was studied to elucidate biomechanical consequences of treatments and help targeting strength training programs. Muscle force analyses were used to clarify the role of lower-limb muscles in the abnormal gait, estimate the changes in tibiofemoral

contact force with crouch severity and examine how much muscle groups could be weakened before crouch gait was not possible [42–44]. Joint instability and damage in anterior cruciate ligament (ACL) - deficient knee were studied, to analyze shear forces and ligament loads as well as muscle compensation strategies for stabilizing [45,46]. In addition, outcomes of ACL reconstruction were investigated to relate increased knee joint loading to complication from surgery [47]. Musculoskeletal modeling and optimization methods were also used to study ACL and muscle strain injury: the influence of specific neuromuscular control parameters on the risk of ACL injury was examined [48], and hamstring muscle forces during sprinting were compared pre- and post-injury [49]. Some studies reported on the effects of foot orthoses, used to treat knee joint osteoarthritis and pain, on knee joint loading during walking and running [50,51].

Optimization theory applied to multibody dynamics musculoskeletal systems assumes that neuromotor control works in reasonable optimal conditions, i.e., it chooses, among infinite solutions available, muscle activation patterns that minimize a prescribed cost function. The process of neuromotor control is based on how the central nervous system coordinates muscle activities while generating the locomotors patterns, and it can be subject- an task-specific, where the relationship with an assumed performance criterion is not known *a priori*. The assumption of optimal conditions may lead to unrealistic predictions in presence of pathological conditions or sudden and precise motor tasks [33,52,53], where neuromotor control strategy may not be optimal. A method to analyze sub-optimal neuromotor control conditions [54] was proposed to study the range of hip contact forces that are physiological possible during normal walking, leading to a 4 BW range prediction. This raises the relevance of probabilistic approaches in the determination of internal loads, where the probability associated to a sub-optimal solution may be estimated from neuromotor control conditions of the patient. Recently, a stochastic multiscale body-organ model was developed to study spontaneous fractures of the femoral neck during normal walking [7], defining osteopenia, sarcopenia, neuromotor control degradation and task repetition as input stochastic variables. The muscle and joint contact forces predicted with the body-level model previously mentioned [54], were used as inputs to the organ-

level model (i.e., finite element model of a femur). The results showed that spontaneous hip fractures during normal waking are possible in comorbity of severe osteopenia and neuromotor control degradation.

One major obstacle in translating modeling and simulation methods into the clinical practice is represented by the lack of a thorough validation of model predictions. There is no doubt that a validation process would lead to establish that a computer model provides results with an acceptable accuracy according to the application and would assess the error and uncertainty involved, improving model reliability necessary for clinicians to draw decisions and analyze information based on the model predictions. The major issue is related to the current unfeasibility of muscle force measurements in vivo (see I.1). Studies involving muscle force calculations usually compare muscle force, activation or excitation predictions against measured and processed EMG data records of muscle activities, as an estimate of validity [2,28]. Nevertheless, both surface and intramuscular EMG recordings do not directly verify the magnitude of muscle forces, preventing the possibility of quantitative validation of skeletal loading conditions. In addition, EMG recordings are affected by some lack of reliability due to intrinsic limitations. The alternative form of validation is represented by direct comparison of predicted joint contact forces with measurements from instrumented implants [55,56]. Since muscle forces are the major contributors to joint loading, this validation also provides an indirect estimate of validity of predicted muscle forces. However, joint contact force measurements are limited to a few implanted patients, and are representative only of specific post-operative subjects. Therefore, few model predictions were directly validated against experimental measurements obtained through instrumented prostheses.

The described limitations in the validation of suitable methods represent a key issue in the assessment of reliability of model predictions and the consequent clinical potential as decision-making tool. Alternatively, sensitivity analyses exist to assess the prediction uncertainties and correlations between variables of any modeling approach, in any application where physiological skeletal loads are predicted. A major element determining the accuracy of model predictions is constituted by the values of the parameters assumed in the model. The biological

structure properties present an intrinsic variability among individuals, some of them cannot be measured non-invasively, and unavoidable uncertainty is associated to the parameters assumed in the model. Sensitivity of skeletal load predictions to different model and simulation parameters has been increasingly studied [28]. The model parameters identified to be critical can be divided into musculotendon and kinematics parameter categories. In the first category, among the studies assessing the sensitivity to musculotendon geometry and dynamics parameters, more critical are considered the position of origin and insertion points of prime mover muscles [57], the number of actuators for broad attachment muscles [58,59] and the tendon slack length values [58,60–62]. In the second category, different joint models has been found to significantly affect muscle and joint contact force predictions [63,64]. Another major element determining prediction accuracy is related to the measurements of body motion adopted for inverse and forward dynamics simulations. Soft tissue artifact is unavoidable using conventional and non-invasive motion capture technologies [65], and newer technologies representing gold standards in body motion measurements, such as single- and bi-plane fluoroscopy and dynamic magnetic resonance images (MRI), are not easily accessible for cost-, time- and ethical-related reasons [66]. Since the calculation of intersegmental joint moments are prone to measurement errors in body motion, this propagates to muscle force predictions when solving the load sharing problem, though it is not easy to be quantified. Although sensitivity studies are increasingly performed, there is a still a need for understanding how some kinematics and musculotendon modeling parameters affects skeletal load predictions, and a complete scenario of critical parameters has not been assessed yet. In addition, few studies adopted a probabilistic approach to account for variability and uncertainty in musculoskeletal model parameters [67]. Probabilistic methods, in conjunction with important increases in computational power, allow to thoroughly characterize how output variables are affected by the variability of input variables, and the interaction between variables. This would not only allow a more holistic assessment of model prediction sensitivity, but also to face clinical questions more efficiently.

I.3 Challenges of subject-specific musculoskeletal modeling and simulation

Most studies involving muscle and joint contact force predictions have utilized generic musculoskeletal models derived from average adult anatomy [2,28]. The lower-limb *Delp model* [68,69] has been widely adopted for a variety of biomechanical investigations. This generic model is based on several experimental studies, and has been altered and refined [70,71] to different purposes. The main issues in the identification of model parameters are related to dataset inconsistency and limited in vivo measurements. For instance, measurement discrepancy on different cadaver specimens were found for some muscle parameters [72,73], optimization methods are used to calculate parameters (e.g., tendon slack length) impossible to measure, adaptation from literature is utilized for unavailable parameters in a certain dataset. This leads to the use of generic models in which the assumption of representation of a wide population may not be robust. Recent models were developed from more consistent datasets based on the geometrical analysis of cadaveric specimens [74,75]. While the first is referred to 21 cadaver specimen measurements, but has not been applied to muscle and joint loading investigations yet, the second involves a single cadaver specimen, i.e. it is not representative of a population, and has been utilized as scaled-generic model for sensitivity and validation analyses [57,59,76].

A growing concern is being raised about the accuracy of scaled-generic models, since they may not be able to account for the substantial variability of musculoskeletal geometry and tissue properties among individuals, and at the same time may not be representative of a specific scenario of a subject. This is particularly relevant when pathological musculoskeletal conditions need to be studied, therefore the purpose of the model should guide the level of subject-specific detail involved for muscle and joint loading analyses. Some studies showed significant differences in muscle moment arm lengths, musculotendon lengths and gait kinematics [77–81] calculated with subject-specific models created from MRI and scaled-generic models. Recent research has demonstrated that using subject-specific musculoskeletal geometry affects calculated muscle and joint forces during gait [81–83] and how this propagates to bone stress

distribution [84]. A few additional studies performed skeletal load investigations using different levels of subject-specific details [7,33,54,85]. Despite the growing concern on the use of scaled-generic model, it can be speculated that few attempts have been made to create subject-specific models for skeletal load predictions, and the current scenario does not clarify to which extent it is important to obtain different subject-specific parameters. Related to this point, beyond the important validation problem of model predictions (see I.2), one should also consider two additional issues: the difficulty in collecting all necessary data in the research and clinical practice, and the lack of valuable methods and frameworks to create subject-specific models and simulations, whose development represents a demanding process requiring extensive effort with skilled expertise and time. For instance, the model identification process involve tissue geometries reconstructions, calculation of tissue inertial properties, definition of location and orientation of joint axes from anatomical landmarks, definition of musculotendon architecture. Tissue reconstructions from CT and MRI provide valuable methods to model the musculoskeletal anatomy with a good accuracy and low level of invasiveness. The level of subject-specific detail also involves additional measurements, e.g., body motion, ground reaction forces, muscle activity, which can be obtained through technologies for human movement analysis such as stereophotogrammetry, 3D fluoroscopy, EMG, force platforms.

The first issue concerning the availability of data implies that subject-specific information cannot be always collected in the research and clinical practice since it is related to the use of the mentioned technologies. In addition, this arises time- and cost-related problems that may not be negligible in some contexts. The second issue concerning the demanding process involved is related to the lack of valuable methods and frameworks available. For instance, MR-based musculoskeletal modeling has not yet become a standard in biomechanical analyses of movement. Important research has been performed to incorporate more accurate MR-based models of musculotendon geometry into multibody musculoskeletal models [86–88], however the lack of automatic methods leads to an intensive manual processing that makes this approach too effort-intensive and costly. Recently, a custom-built software tool was developed for automated

definition of subject-specific muscle paths using non-rigid image registration between an atlas image and the subject's MR images [89], reporting on increased accuracy in the definition of musculotendon paths and 70% of time saved. Although the application of this method showed large percentage differences in calculated moment arm lengths between subject-specific and scaled-generic models [80], the influence on skeletal load predictions have not been assessed yet. Another relevant computer-based procedure called Virtual Palpation [90], has been proposed that allows to locate anatomical landmarks on the available clinical images with and uncertainty up to 3 mm.

The calculation of muscle and joint forces for biomechanical analyses are increasingly performed through the use of commercial, freeware and in-house custom-built software, and several generic models are available for the biomechanical community. When including subject-specific details, the software users and developers have to necessarily set up specific modeling frameworks that involve an important pre-processing phase to create the models, before the desired solutions can be achieved. The process needs a skilled expertise to process imaging data, define the features of the multibody systems, create models and simulation setups in the appropriate file formats depending on the software used, and thus particularly develop codes to create efficient modeling frameworks. All this necessarily involves an effort-intensive, timely and costly process. The lack of available efficient frameworks integrating the various steps described above, represents a key difficulty that limits wider biomechanical investigations on a subject-specific basis, and so the process leading to the translation of computational methods into the orthopedic and neurological practice.

I.4 Aim and outline of the thesis

The overall aim of the research performed during the PhD was to develop subject-specific multibody models of the lower-limb musculoskeletal system and efficient modeling methods, to predict and analyze skeletal loading conditions and the sensitivity of model predictions to relevant modeling parameters. The performed research contributes to improving the state-of-the-art musculoskeletal modeling for physiological loading predictions. This allows to increase the

modeling reliability and represents a further step to bridge the gap between current musculoskeletal modeling and simulation methods and clinical applicability.

Particularly, the purpose was threefold:

(i) Develop subject-specific musculoskeletal models of the lower limbs from medical images (i.e. CT and MRI) and adopt dynamic simulation methods to predict skeletal loads (i.e. muscle and joint contact forces) during motion tasks

(ii) Analyze the sensitivity of model predictions to modeling hypotheses related to musculotendon model parameters and kinematic uncertainties, to understand the accuracy of the models and investigate clinical questions

(iii) Design a software tool to create subject-specific musculoskeletal models as an efficient framework integrating and simplifying the effort-intensive phases of modeling pre-processing

The research presented in this thesis is organized in four parts:

Part I – Presents modeling and simulation methods adopted to create subject-specific models of the lower limbs for the prediction of skeletal loads during motion, with two different applications. *Chapter 1* focuses on a clinical analysis of the femoral loads during walking in a case of massive skeletal reconstruction; *Chapter 2* reports on a methodological study comparing the predictions between subject-specific and generic-scaled modeling.

Part II – Presents sensitivity studies to musculotendon modeling, including the definition of musculotendon paths and force-generating capacity. In *Chapter 3*, a method for the discretization of the musculotendon units from a mechanical standpoint is reported; in *Chapter 4* this method is applied to analyze the sensitivity of the skeletal loads predictions to the number and position of the musculotendon lines of action. *Chapter 5* focuses on the sensitivity of joint contact forces to the force-generating capacity of the hip abductor muscles.

Part III – Presents sensitivity studies to kinematics parameters, including the uncertainties associated to the location and orientation of joint axes and the joint kinematics calculated with different methods. *Chapter 6* presents a sensitivity study of skeletal loads to the uncertainties associated to the identification of the lower-limb joint axes when clinical images are available; in *Chapter 7* the influence of different methods for the calculation of joint kinematics is analyzed on the skeletal load predictions.

Part IV – *Chapter 8* summarizes the design and development of an open-source software to create subject-specific multibody models. The software, developed within a project funded by the European Union, integrates a pre-processing and data manager software with a state-of-the art multibody-dynamics software for musculoskeletal applications, and represents an efficient framework to create and edit subject-specific models.

I.5 References

[1] Zajac F. E., Neptune R. R., and Kautz S. A., 2002, "Biomechanics and muscle coordination of human walking. Part I: introduction to concepts, power transfer, dynamics and simulations," Gait Posture, **16**(3), pp. 215-232.

[2] Pandy M. G., and Andriacchi T. P., 2010, "Muscle and joint function in human locomotion," Annu Rev Biomed Eng, **12**, pp. 401-433.

[3] Cappozzo A., Della Croce U., Leardini A., and Chiari L., 2005, "Human movement analysis using stereophotogrammetry. Part 1: theoretical background," Gait Posture., **21**(2), pp. 186-96.

[4] Wu J. Z., Herzog W., and Epstein M., 2000, "Joint contact mechanics in the early stages of osteoarthritis.," Medical engineering & physics, **22**(1), pp. 1-12.

[5] Eckstein F., Faber S., Mühlbauer R., Hohe J., Englmeier K.-H., Reiser M., and Putz R., 2002, "Functional adaptation of human joints to mechanical stimuli.," Osteoarthritis and cartilage / OARS, Osteoarthritis Research Society, **10**(1), pp. 44-50.

[6] Wong M., and Carter D. ., 2003, "Articular cartilage functional histomorphology and mechanobiology: a research perspective," Bone, **33**(1), pp. 1-13.

[7] Viceconti M., Taddei F., Cristofolini L., Martelli S., Falcinelli C., and Schileo E., 2012, "Are spontaneous fractures possible ? An example of clinical application for personalised , multiscale neuro-musculo-skeletal modelling," Journal of Biomechanics, **45**(3), pp. 421-426.

[8] Felson D. T., 2004, "Obesity and Vocational and Avocational Overload of the Joint as Risk Factors for Osteoarthritis," Journal of Rheumatology, **31**(70), pp. 2-5.

[9] Lafeber F. P. J. G., Intema F., Van Roermund P. M., and Marijnissen A. C. a, 2006, "Unloading joints to treat osteoarthritis, including joint distraction.," Current opinion in rheumatology, **18**(5), pp. 519-25.

[10] Amaro A., Amado F., Duarte J. a, and Appell H.-J., 2007, "Gluteus medius muscle atrophy is related to contralateral and ipsilateral hip joint osteoarthritis.," International journal of sports medicine, **28**(12), pp. 1035-9.

[11] Costa R. A., Oliveira L. M. D., Watanabe S. H., Jones A., and Natour J., 2010, "Isokinetic assessment of the hip muscles in patients with osteoarthritis of the knee," Clinics, **65**(12), pp. 1253-1259.

[12] Claes L., Fiedler S., Ohnmacht M., and Duda G. N., 2000, "Initial stability of fully and partially cemented femoral stems.," Clinical biomechanics (Bristol, Avon), **15**(10), pp. 750-5.

[13] Bitsakos C., Kerner J., Fisher I., and Amis A. A., 2005, "The effect of muscle loading on the simulation of bone remodelling in the proximal femur.," Journal of biomechanics, **38**(1), pp. 133-9.

[14] Bennett D., Ogonda L., Elliott D., Humphreys L., and Beverland D. E., 2006, "Comparison of gait kinematics in patients receiving minimally invasive and traditional hip replacement surgery: a prospective blinded study.," Gait & posture, **23**(3), pp. 374-82.

[15] Deijkers R. L., Bloem R. M., Kroon H. M., Van Lent J. B., Brand R., and Taminiau A. H., 2005, "Epidiaphyseal versus other intercalary allografts for tumors of the lower limb," Clin Orthop Relat Res., **439**, pp. 151-60.

[16] Ogilvie C. M., Crawford E. A., Hosalkar H. S., King J. J., and Lackman R. D., 2009, "Long-term results for limb salvage with osteoarticular allograft reconstruction," Clin Orthop Relat Res., **467**(10), pp. 2685-90. Epub 2009 Feb 13.

[17] Taddei F., Viceconti M., Manfrini M., and Toni A., 2003, "Mechanical strength of a femoral reconstruction in paediatric oncology: a finite element study.," Proceedings of the Institution of Mechanical Engineers. Part H, Journal of engineering in medicine, **217**(2), pp. 111-9.

[18] Kerr Graham H., and Selber P., 2003, “Musculoskeletal aspects of cerebral palsy,” The Journal of Bone and Joint Surgery, **85**(2), pp. 157-166.

[19] Jahnsen R., Villien L., Aamodt G., Stanghelle J. K., and Holm I., 2004, “Musculoskeletal pain in adults with cerebral palsy compared with the general population.,” Journal of rehabilitation medicine : official journal of the UEMS European Board of Physical and Rehabilitation Medicine, **36**(2), pp. 78-84.

[20] Bergmann G., Deuretzbacher G., Heller M., Graichen F., Rohlmann A., Strauss J., and Duda G. N., 2001, “Hip contact forces and gait patterns from routine activities.,” Journal of biomechanics, **34**(7), pp. 859-71.

[21] Fregly B. J., Besier T. F., Lloyd D. G., Delp S. L., Banks S. A., Pandy M. G., and Lima D. D. D., 2012, “Grand Challenge Competition to Predict In Vivo Knee Loads,” Journal of Orthopaedic Research, (April), pp. 503-513.

[22] Pourcelot P., Defontaine M., Ravary-Plumioën B., Lematre M., and Crevier-Denoix N., 2005, “A non-invasive method of tendon force measurement,” Journal of Biomechanics, **38**, pp. 2124-2129.

[23] Crevier-Denoix N., Ravary-Plumioën B., Evrard D., and Pourcelot P., 2009, “Reproducibility of a non-invasive ultrasonic technique of tendon force measurement, determined in vitro in equine superficial digital flexor tendons.,” Journal of biomechanics, **42**(13), pp. 2210-3.

[24] Cavagna G. A., Thys H., and Zamboni A., 1976, “The sources of external work in level walking and running.,” The Journal of physiology, **262**(3), pp. 639-57.

[25] Pandy M. G., 2003, “Simple and complex models for studying muscle function in walking.,” Philosophical transactions of the Royal Society of London. Series B, Biological sciences, **358**(1437), pp. 1501-9.

[26] Crowninshield R. D., 1978, “Use of Optimization Techniques to Predict Muscle Forces,” Journal of Biomechanical Engineering, **100**(2), p. 88.

[27] Crowninshield R. D., and Brand R. A., 1981, “A physiologically based criterion of muscle force prediction in locomotion.,” Journal of biomechanics, **14**(11), pp. 793-801.

[28] Erdemir A., McLean S., Herzog W., and van den Bogert A. J., 2007, “Model-based estimation of muscle forces exerted during movements,” Clin Biomech (Bristol, Avon), **22**(2), pp. 131-154.

[29] Anderson F. C., and Pandy M. G., 2001, “Static and dynamic optimization solutions for gait are practically equivalent,” J Biomech, **34**(2), pp. 153-161.

[30] Lloyd D. G., and Besier T. F., 2003, "An EMG-driven musculoskeletal model to estimate muscle forces and knee joint moments in vivo," J Biomech, **36**(6), pp. 765-776.

[31] Buchanan T. S., Lloyd D. G., Manal K., and Besier T. F., 2004, "Neuromusculoskeletal modeling: estimation of muscle forces and joint moments and movements from measurements of neural command.," Journal of applied biomechanics, **20**(4), pp. 367-95.

[32] Buchanan T. S., Lloyd D. G., Manal K., and Besier T. F., 2005, "Estimation of Muscle Forces and Joint Moments Using a Forward-Inverse Dynamics Model," Medicine & Science in Sports & Exercise, **37**(11), pp. 1911-1916.

[33] Besier T. F., Fredericson M., Gold G. E., Beaupre G. S., and Delp S. L., 2009, "Knee muscle forces during walking and running in patellofemoral pain patients and pain-free controls," J Biomech, **42**(7), pp. 898-905.

[34] Thelen D. G., and Anderson F. C., 2006, "Using computed muscle control to generate forward dynamic simulations of human walking from experimental data," J Biomech, **39**(6), pp. 1107-1115.

[35] Seth A., and Pandy M. G., 2007, "A neuromusculoskeletal tracking method for estimating individual muscle forces in human movement.," Journal of biomechanics, **40**(2), pp. 356-66.

[36] Lin Y.-C., Dorn T. W., Schache a. G., and Pandy M. G., 2011, "Comparison of different methods for estimating muscle forces in human movement," Proceedings of the Institution of Mechanical Engineers, Part H: Journal of Engineering in Medicine.

[37] Delp S. L., Anderson F. C., Arnold A. S., Loan P., Habib A., John C. T., Guendelman E., and Thelen D. G., 2007, "OpenSim: open-source software to create and analyze dynamic simulations of movement.," IEEE transactions on bio-medical engineering, **54**(11), pp. 1940-50.

[38] Heller M. O., Bergmann G., Deuretzbacher G., Claes L., Haas N. P., and Duda G. N., 2001, "Influence of femoral anteversion on proximal femoral loading: measurement and simulation in four patients.," Clinical biomechanics (Bristol, Avon), **16**(8), pp. 644-9.

[39] Heller M. O., Bergmann G., Kassi J.-P., Claes L., Haas N. P., and Duda G. N., 2005, "Determination of muscle loading at the hip joint for use in pre-clinical testing.," Journal of biomechanics, **38**(5), pp. 1155-63.

[40] Lenaerts G., Mulier M., Spaepen A., Van der Perre G., and Jonkers I., 2009, "Aberrant pelvis and hip kinematics impair hip loading before and after total hip replacement.," Gait & posture, **30**(3), pp. 296-302.

[41] Crossley K. M., Dorn T. W., Ozturk H., van den Noort J., Schache a G., and Pandy M. G., 2012, "Altered hip muscle forces during gait in people with patellofemoral osteoarthritis.," Osteoarthritis and cartilage / OARS, Osteoarthritis Research Society, **20**(11), pp. 1243-9.

[42] Steele K. M., Demers M. S., Schwartz M. H., and Delp S. L., 2012, "Compressive tibiofemoral force during crouch gait.," Gait & posture, **35**(4), pp. 556-60.

[43] Steele K. M., Seth A., Hicks J. L., Schwartz M. S., and Delp S. L., 2010, "Muscle contributions to support and progression during single-limb stance in crouch gait.," Journal of biomechanics, **43**(11), pp. 2099-105.

[44] Steele K. M., van der Krogt M. M., Schwartz M. H., and Delp S. L., 2012, "How much muscle strength is required to walk in a crouch gait?," Journal of biomechanics, **45**(15), pp. 2564-9.

[45] Shelburne K., Pandy M. G., and Torry M. R., 2004, "Comparison of shear forces and ligament loading in the healthy and ACL-deficient knee during gait," Journal of Biomechanics, **37**(3), pp. 313-319.

[46] Shelburne K. B., Torry M. R., and Pandy M. G., 2005, "Effect of Muscle Compensation on Knee Instability during ACL-Deficient Gait," Medicine & Science in Sports & Exercise, **37**(4), pp. 642-648.

[47] Fernandez J. W., Akbarshahi M., Crossley K. M., Shelburne K. B., and Pandy M. G., 2011, "Model predictions of increased knee joint loading in regions of thinner articular cartilage after patellar tendon adhesion.," Journal of orthopaedic research : official publication of the Orthopaedic Research Society, pp. 1-10.

[48] McLean S. G., Huang X., and van den Bogert A. J., 2008, "Investigating isolated neuromuscular control contributions to non-contact anterior cruciate ligament injury risk via computer simulation methods.," Clinical biomechanics (Bristol, Avon), **23**(7), pp. 926-36.

[49] Schache A. G., Kim H.-J., Morgan D. L., and Pandy M. G., 2010, "Hamstring muscle forces prior to and immediately following an acute sprinting-related muscle strain injury.," Gait & posture, **32**(1), pp. 136-40.

[50] Neptune R. R., Wright I. C., and van den Bogert A. J., 2000, "The influence of orthotic devices and vastus medialis strength and timing on patellofemoral loads during running.," Clinical biomechanics (Bristol, Avon), **15**(8), pp. 611-8.

[51] Shelburne K. B., Torry M. R., Steadman J. R., and Pandy M. G., 2008, "Effects of foot orthoses and valgus bracing on the knee adduction moment

and medial joint load during gait.," Clinical biomechanics (Bristol, Avon), **23**(6), pp. 814-21.

[52] Bergmann G., Graichen F., and Rohlmann A., 2004, "Hip joint contact forces during stumbling.," Langenbeck's archives of surgery / Deutsche Gesellschaft für Chirurgie, **389**(1), pp. 53-9.

[53] Liikavainio T., Bragge T., Hakkarainen M., Karjalainen P. A., and Arokoski J. P., 2010, "Gait and muscle activation changes in men with knee osteoarthritis.," The Knee, **17**(1), pp. 69-76.

[54] Martelli S., Taddei F., Cappello A., van Sint Jan S., Leardini A., and Viceconti M., 2011, "Effect of sub-optimal neuromotor control on the hip joint load during level walking.," Journal of biomechanics, **44**(9), pp. 1716-21.

[55] Heller M. O., Bergmann G., Deuretzbacher G., Dürselen L., Pohl M., Claes L., Haas N. P., and Duda G. N., 2001, "Musculo-skeletal loading conditions at the hip during walking and stair climbing," Journal of Biomechanics, **34**(7), pp. 883-893.

[56] Kim H. J., Fernandez J. W., Akbarshahi M., Walter J. P., Fregly B. J., and Pandy M. G., 2009, "Evaluation of predicted knee-joint muscle forces during gait using an instrumented knee implant.," Journal of orthopaedic research : official publication of the Orthopaedic Research Society, **27**(10), pp. 1326-31.

[57] Carbone V., van der Krogt M. M., Koopman H. F. J. M., and Verdonschot N., 2012, "Sensitivity of subject-specific models to errors in musculo-skeletal geometry.," Journal of biomechanics, **45**(14), pp. 2476-2480.

[58] Xiao M., and Higginson J., 2010, "Sensitivity of estimated muscle force in forward simulation of normal walking.," Journal of applied biomechanics, **26**(2), pp. 142-9.

[59] Cleather D. I., and Bull A. M., 2010, "Lower-extremity musculoskeletal geometry affects the calculation of patellofemoral forces in vertical jumping and weightlifting," Proc Inst Mech Eng H, **224**(9), pp. 1073-1083.

[60] Scovil C. Y., and Ronsky J. L., 2006, "Sensitivity of a Hill-based muscle model to perturbations in model parameters.," Journal of biomechanics, **39**(11), pp. 2055-63.

[61] Redl C., Gfoehler M., and Pandy M. G., 2007, "Sensitivity of muscle force estimates to variations in muscle-tendon properties," Human Movement Science, **26**(2), pp. 306-319.

[62] Ackland D. C., Lin Y.-C., and Pandy M. G., 2012, "Sensitivity of model predictions of muscle function to changes in moment arms and muscle–tendon properties: A Monte-Carlo analysis," Journal of Biomechanics, pp. 1-9.

[63] Sandholm A., Schwartz C., Pronost N., Zee M., Voigt M., and Thalmann D., 2011, "Evaluation of a geometry-based knee joint compared to a planar knee joint," The Visual Computer, **1**.

[64] Dumas R., Moissenet F., Gasparutto X., and Cheze L., 2012, "Influence of joint models on lower-limb musculo-tendon forces and three-dimensional joint reaction forces during gait," Proceedings of the Institution of Mechanical Engineers, Part H: Journal of Engineering in Medicine, **226**(2), pp. 146-160.

[65] Leardini A., Chiari L., Della Croce U., and Cappozzo A., 2005, "Human movement analysis using stereophotogrammetry. Part 3. Soft tissue artifact assessment and compensation," Gait Posture., **21**(2), pp. 212-25.

[66] Fernandez J. W., and Pandy M. G., 2006, "Integrating modelling and experiments to assess dynamic musculoskeletal function in humans.," Experimental physiology, **91**(2), pp. 371-82.

[67] Laz P. J., and Browne M., 2010, "A review of probabilistic analysis in orthopaedic biomechanics," Proceedings of the Institution of Mechanical Engineers, Part H: Journal of Engineering in Medicine, **224**(8), pp. 927-943.

[68] Delp S. L., 1990, "Surgery simulation: a computer graphics system to analyze and design musculoskeletal reconstructions of the lower limb," Stanford University.

[69] Delp S. L., Loan J. P., Hoy M. G., Zajac F. E., Topp E. L., and Rosen J. M., 1990, "An interactive graphics-based model of the lower extremity to study orthopaedic surgical procedures.," IEEE transactions on bio-medical engineering, **37**(8), pp. 757-67.

[70] Anderson F. C., and Pandy M. G., 1999, "A Dynamic Optimization Solution for Vertical Jumping in Three Dimensions.," Computer methods in biomechanics and biomedical engineering, **2**(3), pp. 201-231.

[71] Nagano A., Komura T., Fukashiro S., and Himeno R., 2005, "Force, work and power output of lower limb muscles during human maximal-effort countermovement jumping.," Journal of electromyography and kinesiology : official journal of the International Society of Electrophysiological Kinesiology, **15**(4), pp. 367-76.

[72] Wickiewicz T. L., Roy R. R., Powell P. L., and Edgerton V. R., 1983, "Muscle architecture of the human lower limb.," Clinical orthopaedics and related research, (179), pp. 275-83.

[73] Ward S. R., Eng C. M., Smallwood L. H., and Lieber R. L., 2009, "Are current measurements of lower extremity muscle architecture accurate?," Clin Orthop Relat Res, **467**(4), pp. 1074-1082.

[74] Arnold E. M., Ward S. R., Lieber R. L., and Delp S. L., 2010, "A model of the lower limb for analysis of human movement.," Annals of biomedical engineering, **38**(2), pp. 269-79.

[75] Klein Horsman M. D., Koopman H. F. J. M., van der Helm F. C. T., Prose L. P., and Veeger H. E. J., 2007, "Morphological muscle and joint parameters for musculoskeletal modelling of the lower extremity," Clinical Biomechanics, **22**(2), pp. 239-247.

[76] Modenese L., Phillips a T. M., and Bull a M. J., 2011, "An open source lower limb model: Hip joint validation.," Journal of biomechanics, **44**(12), pp. 2185-2193.

[77] Scheys L., Spaepen A., Suetens P., and Jonkers I., 2008, "Calculated moment-arm and muscle-tendon lengths during gait differ substantially using MR based versus rescaled generic lower-limb musculoskeletal models.," Gait & posture, **28**(4), pp. 640-8.

[78] Scheys L., Van Campenhout A., Spaepen A., Suetens P., and Jonkers I., 2008, "Personalized MR-based musculoskeletal models compared to rescaled generic models in the presence of increased femoral anteversion: effect on hip moment arm lengths," Gait Posture, **28**(3), pp. 358-365.

[79] Scheys L., Desloovere K., Spaepen A., Suetens P., and Jonkers I., 2011, "Calculating gait kinematics using MR-based kinematic models.," Gait & posture, **33**(2), pp. 158-164.

[80] Scheys L., Desloovere K., Suetens P., and Jonkers I., 2011, "Level of subject-specific detail in musculoskeletal models affects hip moment arm length calculation during gait in pediatric subjects with increased femoral anteversion.," Journal of biomechanics, **44**(7), pp. 1346-53.

[81] Correa T. A., Baker R., Graham H. K., and Pandy M. G., 2011, "Accuracy of generic musculoskeletal models in predicting the functional roles of muscles in human gait," Journal of Biomechanics, **44**(11), pp. 2096-2105.

[82] Lenaerts G., De Groote F., Demeulenaere B., Mulier M., Van der Perre G., Spaepen A., and Jonkers I., 2008, "Subject-specific hip geometry affects predicted hip joint contact forces during gait," J Biomech, **41**(6), pp. 1243-1252.

[83] Lenaerts G., Bartels W., Gelaude F., Mulier M., Spaepen A., Van der Perre G., and Jonkers I., 2009, "Subject-specific hip geometry and hip joint centre location affects calculated contact forces at the hip during gait," J Biomech, **42**(9), pp. 1246-1251.

[84] Jonkers I., Sauwen N., Lenaerts G., Mulier M., Van der Perre G., and Jaecques S., 2008, "Relation between subject-specific hip joint loading, stress distribution in the proximal femur and bone mineral density changes after total hip replacement," J Biomech, **41**(16), pp. 3405-3413.

[85] Besier T. F., Gold G. E., Beaupre G. S., and Delp S. L., 2005, "A Modeling Framework to Estimate Patellofemoral Joint Cartilage Stress In Vivo," Medicine & Science in Sports & Exercise, **37**(11), pp. 1924-1930.

[86] Arnold a S., Salinas S., Asakawa D. J., and Delp S. L., 2000, "Accuracy of muscle moment arms estimated from MRI-based musculoskeletal models of the lower extremity.," Computer aided surgery : official journal of the International Society for Computer Aided Surgery, **5**(2), pp. 108-19.

[87] Blemker S. S., and Delp S. L., 2005, "Three-Dimensional Representation of Complex Muscle Architectures and Geometries," Annals of Biomedical Engineering, **33**(5), pp. 661-673.

[88] Blemker S. S., Asakawa D. S., Gold G. E., and Delp S. L., 2007, "Image-based musculoskeletal modeling: applications, advances, and future opportunities.," Journal of magnetic resonance imaging : JMRI, **25**(2), pp. 441-51.

[89] Scheys L., Loeckx D., Spaepen A., Suetens P., and Jonkers I., 2009, "Atlas-based non-rigid image registration to automatically define line-of-action muscle models: A validation study," Journal of Biomechanics, **42**(5), pp. 565-572.

[90] Taddei F., Ansaloni M., Testi D., and Viceconti M., 2007, "Virtual palpation of skeletal landmarks with multimodal display interfaces.," Medical informatics and the Internet in medicine, **32**(3), pp. 191-8.

PART I

Subject-specific modeling and simulation from medical images

Chapter 1

Femoral loads during gait in a case of massive skeletal reconstruction

Chapter 2

MRI-based subject-specific vs. scaled-generic modeling: a comparison of model predictions

Chapter 1

Femoral loads during gait in a case of massive skeletal reconstruction

Fulvia Taddei[1], Saulo Martelli[1], Giordano Valente[1,2], Maria Grazia Benedetti[3], Alberto Leadini[3], Marco Manfrini[4], Marco Viceconti[1]

[1] Laboratorio di Tecnologia Medica, Istituto Ortopedico Rizzoli, Bologna, Italy
[2] DIEM, University of Bologna, Italy
[3] Laboratorio di Analisi del Movimento, Istituto Ortopedico Rizzoli, Bologna, Italy
[4] Oncology Department, Istituto Ortopedico Rizzoli, Bologna, Italy

Journal article published on Clinical Biomechanics 27(3): 273-80, 2012

Author contributions

F. Taddei obtained funding, designed and manged the project, assisted with interpretation of results and writing the paper

S. Martelli designed the project, assisted with model development, interpretation of results and writing the paper

G. Valente developed the model, performed the simulations of gait, post-processed the results and created the figures

M.G. Benedetti and A. Leardini collected the gait data and assisted with interpretation of results

M. Manfrini collected the imaging data and assisted with interpretation of results

M. Viceconti obtained funding, assisted with project management and writing the paper

Abstract

Background. Biological massive skeletal reconstructions in tumours adopt a long rehabilitation protocol aimed at minimising the fracture risk. To improve rehabilitation and surgical procedures it is important to fully understand the biomechanics of the reconstructed limb. The aim of the present study was to develop a subject-specific musculoskeletal model of a patient with a massive biological skeletal reconstruction, to investigate the loads acting on the femur during gait, once the rehabilitation protocol was completed.

Methods. A personalised musculoskeletal model of the patient's lower limbs was built from a CT exam and registered with the kinematics recorded in a gait analysis session. Predicted activations for major muscles were compared to EMG signals to assess the model predictive accuracy.

Findings. Gait kinematics showed only minor discrepancies between the two legs and was compatible with normality data. External moments showed slightly higher differences and were almost always lower on the operated leg exhibiting a lower variability. In the beginning of the stance phase, the joint moments were, conversely, higher on the operated side and showed a higher variability. This pattern was reflected and amplified on the femoral forces where the differences became important: on the hip, a maximum difference of 1.6 BW was predicted. The variability of the forces seemed, generally, lower on the operated leg than on the contralateral one.

Interpretation. Small asymmetries in kinematic patterns might be associated, in massive skeletal reconstruction, to significant difference in the skeletal loads (up to 1.6 BW for the hip joint reaction) during gait.

Keywords

Subject-specific musculoskeletal modeling, Human gait biomechanics, Child, Computed tomography, Muscle forces

Introduction

Limb-salvage surgery is nowadays widely adopted (more than the 80-85% of cases) in the treatment of osteosarcoma, the most common solid malignant diseases of childhood and adolescence (Friedrich et al., 2008). Still debate is open on the best reconstructive technique (Grimer, 2005), especially in immature subjects with the challenge of a still growing skeleton (Lewis, 2005). Biological reconstructions, using intercalary massive bone allograft (MBA), present some recognised advantages when the original bone joints can be spared (Grimer, 2005; Lewis, 2005) and present acceptable long term survival rates of 75-89% at 10 years (Deijkers et al., 2005). Still, however, allograft and plate fractures represent a major complication (Deijkers et al., 2005; Mankin et al., 1996; Muscolo et al., 2004; Ogilvie et al., 2009; Sorger et al., 2001). In order to limit the fracture risk, rehabilitation therapy is managed preventing a complete weight bearing for a long time: usually until radiographic evidence of allograft-host bone union is present (one year on average (Deijkers et al., 2005)). It would be then important to deeply understand the biomechanics of the reconstructed limbs not only to verify if shorter and more aggressive rehabilitation protocols could be adopted, without increasing the fracture risk, but also to possibly improve the surgical technique, with respect to the mechanical failure of the implant. To this aim, the first fundamental step is to quantitatively assess the loads acting on the reconstructed bones, then to investigate how these loads influence the fracture risk and finally how they evolves during follow-up to estimate the most appropriate rehabilitation loading protocol. This is a complex problem that should be addressed in subsequent steps, the first being the evaluation of the loads acting on the reconstruction at the end of the rehabilitation therapy, as currently managed.

Since the non-invasive measure of muscle forces *in-vivo* is impossible, it is necessary to estimate them using computational musculoskeletal models. Estimates of muscle forces using motion data combined with inverse dynamics and static optimisation has been proposed for many years now (Delp et al., 1990). This approach involves the calculation of joint torques and the solution of the muscle load sharing problem by optimisation (Erdemir et al., 2007). This methodology has been already applied in many clinical contexts since the early

90's (Delp et al., 1990). Computational methods gave insight into the mechanism of muscle contribution to locomotion in healthy (Delp et al., 1990) and pathological subjects (Delp et al., 1994; Free and Delp, 1996; Hicks et al., 2007; Higginson et al., 2006; Piazza and Delp, 2001; Schmidt et al., 1999; Vasavada et al., 1994). Surgical outcomes have been studied in both cases of operations on the muscular (Arnold, Allison S. et al., 2001; Arnold, A. S. and Delp, 2001; Delp et al., 1996) and the skeletal system (Delp et al., 1994; Delp et al., 1996; Free and Delp, 1996; Hicks et al., 2007; Piazza and Delp, 2001; Schmidt et al., 1999; Stansfield and Nicol, 2002; Vasavada et al., 1994), supporting the surgery planning and providing information in tuning the rehabilitation process (Shao et al., 2009). However, to the authors' knowledge, no study has been published so far to investigate motion and loads of the lower limb joints in complex skeletal reconstructions, as those performed in tumour surgery.

More recent studies have demonstrated the value of using subject-specific musculoskeletal models (Dao et al., 2009), especially when abnormalities of the skeleton geometry and/or of the muscular system (Scheys et al., 2008) are present. In large skeletal reconstructions following tumour resection, all tissues that are infected by the tumour should be excised along with a portion of tissue free from disease to assure sufficient margin to avoid local recurrences. This may imply significant changes to the geometry of the affected bone, and to the insertion position and physiological cross sectional area (PCSA) of the muscles. Hence, in this particular scenario, subject-specific models are necessary to investigate the loads acting on the reconstructed limb.

The aim of the present study was to develop a subject-specific musculoskeletal model of a patient who underwent a massive biological skeletal reconstruction at the lower limb, in particular to investigate the loads acting on the reconstruction during gait. At the time of the study, the patient had completed the rehabilitation program and had almost recovered a symmetric gait, which was compatible also with normal data. The final scope of the study was to detect whether the symmetry on kinematics and kinetics data, recorded with standard clinical gait analysis, was also reflected on the internal loads acting on the femurs during gait.

Materials and Methods

The studied patient, male, was operated at the age of 10 for a high grade (stage II B) Osteoblastic Osteosarcoma at the distal left femur. The patient was treated with a neo-adjuvant chemotherapy protocol, and surgery. At the date of the last follow-up control (May 2011) the patient was continuously disease free. An intercalary distal femur resection was performed through a medial approach (distal osteotomy was made in the metaphysis at 5 cm from the knee, the proximal at 15 cm from the knee). The resected segment was removed, completely covered by the *Vastus Intermedius* and by the distal portion of the *Vastus Medialis*. The bone was reconstructed by means of MBA in conjunction with vascularised fibular allograft (VFA from contralateral side). Fixation was provided by a Liss titanium plate with screws (Figure 1a). The insertions of the *Adductor Longus*, *Biceps Femoris short head* and distal *Adductor Magnus,* excised with the resected segment, were not restored. The *Peroneus Longus, Peroneus Brevis, Extensor Hallucis*, *Extensor Digitorum* and *Flexor Hallucis* were detached during surgery from the excised fibula, used as autograft, and re-attached to the interosseus membrane approximately in the same original position. Eight months after surgery the distal screws were removed (Figure 1b), allowing the growth of the femur also from the distal growth plate. After surgery, a hip spica cast was applied for a period of approximately 35 days. When the cast was removed, the patient started a program of passive and active exercises for lower limb joint mobility and muscle strength. The fibula remained alive, radiographic union between the VFA and the patient bone was reached and after 15 months from surgery, the patient was allowed to walk with two crutches and partial progressive loading. After 30 months the patient could walk with full weight-bearing. At month 31 of follow-up, when the rehabilitation program was considered completed, the patient was subjected to a Computed Tomography (CT) exam at the lower limbs for routine clinical reasons. In that occasion, a gait analysis session was also performed, and a specific protocol was adopted to enable the spatial registration between the patient's musculoskeletal model, built from the CT dataset, and the kinematics recorded. That model was used to estimate the femoral loads as explained below.

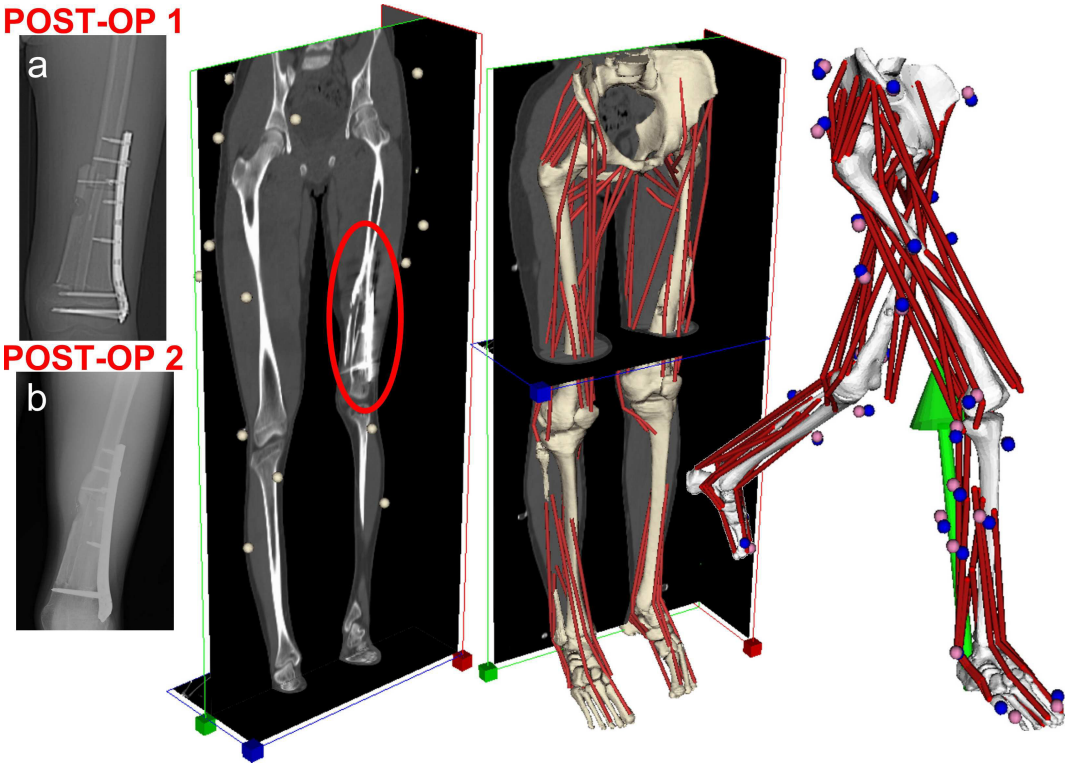

Figure 1 - From left to right: RX of the reconstructed femur immediately after surgery (a) and after removal of distal screws (b); the lower limbs CT exam at month 31 of follow-up with the gait analysis markers visible; the musculoskeletal model superimposed on the CT data (LHPBuilder®, B3C, Italy); the musculoskeletal model in an intermediate frame of a gait cycle (OpenSim 1.9).

CT dataset

Prior to CT scanning, the patient was instrumented with 34 reflective markers (14 mm diameter), visible also on CT images (Figure 1). These markers were positioned following Leardini et al. (2007). From that original marker set, the markers on the feet were removed, as well as those on the two posterior superior iliac spines because of the supine position. To track the pelvis, two additional markers were stuck on the lateral part of this segment. Four additional markers were stuck in the central area of both the thigh and shank, to improve then their pose estimation.

Motion analysis and EMG recordings

A few minutes later, in the motion analysis laboratory, the markers on the feet and those on the two posterior spines were added to the patient, for the standard protocol to run entirely. A 8-camera motion system (Vicon 612 Motion System, Oxford, UK) and two force plates (Kistler, Winterthur, Switzerland) were used for gait analysis. An acquisition in up-right posture and seven repetitions of level walking at a self-selected speed were taken. The force plates values were available only for five repetitions.

EMG registrations were obtained by means of a multichannel recording system (Step32, DemItalia, Italy) for four gait trials. Active clip-type adhesive pregelled disposable Ag/AgCl bipolar 3M EKG electrodes for pediatric application, with an interelectrode distance of 20 mm were used for EMG signal detection. The sampling rate of acquisition was 1000 Hz, low and high cutoff frequencies of the amplifier were 40 Hz and 200 Hz, respectively. The electrodes were positioned on the muscle bells, after appropriate preparation of the skin, according to the Seniam recommendations (Hermens, 1999). The following muscles were explored: *Gluteus Maximum*, *Gluteus Medius*, *Adductor Longus*, *Rectus Femoris*, *Vastus Lateralis*, *Biceps Femoris long head*, *Gastrocnemius* and *Tibialis Anterior*.

The biomechanical musculoskeletal analyses

The skeletal anatomy was segmented from the CT dataset (Amira® v. 4.1, Mercury Computer System, Inc., USA). Since only a small portion of both feet (the talus and approximately half calcaneus) were visible in the CT exam, two complete 3D anatomies of both feet of a suitable size were selected from a public database (www.physiomespace.com) (Testi et al., 2010) and manually registered on the CT volume to complete the skeletal anatomy.

The musculoskeletal model of the lower limbs was defined as a 7-segment, 10 degree-of-freedom (DOF) articulated system, actuated by 82 Hill-type muscle-tendon units (Figure 1). Each leg was modelled as articulated by three ideal joints: a ball-and-socket at the hip (3 DOF) and a hinge (1 DOF) at both the knee and the ankle joints (Jonkers et al., 2008). The identification of joint geometrical parameters, i.e. the pivot point and the axis respectively, was based on relevant

landmarks directly identified on the skeletal model (Taddei et al., 2007) (LHPBuilder®,B3C, Italy). All relevant anatomical landmarks were also identified, following the ISB (International Society of Biomechanics) standards (Wu et al., 2002), and a local coordinate system was computed (Cappozzo et al., 1995) for each segment. The hip centre was defined as the centre of the sphere that best fits the femoral head surface. The joint coordinate system for the hip was defined according to the ISB standards (Wu et al., 2002). The knee flexion axis was defined as the axis connecting the two centres of the medial and the lateral epicondyles (Tanavalee et al., 2001). The axis of the ankle flexion/extension was assumed the one connecting the medial and the lateral tips of the malleoli, which approximates the rotation axis at the tibio-talar joint (Lundberg et al., 1989). The neutral position of the ankle joint was set accordingly to the ISB standards (Wu et al., 2002).

The architecture of the generic muscular model of the lower extremities including 82 muscle actuators published by Delp et al. (1990), was manually registered on the subject-specific skeletal anatomy by an expert anatomist. All defined muscle paths were referenced from an anatomy book (Gray and Lewis, 2000), with the attachment points positioned on the segmented bone surfaces. For the main muscles, a visual check of the modelled lines of action was possible by superimposing the model to the CT volume (Figure 1). The muscular system of the operated leg (left) was modified accordingly to the reconstruction surgery. The left *Vastus Intermedius*, the distal fibres of the *Adductor Magnus*, the *Adductor Longus* and the *Biceps Femoris short head* were removed from the model. The origin of the line of action of the *Vastus Medialis* was moved proximally to mimic the surgical detachment of the distal muscle and the muscle PCSA was reduced accordingly. No changes were applied to the muscle models of the right shank, where the fibula was harvested, since surgery left mostly unchanged their original mechanical function.

Each muscle was modelled as a Hill-type actuator (Thelen and Anderson, 2006). The muscle tetanic forces were taken from Delp et al. (1990) and scaled by the body mass (Koopman and Klein Horsman, 2008; Xiao and Higginson, 2010). The optimal fibre lengths and the tendon slack lengths were determined following

Garner and Pandy (2003). All the other necessary parameters were taken from Delp et al. (1990).

The inertial segment parameters were derived from the CT data, assuming homogeneous density properties for both the hard (1.42 g/cm^3) and the soft tissues (1.03 g/cm^3) (Dumas et al., 2005).

The simulations of gait were run using OpenSim (Delp et al., 2007). The marker trajectories were low-pass filtered with a cut-off frequency of 6 Hz to reduce high frequency fluctuations due to skin-to-bone movements (Gunther et al., 2003). A least-square algorithm was used in a preliminary inverse kinematics analysis to predict the joint motions from recordings of the marker trajectories. The ground reaction forces were low-pass filtered with a cut-off frequency of 20 Hz (van der Bogert and Koning, 1996). The musculoskeletal dynamic simulations were run, for the five gait repetitions for which the ground reaction forces were available, using the computed muscle control (CMC) algorithm (Thelen and Anderson, 2006). Relevant biomechanical indicators, i.e. joint kinematics (in degrees), joint net moments (in newton-meter), hip and knee reaction loads (in newton), muscle forces (in newton) and muscle excitation patterns (% full excitation) were calculated, normalised in terms of gait cycle and synchronised. The biomechanical indicators are presented below by reporting, for each instant of gait, average, minimum and maximum values among the gait trials.

Model validation

The predicted excitations of some major muscles of the operated leg (i.e. *Gluteus Maximus, Gluteus Medius, Adductors, Rectus Femoris, Vastus Lateralis, Biceps Femoris, Gastrocnemius* and *Tibialis Anterior*) were qualitatively compared with the corresponding EMG recordings.

Kinematics and Kinetics

General time-distance parameters (i.e. gait period, average speed, cadence, step length, stance and swing fraction), joint kinematics and external moments at the hip, knee and ankle joints were calculated, normalised in terms of body weight (BW) and height (h) of the patient. All data were compared with published values

for ten normal subjects matched for age: 7 males, 3 females, average age 9.7 years (SD 1.2) (Leardini et al., 2007).

Femoral loads

The femoral loads were analysed in terms of joint reactions (normalised by BW) and muscle forces during stance. The differences between legs were also analysed. The muscle forces were analysed by grouping the muscles accordingly to their function and summing each muscle contribution, as follows: hip flexors (*Iliacus, Sartorius, Rectus Femoris*), hip extensors (*Gluteus Maximus, Biceps Femoris long head, Semimembranosus, Semitendinosus*), hip rotators (*Pectineus, Pyriform, Quadratus Femoris, Gemellus*), hip abductors (*Gluteus Medius, Gluteus Minimus, Tensor Fasciae Latae*), hip adductors (*Adductors Magnus, Adductor Longus, Adductor Brevis, Gracilis*), knee flexors (*Biceps Femoris long head, Semimembranosus, Semitendinosus, Biceps Femoris short head, Medial Gastrocnemius, Lateral Gastrocnemius*), knee extensors (*Rectus Femoris, Vasti Lateralis, Medialis and Intermedius*).

Results

Model validation

The EMG recordings were consistent between gaits, and in good agreement with normal subject patterns (Agostini et al., 2010). Predicted muscle excitation patterns were also consistent throughout the five simulated repetitions. Comparing the predicted muscle excitations with the EMG recordings on the operated leg, a global satisfactory agreement was found throughout the entire gait cycle, apart form the *Rectus Femoris* and for the *Tibialis Anterior*. An exemplary comparison of one gait trial is reported in Figure 2.

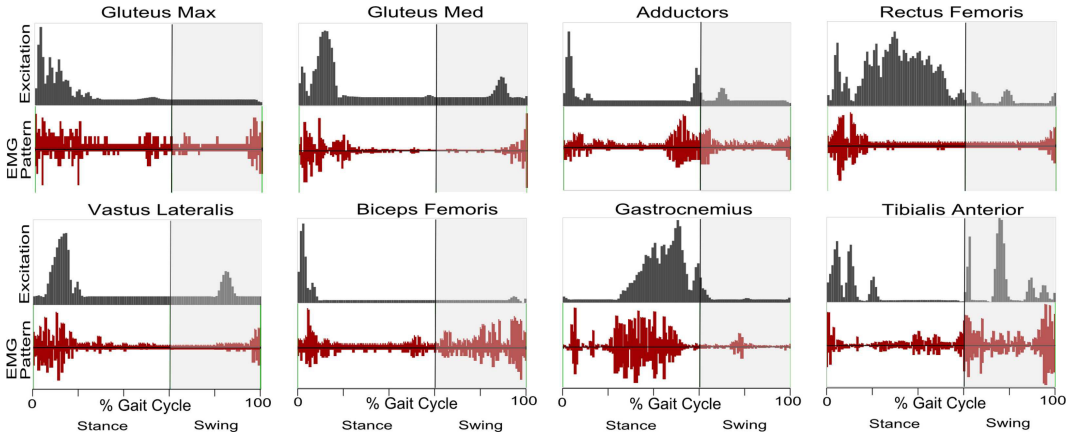

Figure 2 - Comparison of the predicted muscle excitation levels and the corresponding recorded EMG signals, normalised as percentage of maximum values.

Kinematics

Over the five repetitions, the patient walked at an average speed of 1.27 m/s (SD 0.12) and at an average cadence of 1.75 steps/s (SD 0.12). The average duration of stance phase was slightly longer for the healthy leg than for the operated one, being 0.71 s (SD 0.04) and 0.68 s (SD 0.05) respectively, as well as the average step length, being 65 cm (SD 4) and 61 cm (SD 3) respectively.

The joint rotations (Figure 3) were, generally, in agreement with corresponding normal patterns in children (Leardini et al., 2007). Consistent kinematics trends were found for the two legs throughout the entire gait cycle. The largest difference was found on the external rotation of the hip, with an almost 20° offset on the operated leg.

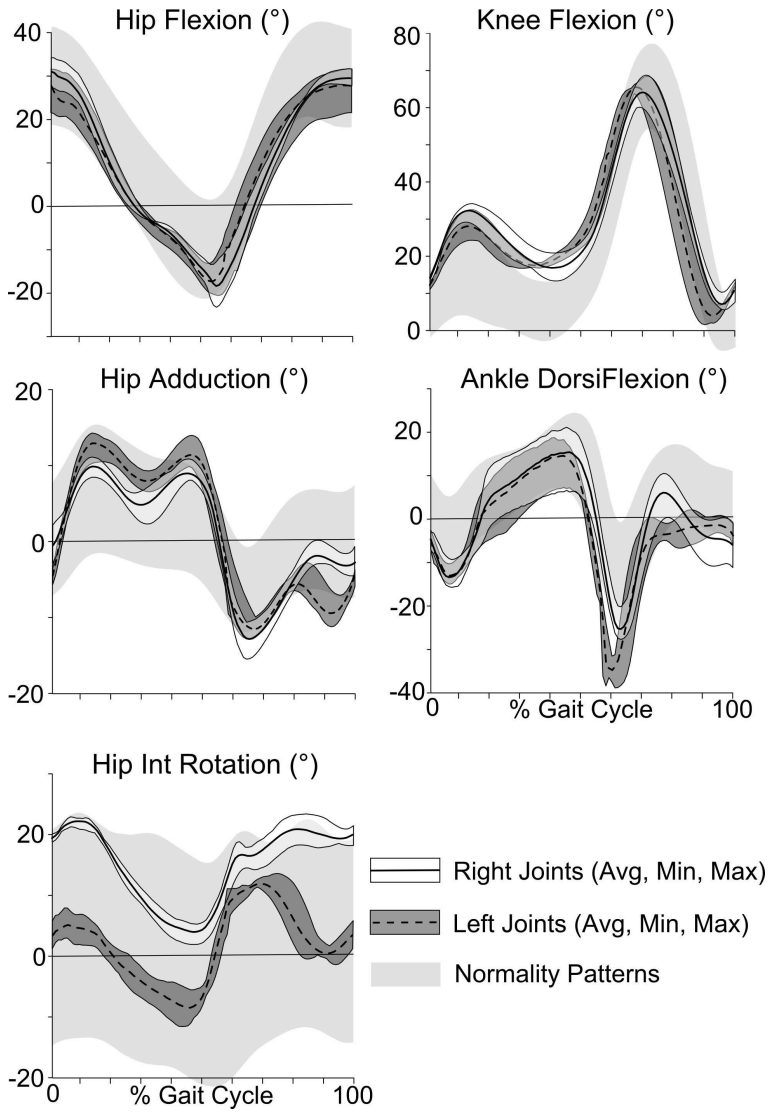

Figure 3 - Kinematics patterns (°) at each of the analysed joint DOFs. The white bands represent the results of the healthy leg (right), whereas the dark grey bands represent the results of the operated leg (left). Average, minimum and maximum values are reported. On the background, in light grey, the reference values for normal children (2 SD) (Leardini et al., 2007) are reported

Kinetics

The net joint moments predicted by the model were, generally, in agreement with the reference data (Figure 4). They were on average lower on the operated leg than on the contralateral one during the whole stance phase, except during early stance, where significantly higher moments were predicted on the hip of the operated leg. These differences reached 2.85 %BW*h.

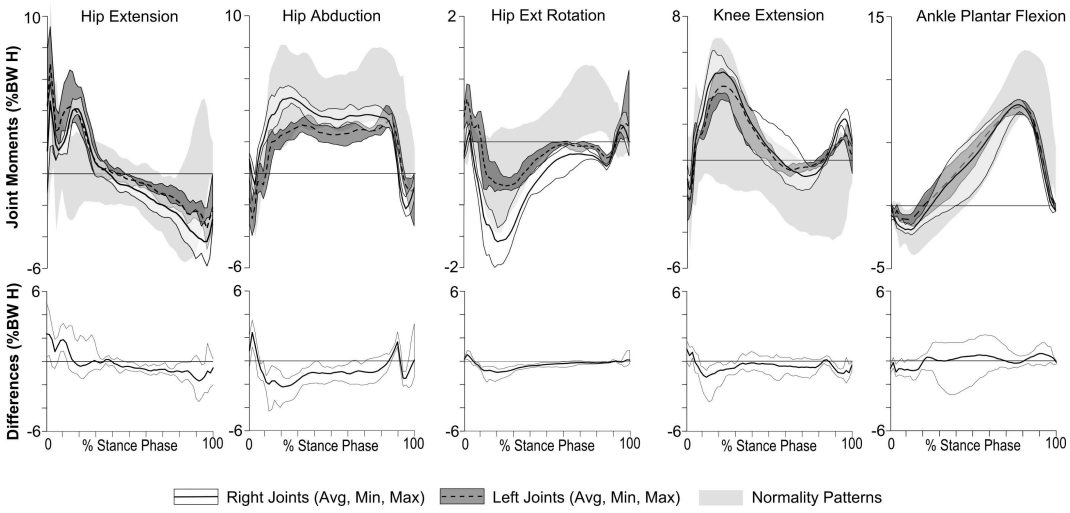

Figure 4 - Joint net moment patterns (%BW*h) at each DOF. Same graphical representation as in Figure 3. The corresponding differences (average, minimum, maximum) between the values of the operated leg and the healthy leg are shown below. On the background, in light grey, the reference values for normal children (2 SD) (Leardini et al., 2007) are reported.

Femoral loads

Joint reaction loads

On average, the hip joint reaction was lower on the operated leg than the contralateral one. This was not true, however, in the first 20% of the stance phase, where the first peak occurred, where the hip joint reaction was on average 30% higher on the operated leg, with a maximum difference of 65% calculated for the peak in one trial, corresponding, in terms of force, to more than 1.5 BW. In the rest of the stance phase, the hip joint reaction was on average 10% lower on the operated leg. The variability of the predicted hip joint reaction also differed between the two legs, exhibiting a higher spread in the first 20% of the stance phase for the operated leg, but a smaller range during the rest of the stance phase.
Apparently the knee joint reaction followed a different trend, being generally higher on the operated leg (Figure 5). However, this difference was, mainly, due to an anticipation of the load increase phase rather than to a higher reaction peak. In fact, the highest differences were calculated just before the first knee joint reaction peak, but the peak itself was lower on the operated leg by 0.1 BW.

Rather, the second peak was higher on the operated leg, but the difference was smaller than 10%.

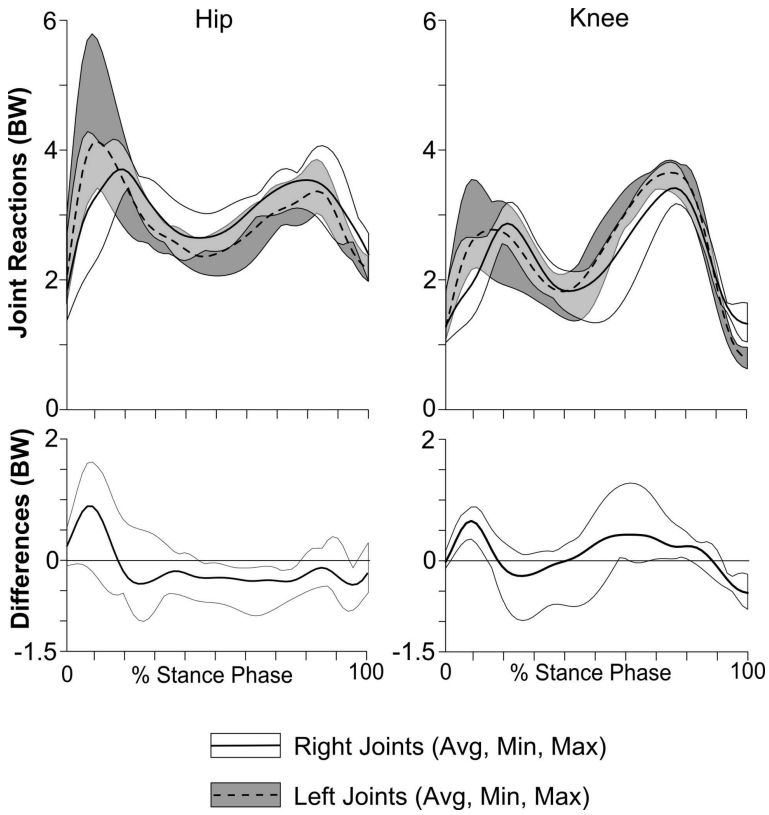

Figure 5 - Joint reaction loads (BW) on the hip (left panel) and on the knee (right panel). Same graphical representation as in Figure 3. The corresponding differences (average, minimum, maximum) between the values of the operated leg and the healthy leg are shown below.

Muscular loads

The most relevant differences between muscle actions were predicted for those groups acting on the hip. In particular, the forces exerted by both hip flexors and extensors during the first 20% of the stance phase were higher on the operated leg than on the contralateral one. The differences in the first peak were, on average, higher than 0.6 BW for both muscle groups and reached 1 BW. During the remaining part of the stance phase, the average forces exerted by the flexor muscles were constantly higher on the operated leg, but the difference was lower, being almost 0.2 BW. Similarly, for the hip rotators, the maximum difference

between the forces was calculated in the same phase of gait, but both absolute values and differences were lower than those predicted for the flexors and the extensors. On the contrary, lower forces were calculated on the operated leg for the abductor muscles throughout the stance phase.

For the muscle groups acting on the knee, the predicted differences were slightly lower, remaining always on average below 0.4 BW. For the knee flexors, higher loads were predicted for the operated leg in the first part of the stance phase, when the first peak was reached, with differences in the order of 0.4 BW.

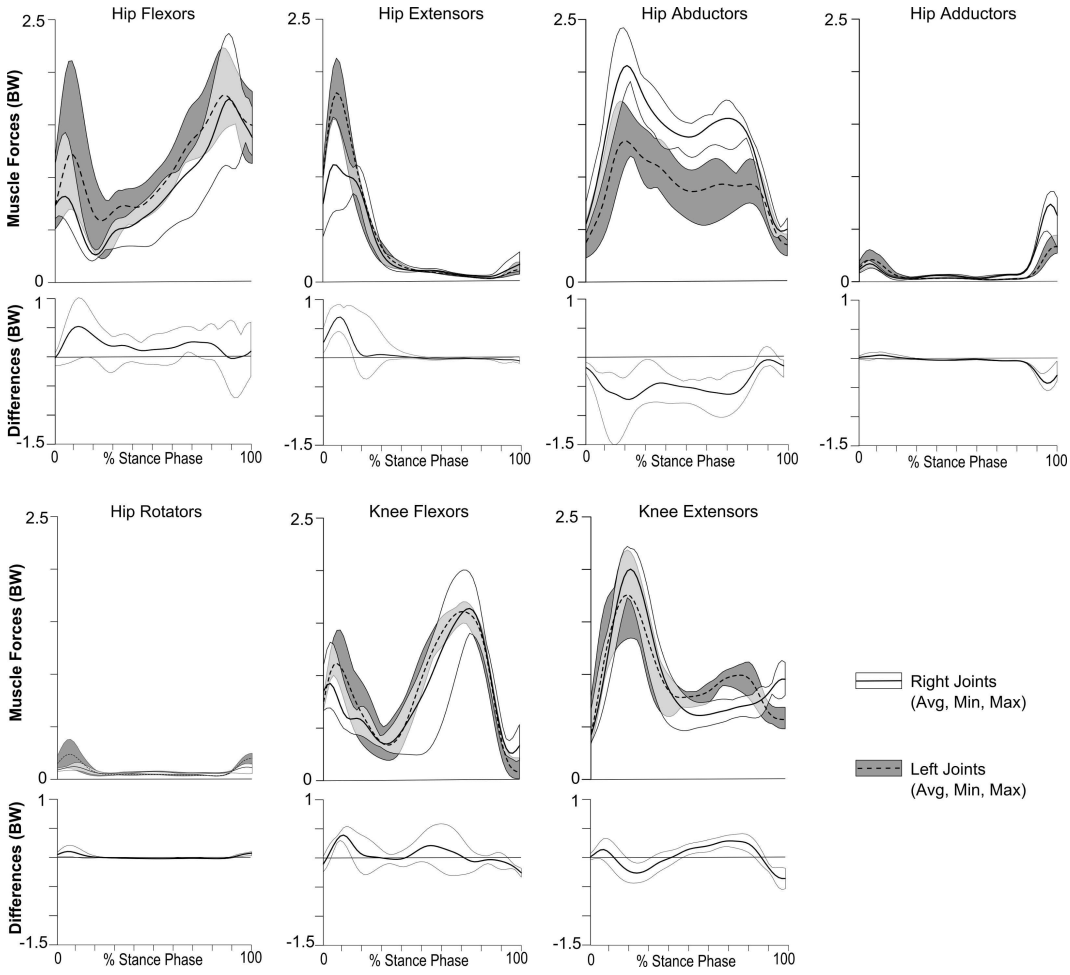

Figure 6 - Muscle forces (BW) grouped by muscle functions. Same graphical representation as in Figure 3. The corresponding differences (average, minimum, maximum) between the values of the operated leg and the healthy leg are shown below.

The second peak reached by the knee flexor muscles was, conversely, comparable between the two legs. For the knee extensors, on the contrary, the first peak was

lower on the operated leg, but a moderate difference of 0.3 BW was predicted in the last part (around 65%) of the stance phase.

Discussion

The aim of the present paper was to investigate the forces acting on a massive femoral reconstruction during gait, to understand if and to which extent were the biomechanical conditions altered due to reconstruction surgery, once the patient had completed the rehabilitation program and was able to walk without exhibiting evident asymmetries between the operated and the contralateral legs. This is a first step to address the complex problems associated to the fracture risk evaluation at the reconstructed femur. To this aim, a subject-specific musculoskeletal model was built, on the basis of an available CT exam of the whole lower limbs, taken for clinical reasons, which was registered to data obtained during a gait analysis session and was used to predict the muscle forces acting on both the femurs during level walking.

At month 31 of follow-up, the patient performed a gait analysis to assess the degree of recovery to normal gait patterns at the operated leg. The results of this exam showed that the patterns of joint rotations and moments were coherent between the two legs at each joint, and compatible with corresponding normal data as obtained from healthy subjects. From a clinical perspective, the rehabilitation therapy could be then considered completed. The major deviation between the kinematics of the two legs was a mean offset of almost 20° at the hip rotation, which could possibly be related to an alteration of the femoral anteversion during surgery, and fell, however, within the normal range. Higher differences were found for the joint external moments, which may indicate a moderate asymmetry in locomotion. This asymmetry could be related to a slight leg length discrepancy (less than 2 cm), but also possibly to a different motor control strategy, for example aimed at protecting the injured leg. The external moments were in fact almost always lower on the operated leg than on the contralateral one and, in addition, exhibited a lower variability somehow indicating a higher level of control of the motion activity. This seemed not true, however, for the transient interval at the beginning of the stance phase where, on

the contrary, the hip and the knee joint moments were higher on the operated side and showed a higher variability. This pattern was reflected and amplified on the forces acting on the femurs, where the differences between the two legs became important. Looking at the hip joint reaction, the same increased variability and average value were predicted on the operated leg with respect to the contralateral one in the early stance phase. On the knee, this effect seemed to be smaller, since the differences between the two legs were mainly due to an anticipation of the phase rather than to a maximum increase. These differences could be relevant: on the hip, a maximum difference of 1.6 BW was predicted, which represented a 65% increment with respect to the contralateral hip reaction. These higher joint reaction forces were due to higher muscle forces acting on the operated femur. Considering the muscles that have an action on the hip joint, both flexors and extensors were predicted to develop, in the early stance phase, higher forces than on the contralateral leg. The flexors then tended to maintain these higher forces throughout the whole stance, whereas for the other muscle groups this did not happen. The rotators actually exhibited a similar pattern, but the forces were lower in magnitude. For the muscles acting on the knee, the same behaviour was predicted for the flexors, where a higher first peak was predicted on the operated leg, whereas for the extensors a higher force was predicted in the second half of the stance phase. The variability of the forces seemed, generally, lower on the operated leg than on the contralateral one. The predicted differences, especially in the first part of the stance phase, may have a non-negligible influence on the risk of fracture that should be further investigated.

A direct comparison of the present results with the literature is impossible, since, to the authors' knowledge, this is the first study that addresses the prediction of the forces acting on a massive skeletal reconstruction during gait. However, some indirect evidences to corroborate the present results can be found. First of all, the accordance of the predicted muscle excitations with the corresponding EMG measurements justifies a good level of confidence in the model predictions. In general, the accordance was good, and comparable with previous similar validation studies (Scheys et al., 2008), the only two exceptions being the non-negligible activation of the *Rectus Femoris* in mid-late stance, which was not

observed from EMG and, on the contrary, the observed activation of the *Tibialis Anterioris* in late stance, which was not predicted by the model. While the latter was likely due to a cross-talk problem, being the *Gastrocnemii* active as well, the inconsistency of the *Rectus Femoris* activation is less simple to explain. Having good confidence in the predicted skeletal kinematics, due to the specific protocol adopted, it is possible that this discrepancy was related to the crude approximation of the knee and ankle joints with simple hinges, but further studies are necessary to support this. However, to the authors' opinion, this mismatch does not invalidate the conclusions for the following reasons. First of all, similar patterns of the *Rectus Femoris* activation were found also in the contralateral intact leg, hence, all the direct comparison between the legs still remains valid. In addition, the predicted muscle excitations in the first phase of stance, where the biggest differences between the two legs were predicted, were in very good agreement with the EMG measurements. On average, the net effect of muscle forces seemed realistic, as the joint reaction loads were in good agreement with measured values reported in the literature (Bergmann, 2011), when considering similar walking speeds. A further indirect confirmation of the present results is that the predicted activation patterns for the healthy leg are in very good agreement with those obtained in a recent study (Xiao and Higginson, 2010) with a similar model scaled onto three healthy young volunteers, analysed at a walking speed very similar to the present (1.3 m/s). The only significant difference regarded the activation of the *Rectus Femoris* in mid stance, already discussed above.

Even though musculoskeletal models are a valuable tool to investigate the loads acting on the skeleton during gait, the current techniques, including the one here adopted, still present several limitations. The joints, especially the knee and the ankle, are crudely modelled, the muscle volumes are represented by a few muscle lines of action, and several parameters defining the muscle functions cannot be truly subject-specific, but rely on published values measured on a limited sample of cadaveric specimens. In addition to those limitations related to the modelling techniques, in the presented model there is another one related to the lack of completeness of the used CT data. The absence of the foot was solved merging a different, although antropometrically similar, anatomy and this may have

introduced an additional error. However, the same strategy was adopted for both limbs, hence the comparative analysis should not be invalidated. Last, but not least, the neuromotor control strategy was always assumed to pursue an optimal goal, but this may not be true. The effects of all these modelling assumptions on the final predicted muscle forces are still largely unknown. Some interesting sensitivity studies have been recently reported (Xiao and Higginson, 2010), but still there is the need for much additional work.

Although with the limitations discussed here above, the results presented in this study showed that small asymmetries in gait patterns, on average lower than 5° apart from the hip rotation and still consistent with normal data, could result in significant differences in musculoskeletal loads (up to 1.6 BW on the hip joint reaction), in patients with large skeletal reconstructions. The influence of such load differences may induce higher risk of fracture of the reconstructed bone. However, how this risk can evolve along the follow-ups needs further investigation and was out of the scope of the present work. Once the picture is complete, the present modelling technique could provide useful information to be used for the thorough optimisation of the rehabilitation therapy and/or of the surgical treatment.

References

Agostini, V., Nascimbeni, A., Gaffuri, A., Imazio, P., Benedetti, M.G., Knaflitz, M., 2010. Normative EMG activation patterns of school-age children during gait. Gait Posture. 32, 285-289.

Arnold, A.S., Blemker, S.S., Delp, S.L., 2001. Evaluation of a Deformable Musculoskeletal Model for Estimating Muscle–Tendon Lengths During Crouch Gait. Annals of Biomedical Engineering. 29, 263-274.

Arnold, A.S., Delp, S.L., 2001. Rotational moment arms of the medial hamstrings and adductors vary with femoral geometry and limb position: implications for the treatment of internally rotated gait. J Biomech. 34, 437-447.

Bergmann, G., 2011. Loading of Orthopaedic Implants, in: Berlin: Julius Wolff Institute, Instrumented Implants, Charité - Universitätsmedizin, Berlin.

Cappozzo, A., Catani, F., Croce, U.D., Leardini, A., 1995. Position and orientation in space of bones during movement: anatomical frame definition and determination. Clin Biomech (Bristol, Avon). 10, 171-178.

Dao, T.T., Marin, F., Ho Ba Tho, M.C., 2009. Sensitivity of the anthropometrical and geometrical parameters of the bones and muscles on a musculoskeletal model of the lower limbs. Conf Proc IEEE Eng Med Biol Soc. 2009, 5251-5254.

Deijkers, R.L., Bloem, R.M., Kroon, H.M., Van Lent, J.B., Brand, R., Taminiau, A.H., 2005. Epidiaphyseal versus other intercalary allografts for tumors of the lower limb. Clin Orthop Relat Res. 439, 151-160.

Delp, S.L., Anderson, F.C., Arnold, A.S., Loan, P., Habib, A., John, C.T., et al., 2007. OpenSim: open-source software to create and analyze dynamic simulations of movement. IEEE Trans Biomed Eng. 54, 1940-1950.

Delp, S.L., Arnold, A.S., Speers, R.A., Moore, C.A., 1996. Hamstrings and psoas lengths during normal and crouch gait: implications for muscle-tendon surgery. J Orthop Res. 14, 144-151.

Delp, S.L., Komattu, A.V., Wixson, R.L., 1994. Superior displacement of the hip in total joint replacement: effects of prosthetic neck length, neck-stem angle, and anteversion angle on the moment-generating capacity of the muscles. J Orthop Res. 12, 860-870.

Delp, S.L., Loan, J.P., Hoy, M.G., Zajac, F.E., Topp, E.L., Rosen, J.M., 1990. An interactive graphics-based model of the lower extremity to study orthopaedic surgical procedures. IEEE Trans Biomed Eng. 37, 757-767.

Delp, S.L., Ringwelski, D.A., Carroll, N.C., 1994. Transfer of the rectus femoris: effects of transfer site on moment arms about the knee and hip. J Biomech. 27, 1201-1211.

Delp, S.L., Wixson, R.L., Komattu, A.V., Kocmond, J.H., 1996. How superior placement of the joint center in hip arthroplasty affects the abductor muscles. Clin Orthop Relat Res. 137-146.

Dumas, R., Aissaoui, R., Mitton, D., Skalli, W., de Guise, J.A., 2005. Personalized body segment parameters from biplanar low-dose radiography. IEEE Trans Biomed Eng. 52, 1756-1763.

Erdemir, A., McLean, S., Herzog, W., van den Bogert, A.J., 2007. Model-based estimation of muscle forces exerted during movements. Clin Biomech (Bristol, Avon). 22, 131-154.

Free, S.A., Delp, S.L., 1996. Trochanteric transfer in total hip replacement: effects on the moment arms and force-generating capacities of the hip abductors. J Orthop Res. 14, 245-250.

Friedrich, J.B., Moran, S.L., Bishop, A.T., Wood, C.M., Shin, A.Y., 2008. Free vascularized fibular graft salvage of complications of long-bone allograft after tumor reconstruction. J Bone Joint Surg Am. 90, 93-100.

Garner, B.A., Pandy, M.G., 2003. Estimation of Musculotendon Properties in the Human Upper Limb. Annals of Biomedical Engineering. 31, 207-220.

Gray, H., Lewis, W.H., 2000. Anatomy of the Human Body. Philadelphia: Lea & Febiger,1918: Bartleby.com.

Grimer, R.J., 2005. Surgical options for children with osteosarcoma. Lancet Oncol. 6, 85-92.

Gunther, M., Sholukha, V.A., Kessler, D., Wank, V., Blickhan, R., 2003. Dealing with skin motion and wobbling masses in inverse dynamics. JMMB. 3, 309-335.

Hermens, H., 1999. European Recommendations for Surface Electromyography: Results of the Seniam Project (SENIAM). Enschede: Roessingh Research and Development.

Hicks, J., Arnold, A., Anderson, F., Schwartz, M., Delp, S., 2007. The effect of excessive tibial torsion on the capacity of muscles to extend the hip and knee during single-limb stance. Gait Posture. 26, 546-552.

Higginson, J.S., Zajac, F.E., Neptune, R.R., Kautz, S.A., Delp, S.L., 2006. Muscle contributions to support during gait in an individual with post-stroke hemiparesis. J Biomech. 39, 1769-1777.

Jonkers, I., Sauwen, N., Lenaerts, G., Mulier, M., Van der Perre, G., Jaecques, S., 2008. Relation between subject-specific hip joint loading, stress distribution in the proximal femur and bone mineral density changes after total hip replacement. J Biomech. 41, 3405-3413.

Klein Horsman, M.D., Koopman, H.F.J.M., van der Helm, F.C.T., Prose, L.P., Veeger, H.E.J., 2007. Morphological muscle and joint parameters for musculoskeletal modelling of the lower extremity. Clinical Biomechanics. 22, 239-247.

Koopman, H.F.J.M., Klein Horsman, M.D., 2008. Hip compression force estimation with a comprehensive musculoskeletal model. Proceedings of Measuring Behavior 2008 (Maastricht, The Netherlands, August 26-29, 2008).

Leardini, A., Sawacha, Z., Paolini, G., Ingrosso, S., Nativo, R., Benedetti, M.G., 2007. A new anatomically based protocol for gait analysis in children. Gait Posture. 26, 560-571.

Lewis, V.O., 2005. Limb salvage in the skeletally immature patient. Curr Oncol Rep. 7, 285-292.

Lundberg, A., Svensson, O.K., Nemeth, G., Selvik, G., 1989. The axis of rotation of the ankle joint. J Bone Joint Surg Br. 71, 94-99.

Mankin, H.J., Gebhardt, M.C., Jennings, L.C., Springfield, D.S., Tomford, W.W., 1996. Long-Term Results of Allograft Replacement in the Management of Bone Tumors. Clinical Orthopaedics and Related Research. 324, 86-97.

Muscolo, D.L., Ayerza, M.A., Aponte-Tinao, L., Ranalletta, M., Abalo, E., 2004. Intercalary femur and tibia segmental allografts provide an acceptable alternative in reconstructing tumor resections. Clin Orthop Relat Res. 97-102.

Ogilvie, C.M., Crawford, E.A., Hosalkar, H.S., King, J.J., Lackman, R.D., 2009. Long-term results for limb salvage with osteoarticular allograft reconstruction. Clin Orthop Relat Res. 467, 2685-2690.

Piazza, S.J., Delp, S.L., 2001. Three-dimensional dynamic simulation of total knee replacement motion during a step-up task. J Biomech Eng. 123, 599-606.

Scheys, L., Van Campenhout, A., Spaepen, A., Suetens, P., Jonkers, I., 2008. Personalized MR-based musculoskeletal models compared to rescaled generic models in the presence of increased femoral anteversion: effect on hip moment arm lengths. Gait Posture. 28, 358-365.

Schmidt, D.J., Arnold, A.S., Carroll, N.C., Delp, S.L., 1999. Length changes of the hamstrings and adductors resulting from derotational osteotomies of the femur. Journal of Orthopaedic Research. 17, 279-285.

Shao, Q., Bassett, D.N., Manal, K., Buchanan, T.S., 2009. An EMG-driven model to estimate muscle forces and joint moments in stroke patients. Comput Biol Med. 39, 1083-1088.

Sorger, J.I., Hornicek, F.J., Zavatta, M., Menzner, J.P., Gebhardt, M.C., Tomford, W.W., et al., 2001. Allograft fractures revisited. Clin Orthop Relat Res. 66-74.

Stansfield, B.W., Nicol, A.C., 2002. Hip joint contact forces in normal subjects and subjects with total hip prostheses: walking and stair and ramp negotiation. Clin Biomech (Bristol, Avon). 17, 130-139.

Taddei, F., Ansaloni, M., Testi, D., Viceconti, M., 2007. Virtual palpation of skeletal landmarks with multimodal display interfaces. Informatics for Health and Social Care. 32, 191-198.

Tanavalee, A., Yuktanandana, P., Ngarmukos, C., 2001. Surgical epicondylar axis vs anatomical epicondylar axis for rotational alignment of the femoral component in total knee arthroplasty. J Med Assoc Thai. 84 Suppl 1, 401-408.

Testi, D., Quadrani, P., Viceconti, M., 2010. PhysiomeSpace: digital library service for biomedical data. Philos Transact A Math Phys Eng Sci. 368, 2853-2861.

Thelen, D.G., Anderson, F.C., 2006. Using computed muscle control to generate forward dynamic simulations of human walking from experimental data. J Biomech. 39, 1107-1115.

Van der Bogert, A.J., Koning, J.J., 1996. On optimal filtering for inverse dynamics analysis, in: 9th Biennial Conference of the Canadian Society for Biomechanics, Vancouver, pp. 214-215.

Vasavada, A.N., Delp, S.L., Maloney, W.J., Schurman, D.J., Zajac, F.E., 1994. Compensating for changes in muscle length in total hip arthroplasty. Effects on the moment generating capacity of the muscles. Clin Orthop Relat Res. 121-133.

Wu, G., Siegler, S., Allard, P., Kirtley, C., Leardini, A., Rosenbaum, D., et al., 2002. ISB recommendation on definitions of joint coordinate system of various joints for the reporting of human joint motion- part I: ankle, hip, and spine. International Society of Biomechanics. J Biomech. 35, 543-548.

Xiao, M., Higginson, J., 2010. Sensitivity of estimated muscle force in forward simulation of normal walking. J Appl Biomech. 26, 142-149.

Chapter 2

MRI-based subject-specific vs. scaled-generic modeling: a case study using the NMSBuilder software

Giordano Valente[1,2], Lorenzo Pitto[1], Maria Cristina Bisi[3], Rita Stagni[3], Luca Cristofolini[2], Fulvia Taddei[1]

[1] Laboratorio di Tecnologia Medica, Istituto Ortopedico Rizzoli, Bologna, Italy
[2] Department of Industrial Engineering, Univerisity of Bologna, Italy
[3] Department of Electric, Electronic and Information Engineering, Univerisity of Bologna, Italy

Unpublished work submitted to the 5th International Conference on Computational Bioengineering (ICCB), Belgium, 2013

Author contributions

G. Valente assisted with project design and management, developed the models, performed the simulations of motion, interpreted the results

L. Pitto segmented the imaging data, post-processed the gait data, developed the models, performed the simulations of gait

M.C. Bisi and R. Stagni collected the gait data, assisted with imaging data collection

L. Cristofolini assisted with project management and imaging data collection

F. Taddei obtained funding, assisted with project management and modeling development

Introduction

Multibody-dynamics modeling of the musculoskeletal system is the only practicable method providing a valuable approach to muscle and joint loading analyses in-vivo. Recent increases in computing power are driving musculoskeletal modeling towards relevant challenges, contributing in the improvement of several orthopedics and neurological treatments. A considerable interest is raising on subject-specific modeling, providing more accurate results compared to generic modeling, particularly when dealing with musculoskeletal pathologies [Pandy, 2010]. One key difficulty concerns the inability to model accurately musculoskeletal geometry on a subject-specific basis, also related to expensive processes in effort and time. Recently, a freely available software toolkit, i.e. NMSBuilder[1], was developed within the European Union-funded project NMS Physiome[2], enabling to create and edit musculoskeletal models from imaging data, create OpenSim model files and perform movement simulations through the OpenSim Application Programming Interface (API)[3] [Delp, 2007]. This study aims at comparing muscle and joint forces during motion predicted by a subject-specific model and a scaled-generic model, and demonstrating how the NMSBuilder modeling framework reduces effort and time to create subject-specific models from MRI.

Methods

Lower-limb MRI and conventional gait analysis measurements were acquired for a healthy subject. A 7 segment, 10 degree of freedom musculoskeletal model, actuated by 82 musculotendon units, was created from the imaging data. NMSBuilder was used to create the OpenSim model, allowing to import the segmented surfaces, calculate rigid body properties, define joint reference frames and kinematical constraints, define musculotendon paths and parameters (Figure 1A). A state-of-the-art generic model [Delp, 1990] was scaled to match the

[1] https://www.biomedtown.org/biomed_town/nmsphysiome/reception/alpha/; see also Part IV of the thesis

[2] http://www.nmsphysiome.eu/; see also Part IV of the thesis

[3] https://simtk.org/api_docs/opensim/api_docs/

subject's anthropometry and mass (Figure 1B). Inverse Kinematics, Static Optimization and Joint Reaction Analysis of the stance phase of seven walking trials were performed using OpenSim, to calculate joint kinematics, muscle and joint contact forces. Predicted muscle activations were compared with experimental EMG, and peak force values compared between the two models.

Results

The subject-specific modeling framework required few days to be completed. A satisfactory agreement was found comparing activations from both subject-specific and scaled-generic models with EMG, with a similar discrepancy. The scaled-generic model predictions tended to a general force overestimation compared to subject-specific predictions. The largest average difference in muscle forces was 0.5 BW in the soleus, while in joint forces was 0.9 BW in the hip.

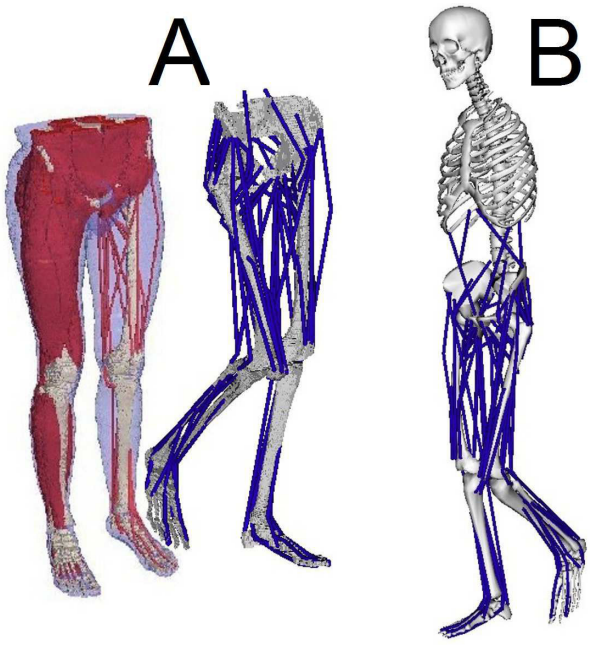

Figure 1 - Subject-specific (A) and scaled-generic (B) musculoskeletal models

Discussion

Subject-specific model predictions present some significant differences compared to scaled-generic, even without musculoskeletal pathologies involved. More refined subject-specific knee and ankle models are being implemented as well as simulations of different motor tasks.

NMSBuilder contributes in simplifying subject-specific modeling frameworks, making appealing the use of such modeling tools to accurately model musculoskeletal geometry.

References

Delp S.L., et al., An interactive graphics-based model of the lower extremity to study orthopaedic surgical procedures, IEEE Trans Biomed Eng. 37:757-67, 1990.

Delp S.L., et al., OpenSim: open-source software to create and analyze dynamic simulations of movement, IEEE Trans Biomed Eng. 54:1940-50, 2007.

Pandy M.G., and Andriacchi T.P., Muscle and joint function in human locomotion, Annu Rev Biomed Eng, 12:401-33, 2010.

PART II

Sensitivity of model predictions to muscular parameters

Chapter 3

Muscle discretization affects the loading transferred to bones in lower-limb musculoskeletal models

Chapter 4

Influence of lower-limb muscle discretization of the prediction of skeletal loads during walking

Chapter 5

Influence of weak hip abductor muscles on joint contact forces during normal walking: a probabilistic modeling analysis

Chapter 3

Muscle discretization affects the loading transferred to bones in lower-limb musculoskeletal models

Giordano Valente[1,2], Saulo Martelli[1], Fulvia Taddei[1], Giovanna Farinella[3], Marco Viceconti[1,3]

[1] Laboratorio di Tecnologia Medica, Istituto Ortopedico Rizzoli, Bologna, Italy
[2] DIEM, University of Bologna, Italy
[3] Laboratorio di BioIngegneria Computazionale, Istituto Ortopedico Rizzoli, Bologna, Italy

Journal article published on Proc. IMechE, Part H: J. Engineering in Medicine, 226(2): 161-70, 2012

Author contributions

G. Valente developed the models, performed calculations, post-processed the results, created the figures and wrote the paper

S. Martelli designed the project, assisted with model development, performance of calculations and writing the paper

F. Taddei obtained funding, assisted with project design and management, performance of calculations and writing the paper

G. Farinella assisted with model developments and performance of calculations

M. Viceconti obtained funding, assisted with project management and writing the paper

Abstract

Modelling the mechanical effect of muscles is important in several research and clinical contexts. However, few studies have investigated the effect of different muscle discretizations from a mechanical standpoint. The present study evaluated the errors of a reduced discretization of the lower limb muscles in reproducing the muscle loading transferred to bones. Skeletal geometries and a muscle data collection were derived from clinical images and dissection studies of two cadaver specimens. The guidelines of a general method previously proposed for a different anatomical district were followed. The data collection was used to calculate the mechanical effect of muscles, i.e. the generalized force vectors, and the errors between a large and a reduced discretization, in a reference skeletal pose and in the extreme poses of the range of motion of joints. The results showed that the errors committed using a reduced representation of muscles could be significant and higher than those reported for a different anatomical region. In particular, the calculated errors were found dependent on the individual anatomy and on the skeletal pose. Since different biomechanical applications may require different discretization levels, care is suggested in identifying the number of muscle lines of action to be used in musculoskeletal models.

Keywords

Muscle discretization, Muscle mechanical effect, Subject-specific musculoskeletal modeling, Lower limb, Range of motion of joints

Introduction

Computational models of the musculoskeletal system have been widely used in several biomechanics investigations [1, 2]. Regarding such models, a strong consensus exists in modelling the mechanical effect of muscles with one-dimensional actuators, implying a discretization of the continuum muscle-tendon elements. This process leads to lumped parameter models and an error in describing the force and moment generating capacity of muscles is involved. Intuitively, the more actuators are used to model each muscle, the lower will be this error, and the larger will be the modelling and computational complexity involved. To date there is no consensus on an adequate number of muscle lines of action to be used in lower limb models and significant differences can be found. For instance, the *Gluteus Maximus* has been modelled with one line [3-6], two lines [7, 8] or three lines [9-12]. In general, in the majority of models presented in the literature, a small number of muscle lines of action is adopted. Actually, one of the most widely adopted discretizations [13-16], proposed by Delp *et al.* [9, 17], consists of 43 line elements per leg, where single lines of action are used except for a few muscles (*Gluteus Maximus*, *Gluteus Medius*, *Gluteus Minimus*, *Adductor Magnus*) discretized with three elements. Nevertheless, in a more recent work, a lower limb model with a markedly larger number of elements (163 per leg) has been proposed [18]: with an heuristic choice, most muscles were divided into parts and each one was discretized with a minimum number of elements. The importance of the discretization choice on the biomechanics investigations surely depends on the objective of the modelling activity, but, to date, no conclusive sensitivity studies have been performed on the lower limb muscles. As a consequence, the effect of the discretization level on the mechanical effect of the lower limb muscles on bones is still unclear.

To the authors' knowledge, only one single study [19] has been published on the methodological problem of assessing an adequate number of muscle lines of action. In that work, a musculoskeletal model of the shoulder region was built from accurate dissection measurements taken from a cadaver study on bones and muscle attachment areas. It was there assumed that 200 lines of action could correctly reproduce the muscle mechanical effect on bones, represented by the

resulting force and moment vectors with respect to the centroid of the attachment areas. Then the mechanical effect was calculated for a large number (200) and a reduced number (up to six) of lines of action, in order to analyse the resulting error between the two representations in a reference pose. The results showed that the highest absolute errors were found for the muscles with larger attachment areas and the relative errors did not exceed 15% for most muscles.

Although important, the results of the cited study [19] cannot be directly transferred to lower limb models, due to the significant differences between the two anatomical regions. In addition, it would be interesting to understand if, and to which extent, the results obtained from one anatomy and one pose can be extended to different geometries and poses in the range of motion (ROM) of joints. In fact, it is well known that lower limb muscle attachments and moment arms show a wide anatomical variability [20], but it is not evident *a priori* if this variability may influence or not the error related to the muscle discretization, which is an aspect neglected in the reference cited work.

The aim of the present study is twofold: first, to replicate the mentioned work [19] for the lower limbs in order to evaluate the errors of the muscle discretization in reproducing the mechanical effect of muscles on bones, for a given muscle force, in a reference skeletal pose; second, to extend the study to the extreme poses of the ROM of lower limb joints. To the purpose, data from both limbs of two cadaver specimens were used, and the variability of the calculated mechanical effect of muscles was studied when varying the musculoskeletal geometry and the model pose.

Materials and Methods

Data Collection

Lower limb data of two cadaver specimens were obtained from detailed multiscale datasets [21], publicly available through the Physiome Space service[1] [22] (Fig. 1). The data collection includes the bone segments and the muscle anatomies. The muscular data collection of the lower limbs includes 66 muscles for a specimen

[1] https://www.physiomespace.com/

(missing *Gemellus Superior* and *Inferior, Obturator Externus* and *Internus, Quadratus Femoris, Plantaris, Extensor* and *Flexor Digitorum Brevis*) and 69 muscles for the other (missing *Gluteus Maximus, Left Pyriform, Semitendinosus, Biceps Femoris Caput Brevis, Peroneus Tertius, Soleus, Medial* and *Lateral Gastrocnemius*), and consists of three-dimensional coordinates of the points defining the attachment locations of muscles, superficial paths of the muscle fibres, muscle volumes and lengths.

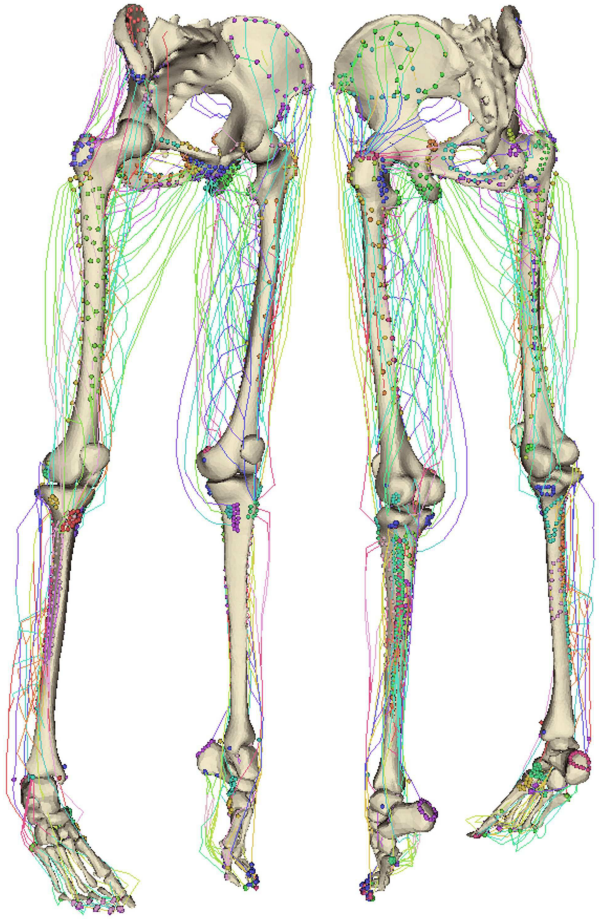

Figure 1 - Complete lower limb dataset of a cadaver specimen: bone geometries, digitised muscle attachment points and superficial fibre paths, loaded and spatially registered in a dedicated software (LHPBuilder, SCS, Italy)

Modelling the mechanical effect of the lower limb muscles

Discretizing the muscle attachment areas

The muscle attachment areas were modelled according to their shapes, following the method proposed for the shoulder muscles [19]: (1) approximation by a point (considered as line with order zero) for relatively small areas, (2) approximation by a straight line (first order) or curved line (third order) for areas with relatively large length/width ratio, (3) approximation by a plane for relatively large areas. In three-dimensional space a muscle can influence up to six degrees of freedom (DOF) of each bone, depending on the shape of the attachment area and the direction of the muscle fibres. In general, nine combinations of areas are possible, and each muscle with a combination of attachment areas can influence a specific number of DOF. The minimum number of lines of action necessary to the muscle representation is given by the number of DOF that the muscle can influence independently. This minimum number of elements is equal to the rank of matrix **A** (eq. 2.2, section 2.2.2) [19]. In the lower limb region, five combinations of geometrical shapes of attachment areas were identified, and each muscle was schematised with a combination of them (Table 1). The muscles whose attachment areas were both approximated by a single point, were represented by a single line of action. Some muscles exerting a negligible force were not included in the models (*Extensor* and *Flexor Digitorum, Extensor* and *Flexor Hallucis, Obturator Externus* and *Internus, Peronei Brevis, Longus* and *Tertius, Popliteus*). For the muscles *Iliacus, Tibialis Anterior* and *Tibialis Posterior*, points dividing the involved muscles in series of two straight line segments (i.e. via-points) and fixed to the proximal segment were defined on the superficial fibre paths, identifying a proximal and a distal part of the muscles.

Table 1 - Modelling the muscle attachment areas according to their shape: origin and insertion areas described as plane, line (order) or point, with the corresponding minimum number of elements necessary for the muscle representation. The muscle datasets include four samples per muscle, except for: * two samples, ** three samples

Muscle	Shape Description		Min number of elements
	Origin	Insertion	
Adductor Brev	Point	Line (3)	3
Adductor Long	Point	Line (1)	2
Adductor Magn	Line (1)	Line (3)	5
Biceps Fem CB *	Line (3)	Point	3
Biceps Fem CL	Point	Point	1
Gastrocn Lat *	Point	Point	1
Gastrocn Med *	Point	Point	1
Gemellus *	Point	Point	1
Gluteus Max *	Plane	Line (3)	6
Gluteus Med	Plane	Point	4
Gluteus Min	Plane	Point	4
Gracilis	Point	Point	1
Iliacus (dist)	Line (3)	Point	3
Iliacus (prox)	Plane	Line (3)	6
Pectineus	Point	Point	1
Plantaris	Point	Point	1
Pyriform **	Line (1)	Point	2
Quadratus Fem *	Point	Point	1
Rectus Fem	Point	Point	1
Sartorius	Point	Point	1
Semimembr	Point	Point	1
Semitend *	Point	Point	1
Soleus *	Line (1)	Point	2
Tensor Fasc Lat	Point	Point	1
Tibialis Ant (dist)	Point	Point	1
Tibialis Ant (prox)	Line (1)	Point	2
Tibialis Post (dist)	Point	Point	1
Tibialis Post (prox)	Line (1)	Point	2
Vastus Int	Line (1)	Point	2
Vastus Lat	Line (3)	Point	3
Vastus Med	Line (3)	Point	3

A mathematical description of the geometrical shapes was fitted to the data points of the attachment areas, following the previously published method [19, 23] (Fig. 2):

One point-approximated attachment areas: The coordinates of the point-shaped attachment areas were approximated by the centroid of the areas, calculated as the mean of the measured coordinates on bones.

Line-approximated attachment areas: The coordinates of data points of the attachment areas were expressed as polynomials in variable $t_i \in [0,1]$:

$$x = x(t), y = y(t), z = z(t) \quad (2.1)$$

For each coordinate a least squares criterion was used to estimate the parameters of the polynomials. The resulting attachment areas of the muscles were proportionally distributed along the polynomials.

Plane-approximated attachment areas: The coordinates of data points of the attachment areas were expressed by the equation of a plane approximating the attachment areas. Data points were projected on the plane using a least squares criterion to estimate the parameters describing the plane. The area defined by the projected coordinates could be divided in equal parts along the longer axis, and for each part two points were proportionally distributed over the area, resulting in an even number of points describing the surface.

In all combinations of the modelled attachment areas, the geometric muscle model could be created by locating an arbitrary large number of straight lines of action between the origin and the insertion points (including via-points where described above), using a map of the muscle bundle distribution derived from the position data.

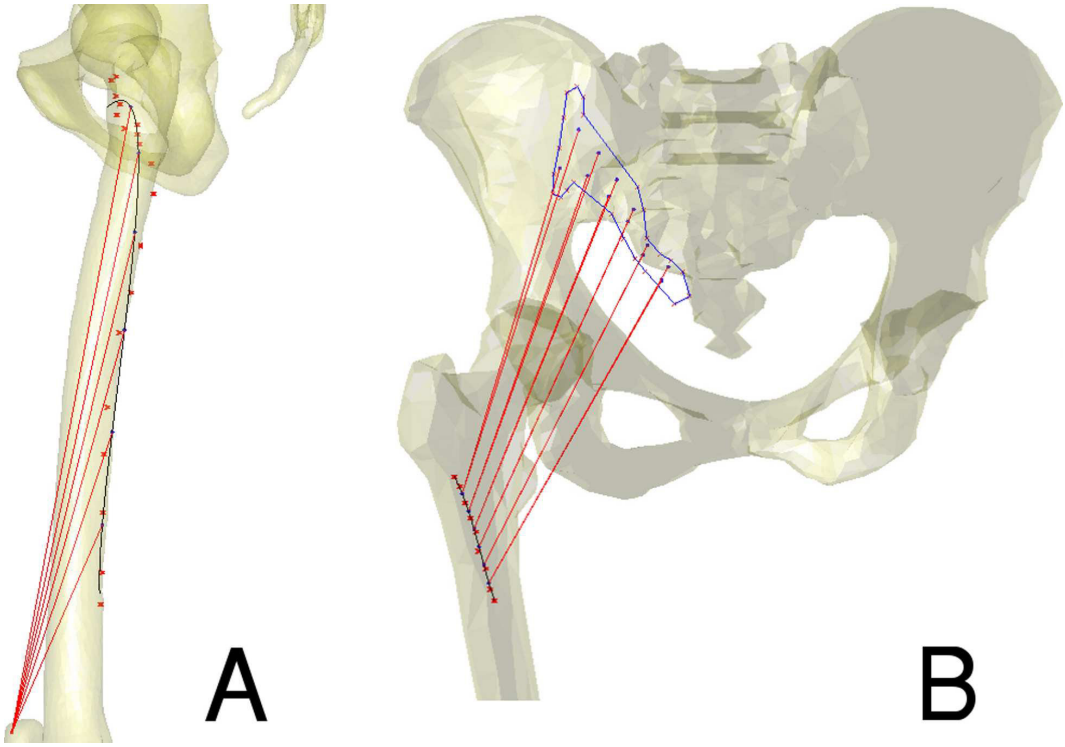

Figure 2 - Examples of modelling the muscle attachment areas and location of an arbitrary number of straight lines of action in two muscles. (A) Line-approximated and point-approximated attachment areas (Vastus Lateralis, six elements shown). (B) Plane-approximated and line-approximated attachment areas (Gluteus Maximus, 12 elements shown). To every point on the line correspond two points on the plane

Computing the mechanical effect of muscles

The muscle force vectors were represented by the lines of action attached to the bone and pointing towards the fibre directions. The mechanical effect of each muscle was described by the resulting force and moment vectors with respect to the centroid of the attachment areas [19], $\boldsymbol{Y_F}$ and $\boldsymbol{Y_M}$, exerted by the muscle lines of action, which can be written in a compact form as generalized force vector:

$$\boldsymbol{Y_n} = \mathbf{A_n} \cdot \boldsymbol{U_n} \tag{2.2}$$

where the matrix **A** accounts for the muscle geometry and $\boldsymbol{U}$ represents the vector of scalar forces, for n number of lines of action. Under the assumption of even activation of each muscle over its entire volume [19], the muscle force u was supposed uniformly distributed between the lines of action:

$$u = \frac{PCSA \cdot \sigma}{n} \tag{2.3}$$

where n represents the number of lines of action, *PCSA* the muscle physiological cross-sectional area and σ the constant muscle tension equal to 30 N/cm^2 [19]. The values of muscle PCSAs were calculated from the muscle data collections as the muscle volume divided by the optimal fibre length l_{opt}, where l_{opt} was calculated as the mean fibre length multiplied by the ratio of the mean sarcomere length and the optimal sarcomere length of 2.7 μm [24].

The muscles that did not feature a point-approximated attachment area (*Gluteus Maximus, Adductor Magnus*) presented non-null moments at both origin (O) and insertion (I) attachments, while all the other muscles showed null moment with respect to the centroid of the point-approximated area. The moments with respect to the centroid of the via-points (*Iliacus*) have not been evaluated.

The mechanical effect of muscles in the ROM of joints

A 7-segment, 10-DOF computational model of the lower limb system was generated for each cadaver specimen. Each leg was articulated by three ideal joints: a ball-and-socket at the hip (3 DOF) and a hinge (1 DOF) at both the knee and the ankle [16]. The identification of the joint parameters was based on relevant landmarks identified on the skeletal surface with a virtual palpation procedure [25]. All anatomical landmarks were identified following the ISB standards and a local coordinate system was defined for each segment [26]. The hip centre was defined as the centre of the sphere that best fitted the femoral head surface. The hip joint orientation was defined accordingly to ISB standards [26]. The axis of knee rotation was defined as the axis connecting the two centres of the medial and lateral epicondyles [27], and the axis of ankle rotation was defined as the axis connecting the medial and the lateral malleoli [28]. The reference pose of the models was defined as the neutral pose where the generalized coordinates were zero, accordingly to the ISB recommendations [29]. The further investigated poses were in correspondence of the minimum and maximum ROM values of each joint DOF. Each movement in the interested poses was performed separately, without considering any combination of joint angle values. Therefore, the investigated skeletal poses were 40 in total, which included the reference pose and the nine extreme poses for the four samples (two sides per specimen). The

extreme ROM values of all considered joints were taken from the mean values of an adult population [30] (Table 2).

Table 2 - Extreme values of active ROM of the modelled lower limb joints

JOINT	DOF	min value (°)	max value (°)
Hip	Extension (-)/Flexion (+)	-12	121
	Abduction (-)/Adduction (+)	-40	26
	Extra (-)/Intra (+) Rotation	-44	44
Knee	Flexion (-)/Extension (+)	-141	0
Ankle	Plantar (-)/Dorsi (+) Flexion	-54	12

Error between the large and the reduced muscle representation

It was assumed that a uniform density of lines of action equal to 1 line/mm constituted a good muscle representation to correctly reproduce the mechanical effect of each entire muscle. This assumption was preliminarily verified through a convergence study, calculating the generalized force vectors for increasing values of line density. Thus the large representation of each muscle was constituted by the number of lines of action corresponding to 1 line/mm, ranging from 41 to 293; the reduced representation was constituted by the number of elements equal to the DOF influenced by the muscle (Table 1). In order to evaluate the error between the two muscle discretizations, the corresponding generalized force vectors, $\boldsymbol{Y}_{large}$ and $\boldsymbol{Y}_{reduced}$, were calculated. Then the absolute error e_a and the percentage relative error e_r were calculated between the two representations as follows:

$$e_a = \left\| \boldsymbol{Y}_{large} - \boldsymbol{Y}_{reduced} \right\| \tag{2.4}$$

$$e_r = 100 \frac{\left\| \boldsymbol{Y}_{large} - \boldsymbol{Y}_{reduced} \right\|}{\left\| \boldsymbol{Y}_{large} \right\|} \tag{2.5}$$

The values of $\boldsymbol{Y}_{large}$, $\boldsymbol{Y}_{reduced}$, e_a, e_r were calculated with respect to the reference pose and the extreme poses of the ROM of each joint DOF. For each muscle, the data were collected as mean, minimum and maximum values between the samples, in order to evaluate the influence of the geometry and the model pose on the muscle mechanical effect. The calculation of all the generalized force vectors of muscles could be performed in few minutes with a common desktop computer.

The errors on the calculated muscle force vectors between the large and the reduced muscle representation were small ($e_{r,f} < 1\%$), therefore only the muscle moments are included in the presented results.

Results

Convergence analysis

All muscle moments showed an asymptotic convergence behaviour with respect to the density of muscle lines of action, in all the investigated poses. The convergence, to which corresponded a relative error below 5%, was achieved with a mean value of 0.35±0.17 lines/mm between all muscles in all the poses, and with a maximum value of 0.76 lines/mm. As an example, the curves of moments and absolute errors for the *Gluteus Medius* in the reference pose are reported (Fig. 3): this muscle shows one of the largest differences of the moments between the

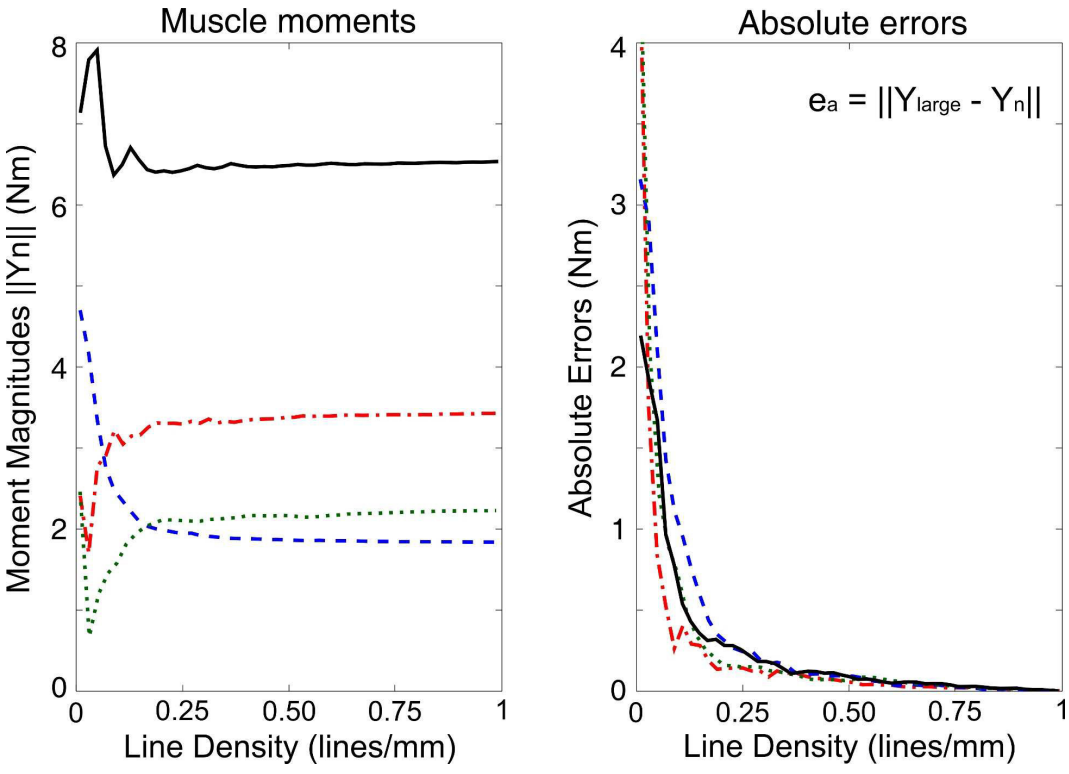

Figure 3 - Convergence curves (magnitudes of muscle moments ||Yn|| and absolute errors ||Ylarge - Yn||) calculated for an increasing density of lines of action, corresponding to an increasing number n of lines of action, used for the discretisation of muscles. The four different curves represent the four samples of the Gluteus Medius

muscle samples, but this does not reflect on the absolute errors.

Influence of the reduced muscle representation

Reference pose

The muscle moments (i.e. $||\boldsymbol{Y}_{large}||$ and $||\boldsymbol{Y}_{reduced}||$) and the absolute errors (i.e. e_a) are presented for each muscle (Figure 4 and 6). The broad attachment muscles (*Gluteus Maximus, Gluteus Medius, Vastus Lateralis, Vastus Medialis, Adductor Magnus*) showed the highest mean values of muscle moments and absolute errors. For these muscles, the mean absolute errors ranged from 0.4 Nm for the *Gluteus Maximus* to 3.4 Nm for the *Vastus Medialis* (Fig. 6). The mean relative error was 34%, ranging from 14% to 60% (found for the *Gluteus Maximus* and *Vastus Medialis* respectively); overall, the muscles, excluding those whose absolute contribute was below 0.1 Nm (i.e. *Tibialis Anterior, Tibialis Posterior, Adductor Longus*), showed an average relative error of 40%, ranging from 14% to 75% (found for the *Gluteus Maximus* and *Gluteus Minimus* respectively). In the majority of cases, the muscle moments showed a relatively high variability between the different modelled anatomies. Considering the broad attachment muscles, the ratio between the moment range and mean value was on average 88% and reached 200% for the *Gluteus Medius*. Similarly, the ratio between the absolute error range and mean value was on average 66% and reached 122% for the *Adductor Magnus*.

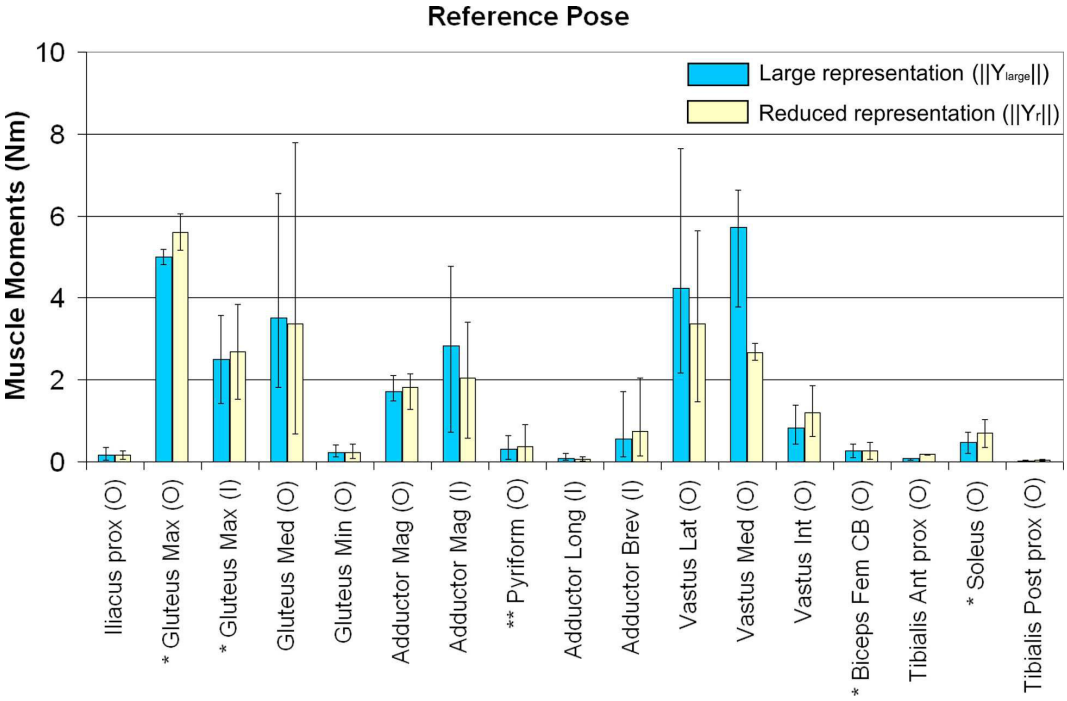

Figure 4 - Norm of muscle moments (||Ylarge|| and ||Yreduced||) presented as mean, minimum and maximum values in the reference pose (four muscle samples, except for: * two muscle samples, ** three muscle samples). A total of four skeletal poses were analysed: four samples (two sides per specimen) in the reference pose. The muscle moments were calculated with respect to the centroid of O = origin attachment, and I = insertion attachment

Extension to the extreme poses of the ROM

The muscle moments and the absolute errors are presented (Figure 5 and 6) in correspondence of the extreme skeletal poses, showing a general tendency towards smaller muscle moments than those calculated in the reference pose. The broad attachment muscles (*Gluteus Maximus, Gluteus Medius*, *Vastus Lateralis*, *Vastus Medialis*, *Adductor Magnus*) showed the highest mean values of muscle moments and absolute errors. For these muscles, the mean absolute errors ranged from 0.4 Nm for the *Gluteus Maximus* to 2.1 Nm for the *Vastus Medialis* (Fig. 6). The mean relative error was 36%, ranging from 13% to 63% (found for the *Gluteus Maximus* and *Vastus Medialis* respectively); overall, the muscles, excluding those whose absolute contribute was below 0.1 Nm (i.e. *Tibialis Anterior, Tibialis Posterior, Adductor Longus*), showed an average relative error of 42%, ranging from 13% to 75% (found for the *Gluteus Maximus* and *Gluteus Minimus* respectively). The variability of the muscle moments increased when

including the effect of the extreme poses in the ROM. Considering the broad attachment muscles, the ratio between the moment range and mean value was on average 165% and reached 290% for *Gluteus Medius*. Similarly, the ratio between the absolute error range and mean value was on average 145% and reached 200% for the *Adductor Magnus.*

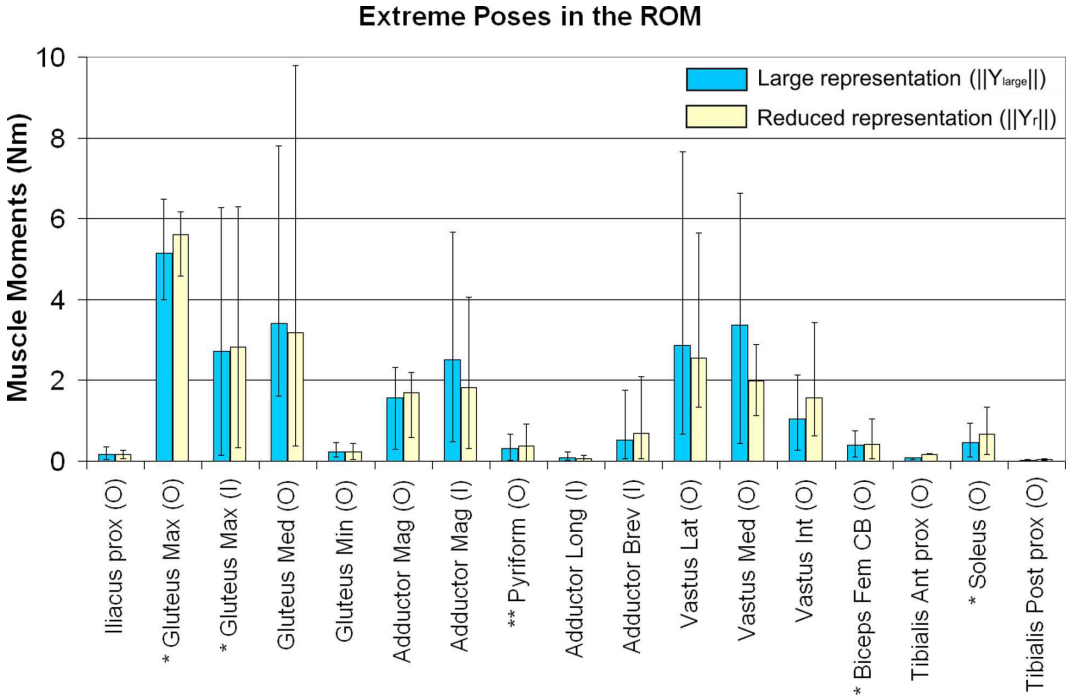

Figure 5 - Norm of muscle moments (||Ylarge|| and ||Yreduced||) presented as mean, minimum and maximum values in the extreme poses of the ROM (four muscle samples, except for: * two muscle samples, ** three muscle samples). A total of 40 skeletal poses were analysed: four samples (two sides per specimen) in 10 extreme poses (six at the hip, two at the knee, two at the ankle). The muscle moments were calculated with respect to the centroid of O = origin attachment, and I = insertion attachment

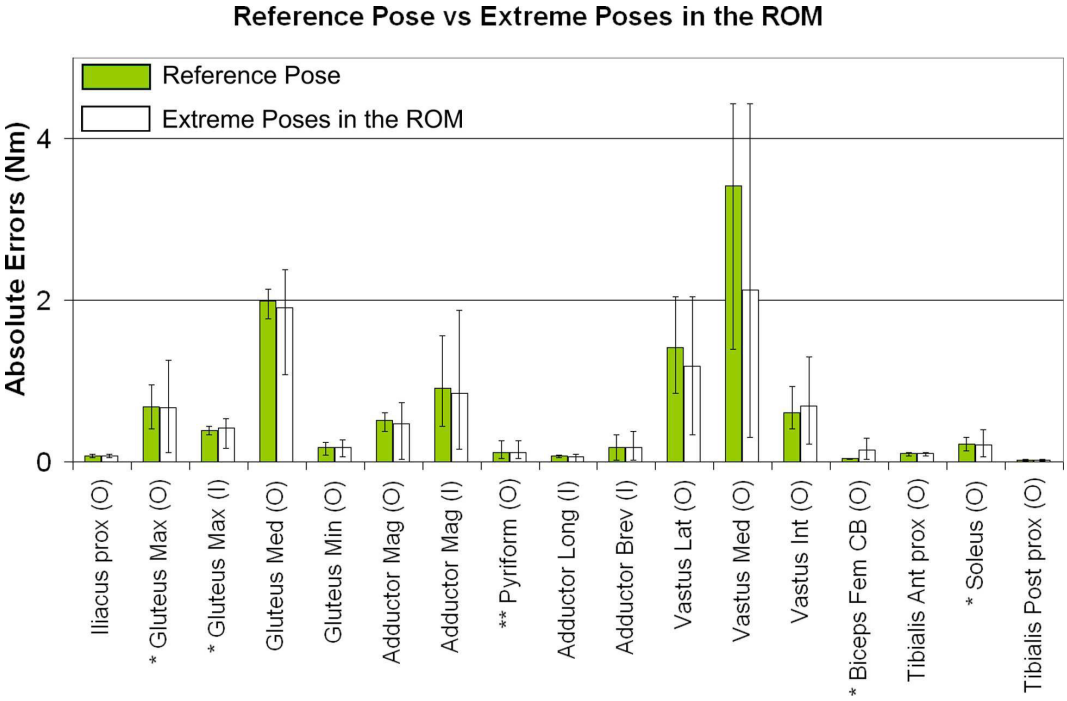

Figure 6 - Absolute errors (ea = ||Ylarge - Yreduced||) presented as mean, minimum and maximum values in the reference pose and in the extreme poses of the ROM (four muscle samples, except for: * two muscle samples, ** three muscle samples). A total of four skeletal poses were analysed in the reference pose, and 40 in the extreme poses of the ROM. The muscle moments were calculated with respect to the centroid of O = origin attachment, and I = insertion attachment

Discussion

In musculoskeletal models, the continuum muscle-tendon units are discretized to represent the muscle mechanical effect with lines of action attached to the bones. The influence of different types of muscle discretization on the mechanical effect of the lower limb muscles had not been addressed yet, particularly when varying the anatomy and the skeletal pose. Then the aim of the present study was to evaluate the error of a reduced muscle representation in reproducing the mechanical effect on the skeletal system, varying the musculoskeletal geometry and the model pose.

It was found that one muscle line of action per millimetre represented a good assumption to correctly reproduce the muscle mechanical effect on bones (Fig. 3), since the convergence was achieved for all muscles with a markedly lower line density. When passing from the large representation with the maximum line

density to the minimum representation (up to six lines of action), the error on the force vector was small in all cases ($e_{r,f} < 1\%$), confirming previous findings [19], while the errors on the muscle moments with respect to the centroid of the attachment areas could be significant. In particular, mean relative errors up to 75% were predicted, and even restricting the analysis to the muscles with broad attachment areas, the mean relative error remained above 30%. The calculated errors were found dependent on the individual anatomy and on the skeletal pose. The average increase of error variability due to the inclusion of the different skeletal poses was comparable to the original variability related only to the different anatomies. Thus it seems that both factors have similar role.

To the authors' knowledge, this is the first study addressing the influence of the discretization of the lower limb muscles on their mechanical effect. A similar study was proposed for a different anatomical district (i.e. the shoulder) on one specimen in a single reference pose [19]. That study shows that the broad attachment muscles are affected by the largest absolute errors (i.e. e_a) and lower relative errors (i.e. e_r), in accordance with the present findings. However, for the lower limbs, the relative errors were found higher than those reported for the shoulder. Indeed, e_r for the reference pose was up to 75%, with a mean value of 40%, while the errors for the shoulder muscles do not exceed 15%. Also the mean error for the broad attachment muscles (34%) was found to be significantly higher than the maximum value reported for the shoulder muscles. It was also shown a significant variability of the muscle moments and moment errors due to the different anatomies (Fig. 4 - 6), which take into account both intra-subject and inter-subject variability. This result appears consistent with the large range of muscle forces predicted with different models mimicking the same activity [31, 32], and with the observed wide anatomical variability for the femoral muscle attachments [20].

The present study is affected by some limitations. First, a uniform distribution of the muscle force over the vector $\boldsymbol{u}$ was assumed [19], supposing an even activation of each muscle over its entire volume. However, this methodological hypothesis allowed for separating the effect of independent activations, to study the effect of muscle discretization only. In addition, the adoption of the same

assumptions of the original method [19] allowed for a direct comparison of the results. Moreover, strategies for extrapolating the results to non-uniform distributions have been already discussed [19]. Second, via-points were included in few muscles (*Iliacus, Tibialis Anterior* and *Tibialis Posterior*); however, the adopted muscle paths have been previously used in musculoskeletal models and the inclusion of via-points would result in smaller moments and absolute errors. Last, data from two cadaver specimens were used, not representing a consistent sample size for a full characterisation of the error between large and reduced muscle representations. However, extending the study to more specimens, the error committed could only be equal or bigger, leaving unchanged the majority of the conclusions and highlighting the relevance of subject-specific modelling.

The presented results might have implications on the generation of musculoskeletal models. The calculated line densities of convergence correspond to an accurate number of muscle lines of action which is always larger than the reduced representation of each muscle (Table 1), and the reduced representation includes a number of elements larger than commonly adopted discretizations. Moreover, the line densities of convergence showed an important dependence on the single muscle and the pose considered (0.35±0.17 lines/mm), resulting in a variable number of lines of action needed. For instance, regarding the broad attachment muscles, the number of elements ranged from 21±2 (*Adductor Magnus*) to 35±9 (*Vastus Medialis*). Therefore, care should be taken in using the proposed error indication to identify the minimum number of muscle elements to be used, since different application (e.g. structural analyses of bone stresses and musculoskeletal models for the prediction of muscle forces during motion) may require different discretization levels. In fact, the choice of the point used for the calculation of the moment vectors is crucial for the computation of the errors. The choice of the centroid of the attachment areas as the reference point is the one that produces the highest relative errors, since it is the point producing the minimum moment vector for each muscle [19]. Further investigations will involve the calculation of the muscle moments with respect to the joint centres, in order to calculate an adequate muscle discretization suitable for applications of models for dynamic simulations of motion.

In conclusion, it was compared the mechanical effect of the lower limb muscles on bones produced by two muscle representations: a large discretization, i.e. one line of action per millimetre, correctly reproducing the muscle mechanical effect, and a reduced discretization, with a number of elements equal to the DOF that the muscle can influence independently. It was considered up to four anatomies in a reference skeletal pose and in the extreme poses of the ROM. It was found that the error committed using the reduced representation could be larger than that reported for the shoulder muscles [19], and it was dependent on the individual anatomy and the skeletal pose.

Ackowledgements

The present study was financially supported by the EU funded projects LHDL (reference 026932) and NMS Physiome (reference 248189). The authors wish to acknowledge Prof. Serge Van Sint Jan (Université Libre de Bruxelles, Belgium) for the dissection study of the cadaver specimens and Mauro Ansaloni (Istituto Ortopedico Rizzoli, Bologna, Italy) for the segmentation of the CT volumes.

References

1 **Erdemir, A., McLean, S., Herzog, W. and van den Bogert, A.J.** Model-based estimation of muscle forces exerted during movements. *Clin Biomech (Bristol, Avon)*, 2007, **22**(2), 131-154.

2 **Piazza, S.J.** Muscle-driven forward dynamic simulations for the study of normal and pathological gait. *J Neuroeng Rehabil*, 2006, **3**, 5.

3 **Hoy, M.G., Zajac, F.E. and Gordon, M.E.** A musculoskeletal model of the human lower extremity: the effect of muscle, tendon, and moment arm on the moment-angle relationship of musculotendon actuators at the hip, knee, and ankle. *J Biomech*, 1990, **23**(2), 157-169.

4 **Jonkers, I., Stewart, C. and Spaepen, A.** The study of muscle action during single support and swing phase of gait: clinical relevance of forward simulation techniques. *Gait Posture*, 2003, **17**(2), 97-105.

5 **Thelen, D.G., Anderson, F.C. and Delp, S.L.** Generating dynamic simulations of movement using computed muscle control. *J Biomech*, 2003, **36**(3), 321-328.

6 Higginson, J.S., Zajac, F.E., Neptune, R.R., Kautz, S.A. and Delp, S.L. Muscle contributions to support during gait in an individual with post-stroke hemiparesis. *J Biomech*, 2006, **39**(10), 1769-1777.

7 Kepple, T.M., Sommer, H.J., 3rd, Lohmann Siegel, K. and Stanhope, S.J. A three-dimensional musculoskeletal database for the lower extremities. *J Biomech*, 1998, **31**(1), 77-80.

8 Anderson, F.C. and Pandy, M.G. Dynamic optimization of human walking. *J Biomech Eng*, 2001, **123**(5), 381-390.

9 Delp, S.L., Loan, J.P., Hoy, M.G., Zajac, F.E., Topp, E.L. and Rosen, J.M. An interactive graphics-based model of the lower extremity to study orthopaedic surgical procedures. *IEEE Trans Biomed Eng*, 1990, **37**(8), 757-767.

10 Scheys, L., Van Campenhout, A., Spaepen, A., Suetens, P. and Jonkers, I. Personalized MR-based musculoskeletal models compared to rescaled generic models in the presence of increased femoral anteversion: effect on hip moment arm lengths. *Gait Posture*, 2008, **28**(3), 358-365.

11 Brand, R.A., Crowninshield, R.D., Wittstock, C.E., Pedersen, D.R., Clark, C.R. and van Krieken, F.M. A model of lower extremity muscular anatomy. *J Biomech Eng*, 1982, **104**(4), 304-310.

12 Heller, M.O., Bergmann, G., Deuretzbacher, G., Dürselen, L., Pohl, M., Claes, L., Haas, N.P. and Duda, G.N. Musculo-skeletal loading conditions at the hip during walking and stair climbing. *Journal of Biomechanics*, 2001, **34**(7), 883-893.

13 Besier, T.F., Gold, G.E., Beaupre, G.S. and Delp, S.L. A modeling framework to estimate patellofemoral joint cartilage stress in vivo. *Med Sci Sports Exerc*, 2005, **37**(11), 1924-1930.

14 Hicks, J., Arnold, A., Anderson, F., Schwartz, M. and Delp, S. The effect of excessive tibial torsion on the capacity of muscles to extend the hip and knee during single-limb stance. *Gait Posture*, 2007, **26**(4), 546-552.

15 Lenaerts, G., De Groote, F., Demeulenaere, B., Mulier, M., Van der Perre, G., Spaepen, A. and Jonkers, I. Subject-specific hip geometry affects predicted hip joint contact forces during gait. *J Biomech*, 2008, **41**(6), 1243-1252.

16 Jonkers, I., Sauwen, N., Lenaerts, G., Mulier, M., Van der Perre, G. and Jaecques, S. Relation between subject-specific hip joint loading, stress distribution in the proximal femur and bone mineral density changes after total hip replacement. *J Biomech*, 2008, **41**(16), 3405-3413.

17 Delp, S.L. and Loan, J.P. A graphics-based software system to develop and analyze models of musculoskeletal structures. *Comput Biol Med*, 1995, **25**(1), 21-34.

18 Horsman, K., Koopman, H.F.J.M., van der Helm, F.C.T., Prose, L.P. and Veeger, H.E.J. Morphological muscle and joint parameters for musculoskeletal modelling of the lower extremity. *Clinical Biomechanics*, 2007, **22**(2), 239-247.

19 Van der Helm, F.C. and Veenbaas, R. Modelling the mechanical effect of muscles with large attachment sites: application to the shoulder mechanism. *J Biomech*, 1991, **24**(12), 1151-1163.

20 Duda, G.N., Brand, D., Freitag, S., Lierse, W. and Schneider, E. Variability of femoral muscle attachments. *J Biomech*, 1996, **29**(9), 1185-1190.

21 Viceconti, M., Clapworthy, G. and Van Sint Jan, S. The Virtual Physiological Human - a European initiative for in silico human modelling. *J Physiol Sci*, 2008, **58**(7), 441-446.

22 Testi, D., Quadrani, P. and Viceconti, M. PhysiomeSpace: digital library service for biomedical data. *Philos Transact A Math Phys Eng Sci*, 2010, **368**(1921), 2853-2861.

23 Van der Helm, F.C., Veeger, H.E., Pronk, G.M., Van der Woude, L.H. and Rozendal, R.H. Geometry parameters for musculoskeletal modelling of the shoulder system. *J Biomech*, 1992, **25**(2), 129-144.

24 Walker, S.M. and Schrodt, G.R. I segment lengths and thin filament periods in skeletal muscle fibers of the Rhesus monkey and the human. *Anat Rec*, 1974, **178**(1), 63-81.

25 Taddei, F., Ansaloni, M., Testi, D. and Viceconti, M. Virtual palpation of skeletal landmarks with multimodal display interfaces. *Med Inform Internet Med*, 2007, **32**(3), 191-198.

26 Wu, G., Siegler, S., Allard, P., Kirtley, C., Leardini, A., Rosenbaum, D., Whittle, M., D'Lima, D.D., Cristofolini, L., Witte, H., Schmid, O. and Stokes, I. ISB recommendation on definitions of joint coordinate system of various joints for the reporting of human joint motion--part I: ankle, hip, and spine. International Society of Biomechanics. *J Biomech*, 2002, **35**(4), 543-548.

27 Tanavalee, A., Yuktanandana, P. and Ngarmukos, C. Surgical epicondylar axis vs anatomical epicondylar axis for rotational alignment of the femoral component in total knee arthroplasty. *J Med Assoc Thai*, 2001, **84 Suppl 1**, S401-408.

28 Lundberg, A., Svensson, O.K., Nemeth, G. and Selvik, G. The axis of rotation of the ankle joint. *J Bone Joint Surg Br*, 1989, **71**(1), 94-99.

29 Wu, G. and Cavanagh, P.R. ISB recommendations for standardization in the reporting of kinematic data. *J Biomech*, 1995, **28**(10), 1257-1261.

30 Boone, D.C. and Azen, S.P. Normal range of motion of joints in male subjects. *J Bone Joint Surg Am*, 1979, **61**(5), 756-759.

31 Xiao, M. and Higginson, J. Sensitivity of estimated muscle force in forward simulation of normal walking. *J Appl Biomech*, 2010, **26**(2), 142-149.

32 Cleather, D.I. and Bull, A.M. Lower-extremity musculoskeletal geometry affects the calculation of patellofemoral forces in vertical jumping and weightlifting. *Proc Inst Mech Eng H*, 2010, **224**(9), 1073-1083.

Chapter 4

Influence of lower-limb muscle discretization on the prediction of skeletal loads during walking

Giordano Valente[1,2], Saulo Martelli[1,3], Marco Viceconti[1,4], Fulvia Taddei[1]

[1] Laboratorio di Tecnologia Medica, Istituto Ortopedico Rizzoli, Bologna, Italy
[2] DIEM, University of Bologna, Italy
[3] Department of Mechanical Engineering, University of Melbourne, Australia
[4] Department of Mechanical Engineering, University of Sheffield, UK

Conference Proceedings published on The Proceedings of the 10th Symposium on Computational Methods in Biomechanics and Biomedical Engineering, 2012, ISBN: 978-0-9562121-5-3

Author contributions

G. Valente developed the models, performed simulations of gait, post-processed the results, created the figures, wrote the paper, designed the project
S. Martelli assisted with project design, model developments and writing the paper
M. Viceconti obtained funding, assisted with project design and writing the paper
F. Taddei obtained funding, assisted with project design, model developments and writing the paper

Abstract

Computational models of the musculoskeletal system represents the state-of -the-art for the prediction of skeletal loads during motion, and there is a growing need for understanding the sensitivity of model predictions to several parameters and assumptions involved. Modelling the musculotendon units as one-dinemsional actuators implies a discretization process, whose choice should rely on the modelling objectives; however the sensitivity of the muscle and joint forces to the muscle discretization has not been systematically assessed yet. The present study aims at evaluating the influence of the lower-limb muscle discretization, using a published discretization method and a subject-specific data collection. Different models with increasing discretization levels (up to an optimal model) were built and simulations of motion were run solving a traditional inverse dynamics and static optimization problem. The results showed that the errors on the peaks of joint contact forces might be significant (up to 14%) and with a tendency of force underestimation.

Introduction

Multibody-dynamics models of the musculoskeletal system have been widely used to assess skeletal loads or muscle functions in normal and pathological conditions (1,2). The use of such models represents the only viable solution for the prediction of muscle forces during movement, since it is not feasible to obtain in-vivo measurements with non-invasive means. In the past few years, there has been a markedly growing use of computational models in combination with different methods for muscle-force estimates (3), making necessary the knowledge of the reliability of the models in terms of accuracy of the estimates. Since only indirect validation of model predictions can be performed, it is important to understand the sensitivity of model predictions to the several parameters assumed in the modelling process.

Focusing on the lower-limb system, several models with different muscle discretizations, i.e. the number of muscle actuators discretizing the muscle-tendon units, have been used for biomechanics investigations, implying different modelling and computational complexity (4). The choice of the discretization

should rely on the objective of research and clinical application, however no conclusive sensitivity study has been performed on the lower-limb muscles. Only one study was found to analyze the predicted muscle forces perturbing the number of model actuators (5): the results showed that the muscles could achieve the same force pattern but different magnitude, but the discretization method was there based on heuristic choices. Therefore the influence of the muscle discretization on the prediction of the loads acting on the skeletal system still represents an important issue to be investigated in order to give more insights into the sensitivity of musculoskeletal models.

In a published study (4), using a discretization method based on a mechanical standpoint, it has been shown how the loading transferred to bones is affected by the lower-limb muscle discretization, depending on the individual anatomy and skeletal pose. However this method has not been applied to models for dynamic simulation of motion and thus the influence of different discretization levels on models predictions has not been assessed yet.

Therefore, the present study aims at applying the previously published method (4) to calculate an optimal muscle discretization of the lower limbs, and use it in a subject-specific model for the prediction of skeletal loads during walking, to then compare the results with those obtained through models with an increasing muscle discretization level.

Materials and Methods

Data collection

The musculoskeletal models were developed from a detailed multiscale data collection, publicly available at www.physiomespace.com. The lower-limb dataset includes bone segments and muscle anatomies (further details on (4)), while gait analysis data from a body-matched volunteer include 3D motion, ground reaction forces and lower-limb muscle activities (further details on (6)).

The musculoskeletal models

The base skeletal model used in this study was previously developed and validated (6): it consists of a 7-segment, 10-degree-of-freedom system, articulated

by a ball-and-socket joint at the hip, and a hinge joint at both knee and ankle, where the definition of the joint parameters was based on skeletal anatomical landmarks identified on the skeletal surfaces and following the ISB standards (Fig. 1).

A total of five musculoskeletal models were built with different muscle discretization. The first model (*Mod1*) included one line of action per muscle (resulting in 68 muscle elements), the last one (*Mod5*) included an optimal number of lines of action (resulting in 344 muscle elements) as defined in the following paragraph. The other models included a 25% increase of each muscle lines of action from the coarser to the most refined discretization. The maximum isometric force that each muscle could exert was defined from each muscle physiological cross sectional area (PCSA), assuming the tetanic muscle stress (TMS) equal to 1 N/mm^2 (7).

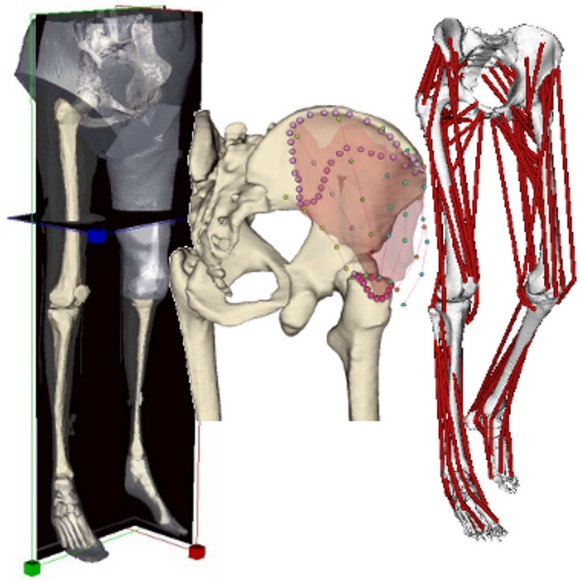

Figure 1 - One of the musculoskeletal models built from the subject-specific data collection

Lower-limb muscle discretization

In the *Mod1* model, each muscle attachment area was discretized with its centroid. For the optimal model (*Mod5*), a discretization method was applied (4), which allowed to discretize the muscle attachment areas according to their shapes, locate

an arbitrary number of line of actions and calculate the generalized force vectors with respect to a chosen point. In the present study, the number of lines of action were computed for each muscle such that the muscle moments with respect to the corresponding joint center reached convergence, in a reference pose and in the extreme poses of the range of motion of normal walking. For each muscle, the maximum value between the poses was chosen for the model. For the intermediate models (i.e. *Mod2, Mod3, Mod4*), the muscles were discretized with the same method such to have a 25% increase of each muscle lines of action from the coarser to the most refined discretization.

Skeletal load calculations

Simulations of one cycle of normal walking were run with the different models, solving a traditional inverse dynamics and static optimization problem using the OpenSim software (8), to calculate muscle and joint contact forces during motion. The calculated forces (F) obtained with the different muscle discretization models were normalized in terms of gait cycle and body weight, and analyzed in correspondence of the peaks of joint contact loads, calculating the errors between the optimal model (i.e. maximum discretization level) and the other models with increasing discretization level:

$$(F_{Mod5} - F_{Mod\,i})/F_{Mod5} \quad [1]$$

where i = 1,2,3,4.

Results

Muscle discretization

The gluteals and the vastus medialis were the muscles that required more lines of action to reach convergence (Fig. 2). The majority of muscles required only one line of action to be modelled.

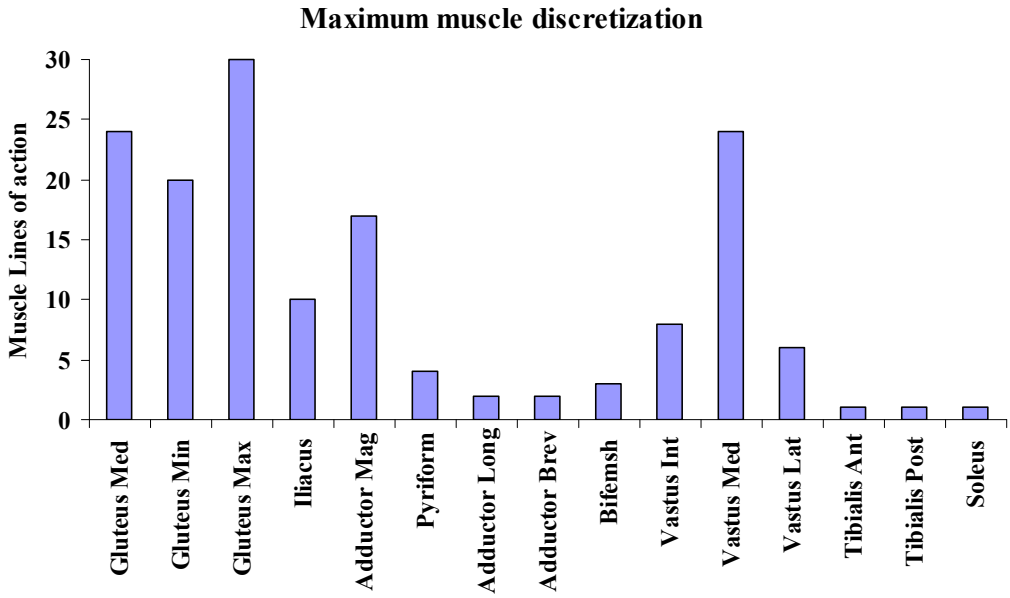

Figure 2 - Number of lines of action necessary to model the major lower-limb muscles, corresponding to the elements such that the exerted moments reached convergence in the poses of the range of motion of normal walking

Influence on the skeletal loads

The patterns of the calculated joint contact forces (i.e. hip, knee and ankle forces) during the gait cycle were the same using *Mod2* to *Mod5* models. Particularly, the force peaks were achieved at the same instant of gait cycle. Exception was found with the coarser discretization model (*Mod1*), where the force patterns slightly differed and showed the force peaks at different instants of gait. The relative errors on the force peaks could be up to 14% and decreased with the increasing discretization level (Fig. 3). The errors were more marked in the knee and hip forces, while the ankle force errors did not exceed 1%.

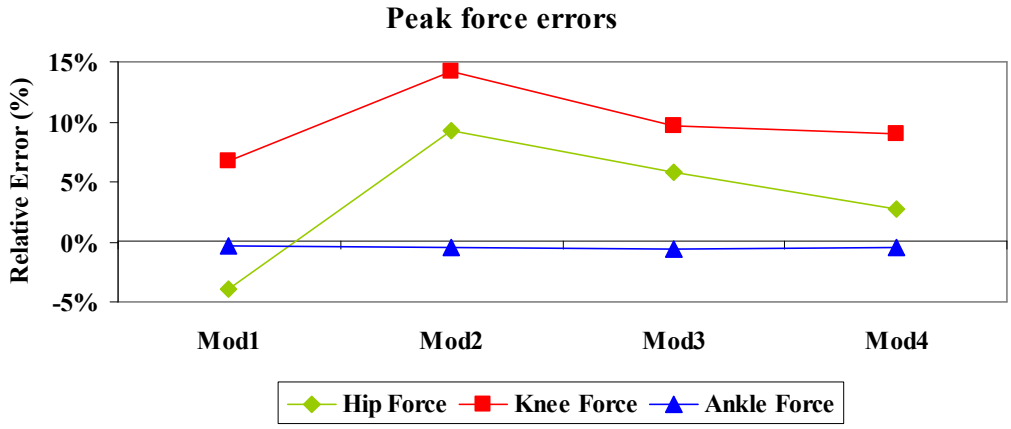

Figure 3 - Relative errors on the peaks of joint contact forces with respect to the values calculated with the most refined muscle discretization model (Mod5)

Discussion

The present study gives insights into the sensitivity of skeletal load predictions to the lower-limb muscle discretization in subject-specific computational models.

The most refined discretization model, calculated with a previously published method [4], presented a number of muscle lines of action markedly larger than those commonly used in such models, with increased modelling and computational complexity.

When predicting joint contact forces during walking, and assuming the most refined model as the most accurate, the hip and knee peak forces were predicted with significant errors (up to 14%), and a tendency of force underestimation was shown. The ankle force errors were markedly lower, since for all muscles spanning the ankle only one line of action was necessary to model them. The coarser model (i.e. one line of action per muscle) was the only predicting different force patterns, suggesting the need of more refined discretizations particularly for broad attachment muscles.

The major limitations of the study were: first, the small sample size of motion trials (one subject and one gait cycle), thus it is planned to extend it to more gait trials and motion tasks; second, not all muscles included via-points in the line-of-action model, and this might affect the calculation of force magnitudes, particularly for major muscles such gluteus maximus and vasti.

In conclusion, this work might help improving the reliability of musculoskeletal models, moving a further step towards the assessment of the sensitivity to the several parameters involved in the modelling and simulation process.

References

1. Piazza S. J., Muscle-driven forward dynamic simulations for the study of normal and pathological gait, Journal of neuroengineering and rehabilitation, 2006, 3: 5
2. Erdemir A., McLean S., Herzog W., van den Bogert A. J., Model-based estimation of muscle forces exerted during movements, Clin Biomech (Bristol, Avon), 2007, 22(2): 131–154.
3. Lin Y.-C., Dorn T. W., Schache A. G., Pandy M. G., Comparison of different methods for estimating muscle forces in human movement, Proceedings of the Institution of Mechanical Engineers, Part H: Journal of Engineering in Medicine, 2012, 226(2): 103-112
4. Valente G., Martelli S., Taddei F., Farinella G., Viceconti M., Muscle discretization affects the loading transferred to bones in lower-limb musculoskeletal models, Proceedings of the Institution of Mechanical Engineers, Part H: Journal of Engineering in Medicine, 2012, 226(2): 161–169
5. Xiao M., Higginson J., Sensitivity of estimated muscle force in forward simulation of normal walking, Journal of applied biomechanics, 2010, 6(2): 142–149
6. Martelli S., Taddei F., Cappello A., van Sint Jan S., Leardini A., Viceconti M., Effect of sub-optimal neuromotor control on the hip joint load during level walking. Journal of biomechanics, 2011, 44(9): 1716–21
7. Glitsch U., Baumann W., The three-dimensional determination of internal loads in the lower extremity. J Biomech., 1997, 30(11-12): 1123–31.
8. Delp S. L., Anderson F. C., Arnold A. S., Loan P., Habib A., John C. T., et al., OpenSim: open-source software to create and analyze dynamic simulations of movement, IEEE transactions on bio-medical engineering, 2007, 54(11): 1940–50

Chapter 5

Influence of weak hip abductor muscles on joint contact forces during normal walking: a probabilistic modeling analysis

Giordano Valente[1,2], Fulvia Taddei[1], Ilse Jonkers[3]

[1] Laboratorio di Tecnologia Medica, Istituto Ortopedico Rizzoli, Bologna, Italy
[2] Department of Industrial Engineering, University of Bologna, Italy
[3] Department of Biomedical Kinesiology, K.U. Leuven, Belgium

Journal article under review at Journal of Biomechanics, 2012

Author contributions

G. Valente developed the models, performed simulations of gait, post-processed the results, created the figures, wrote the paper, assisted with project design and management

F. Taddei obtained funding, assisted with project design and management and writing the paper

I. Jonkers assisted with project design and management, model developments, and writing the paper

Abstract

The weakness of hip abductor muscles is related to lower-limb joint osteoarthritis, and joint overloading may increase the risk for disease progression. The relation between muscle strength, structural joint deterioration and joint loading makes the latter an important parameter in the study of onset and follow-up of the disease. Since the relation between hip abductor weakness and joint loading still remains an open question, the purpose of this study was to adopt a probabilistic modelling approach to give insights into how the weakness of hip abductor muscles affects ipsilateral joint contact forces during walking, while tracking normal gait kinematics. A generic musculoskeletal model was scaled to each healthy subject included in the study, and the maximum force-generating capacity of each hip abductor muscle in the model was perturbed to evaluate how a broad distribution of muscle dysfunction affected the joint contact forces of the ipsilateral lower limb. In general, we found that the muscular system was able to compensate for abductor weakness. The reduced force-generating capacity of the abductor muscles affected joint contact forces, increasing the risk of overloading at the hip and knee joints, with more marked implication of the latter. The predicted joint loads were found to be most sensitive to gluteus medius weakness, particularly the anterior compartment, focusing the attention of future research on loading condition analysis with clinical data and strength training programs.

Keywords

Musculoskeletal modeling, Dynamic simulations, Monte-Carlo analysis, Weak abductor muscles, Joint contact forces

Introduction

Mechanical factors related to joint loading constitute a major cause in the development and progression of osteoarthritis (OA) (Lafeber et al., 2006). Excessive joint loading during normal daily activities and obesity, in conjunction with local joint vulnerabilities, are confirmed risk factors in the etiopathogenesis of OA, particularly at the hip and knee joints (Felson, 2004). The weakness of hip abductor muscles was related to joint OA in the lower limb: the level of gluteus medius atrophy was found to correlate significantly to radiographic signs of hip OA in both ipsilateral and contralateral legs (Amaro et al., 2007). Significant weakness of hip abductors was also observed in knee OA subjects (Costa et al., 2010; Hinman et al., 2010), although the causal relation between muscle weakness and disease onset could not be established. Hip abductor muscle action prevents joint instability and consequent musculoskeletal overloading during gait (Amaro et al. 2007), and abductor weakness in the support limb is known to induce excessive pelvis drop towards the contralateral limb (Trendelenburg sign). This pelvis instability was extensively documented in patients with hip OA and after total joint replacement (Beaulieu et al., 2010; Madsen et al., 2004; Jandrić, 1997). Likewise, hip abductor weakness was related to excessive medial tibiofemoral compartment loading with consequent risk for disease progression in knee OA patients (Mündermann et al., 2005; Chang et al., 2005), and was found to contribute to functional limitations of patients with total knee arthroplasty (Piva et al., 2011). The suggested relation between muscle strength, articular loading and structural deterioration makes joint loading a relevant parameter in the detection of onset and follow-up of degenerative joint disease in the lower limb (Wilson et al., 2006; Wu et al., 2000). However, joint loading cannot be easily studied in-vivo. The only direct way to measure joint contact forces in-vivo implies the use of instrumented prostheses. This approach is, however, limited to a few subjects and is representative of a post-operative situation. Alternatively, computer models of the musculoskeletal system in combination with dynamic simulations of motion, have been increasingly used (Pandy and Andriacchi, 2010; Erdemir et al., 2007) to calculate joint contact forces, providing a valuable approach to joint

loading analyses in-vivo (Lenaerts et al., 2009; Steele et al., 2011; Taddei et al., 2012).

To the authors' knowledge, the relation between the weakness of hip abductor muscles and the lower-limb joint contact forces was not extensively studied. Lenaerts et al., 2008 used a subject-specific model with halved force-generating capacity of the hip abductor muscles to calculate the hip contact forces during walking using inverse dynamics and static optimization methods. Compared to the normal force-generating capacity model, an increased activation up to the maximal was found for these muscles, but changes in the hip contact forces were not confirmed. In a more recent study, van der Krogt et al., 2012 analyzed the effect of local muscle weakness on gait impairment and muscle forces during walking, using a scaled generic musculoskeletal model and the Computed Muscle Control (CMC) algorithm (Thelen and Anderson, 2006). They concluded that gait was most impaired when hip abductors and ankle plantarflexors were weakened in the model.

However, none of the above studies provided a complete overview on the relation between hip abductor weakness and lower-limb joint loading. Lenaerts et al., 2008 limited their analysis on hip contact forces in one subject and one gait trial, and did not analyze the effect on knee contact forces; in the second study (van der Krogt et al., 2012), muscle weakness was not related to joint contact forces. In addition, no studies were found that included a structured approach to analyze how weakness of the individual compartments of hip abductor muscles correlated with altered joint loading.

Therefore, the aim of the present study was to evaluate the effect of weakness of the different compartments of the hip abductor muscles on joint contact forces of the ipsilateral lower limb, in unaltered normal gait conditions. To address this question, simulations of gait of healthy adult subjects were first generated using a generic musculoskeletal model with representative muscle strength. Then, a probabilistic modelling approach was adopted performing a Monte-Carlo analysis. This allowed to evaluate the effect of a broad distribution of reduced maximum force-generating capacity of each hip abductor muscle on joint contact forces, while imposing the normal gait kinematics to be tracked. The statistical analysis

of the results was focused on the gait instants of maximum joint loads, particularly relevant for overloading risk and osteoarthritis degenerative process.

Materials and Methods

Human experiments

Five healthy male subjects (age: 26 ± 2 yrs; mass: 82 ± 10 kg; height: 182 ± 2 cm) gave informed consent to participate in this study, approved by the local institutional research board. The subjects were fitted with markers for 3D motion capturing, merging the Plug-in-gait (Davis et al., 1991) and the MOCAP (Software for interactive musculoskeletal modelling (SIMM), Motion Analysis Corp., Santa Rosa, USA) marker sets. After a static trial, the subjects were asked to walk at a self-selected speed along the 10 meter walkway in a straight line. Throughout all trials, kinematics were measured at 100 Hz using a Vicon system (Oxford Metrics, Oxford, UK). In a pre-processing phase, the marker coordinates were filtered and smoothed using Woltring's quintic spline routine (Woltring, 1986), implemented in Workstation (Vicon Workstation 5.2 beta 20, Oxford Metrics). Ground reaction forces were measured at 1000 Hz using two AMTI force plates (Advanced Mechanical Technology Inc., Watertown, MA) embedded in the walkway. Surface electromyography (EMG) signals of major lower-limb muscles (i.e. gluteus maximus, rectus femoris, vastus lateralis, biceps femoris long head, semimembranosus, tibialis anterior, gastrocnemius) were recorded at 1000 Hz using a wireless EMG device (Aurion, Italy). EMG data were rectified, bi-directionally low-pass filtered at 6 Hz, and normalized to the peak values of predicted muscle activations (van der Krogt et al., 2012).

Baseline gait simulations

A generic musculoskeletal model (Delp et al., 1990) with 10 rigid bodies, 23 degrees of freedom and 92 muscle-tendon actuators was scaled to match each subject's dimensions and inertial properties, using the experimentally measured position of markers placed on anatomical landmarks and body mass during standing trials. For a representative trial of each subject, OpenSim (Delp et al., 2007) was used to generate and analyze simulations of walking using the scaled

models. Inverse kinematics and Residual Reduction Algorithm (RRA) (Delp et al., 2007) were used in conjunction with the measured marker trajectories and ground reaction forces and moments to enforce dynamic consistency. Then CMC (Thelen and Anderson, 2006) was used to calculate the optimal muscle excitations that generated the necessary joint moments to track the kinematics produced by RRA. The lower-limb joint contact forces were calculated using the Joint Reaction analysis (Steele et al., 2011). To test the accuracy of the simulations, predicted muscle activations were compared with the experimental EMG recordings (Figure 1). In general, a satisfactory agreement was found.

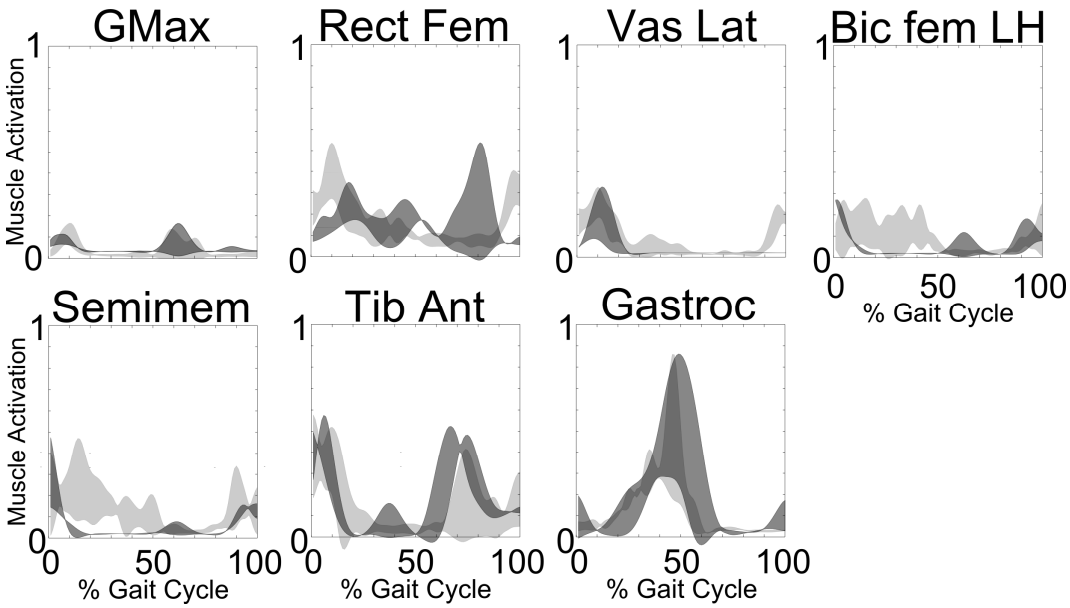

Figure 1 - Comparison between standard deviations of muscle activations predicted with the baseline model (dark gray areas) and experimental EMG recordings (light gray areas), for the muscles of which EMG was available. Data were averaged over five subjects. EMG data were rectified, bi-directionally low-pass filtered at 6 Hz, and normalized to the peak values of predicted muscle activations.

Perturbed gait simulations

A Monte-Carlo analysis was performed to evaluate the sensitivity of joint contact forces to the weakness of hip abductor muscles. Seven stochastic input variables were defined, i.e. the maximum isometric force of each muscle actuator modelling the hip abductors of the ipsilateral leg, including gluteus medius anterior

(GMedA), middle (GMedM) and posterior (GMedP), gluteus minimus anterior (GMinA), middle (GMinM) and posterior (GMinP), and tensor fascia latae (TFL). The effect of the stochastic input variables was evaluated on the following stochastic output variables: 12 joint contact force variables, i.e. antero-posterior (F_x), proximo-distal (F_y) medio-lateral (F_z) components of the ipsilateral hip, knee and ankle joint contact forces, and their respective magnitudes (F).

Each input variable was randomly sampled with a uniform distribution between zero and the maximum isometric force values in the baseline model (Delp et al., 1990). A Latin Hypercube Sampling strategy was applied to perform the Monte-Carlo simulations, generating an efficient distribution of the input variable values (see Appendix). For each set of generated sample values, a corresponding musculoskeletal model with the altered set of maximum isometric forces was created. Consequently, new CMC solutions were calculated with the resulting modified models that aimed to track the original kinematics. Normal gait kinematics was considered successfully tracked if the difference in all joint angles between perturbed and baseline simulations did not exceed one degree (Thelen and Anderson, 2006; van der Krogt et al., 2012). If normal gait kinematics could be achieved, further statistical analyses were performed on the output variables. The models were free to adopt any muscle force values within the imposed maximum force-generating capacity. Finally, subsequent Joint Reaction analyses calculated the perturbed joint contact forces.

A convergence analysis showed that 200 simulations ensured that mean and standard deviation values of the variables reached convergence, being the relative variation of the values across the last 10% of the simulations below 5% of the final step values. Approximately 250-hour computation time was needed to run a total of 1000 simulations (200 per subject) on a common desktop computer.

Statistical analysis

Simulation results confirmed the typical double-peaked curves during the gait cycle for the total hip and knee joint contact forces, and one-peaked curve for the ankle (Figure 2). Further data analysis therefore focused on the gait instants of maximum total joint contact forces, i.e. two instants of maximum hip and knee

force magnitude, and the instant of maximum ankle force magnitude. All force values were normalized to body weights (BW).

Normal gait kinematics could not be successfully tracked in 1.5% of the perturbed simulations at the instants of maximum total joint contact forces. In these cases, the corresponding calculated forces were not included in the following analysis.

To assess the variations in joint contact forces induced by the perturbed strength of the hip abductor muscles, mean, standard deviation (std) and coefficient of variation (CV = 100 x std/mean) of the perturbed output variables were calculated over all simulations.

To evaluate how the perturbed values of joint contact forces differed from the baseline values, the relative mean differences in the output variables between the perturbed and the baseline simulations were calculated and presented as statistical distributions.

Finally, to quantify the sensitivity of the output variables to the perturbed abductor muscle strength, a correlation analysis was performed between all input and output variables, evaluating the Pearson's correlation coefficients (r) and the corresponding p-values. Only significant correlation coefficients ($p < 10^{-4}$) are reported in the results section.

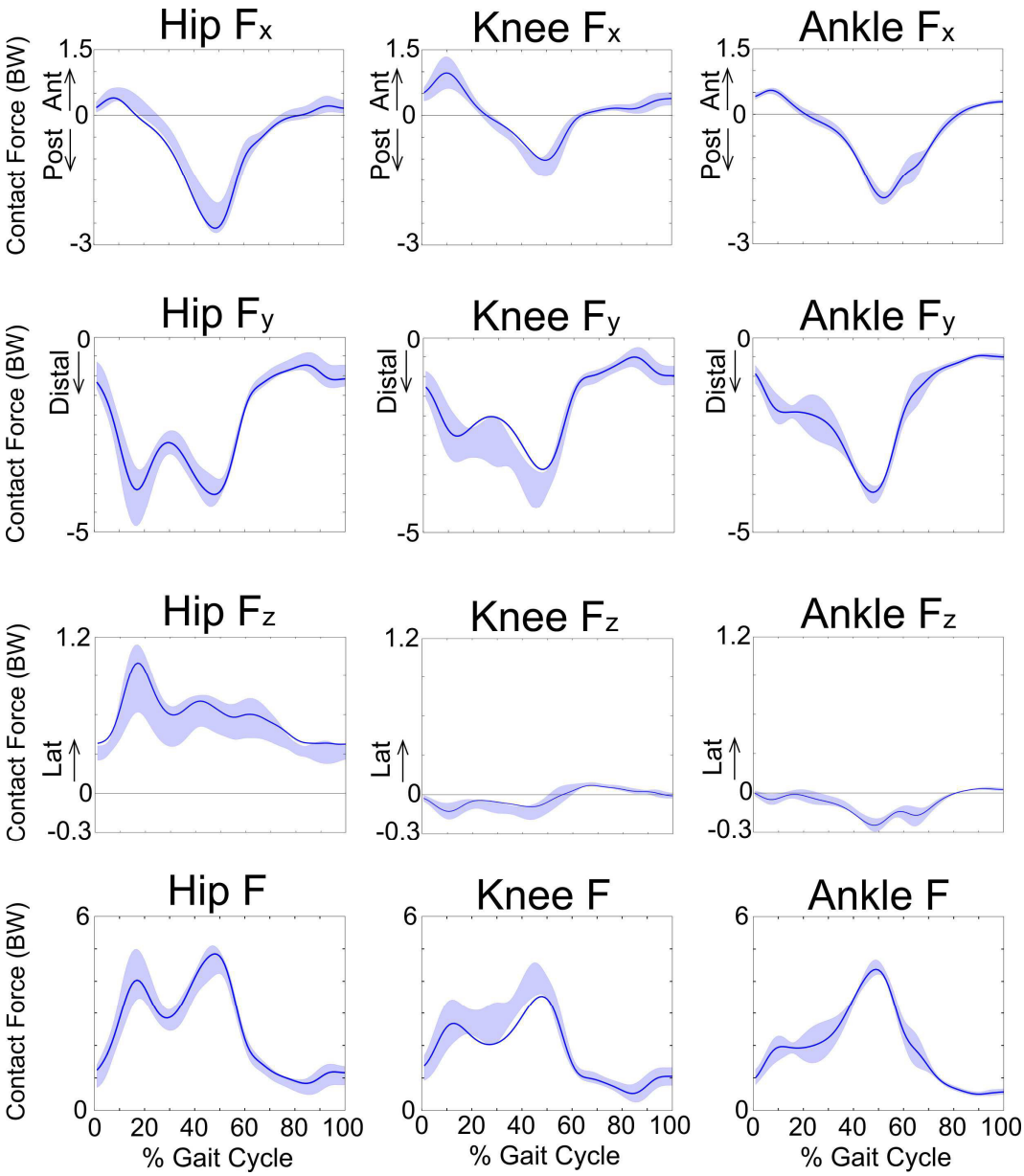

Figure 2 - Variation in the components of the calculated joint contact forces (BW) following the statistical perturbation of the hip abductor muscles strength in the simulated gait cycle. The curves show the standard deviations of the perturbed simulations (shaded area), run within the Monte Carlo analysis, compared to the baseline simulation (solid line). The values were averaged over five subjects. Force components are: antero-posterior (Fx), proximo-distal (Fy), medio-lateral (Fz) and magnitude (F)

Results

Perturbation of the maximum isometric force of the hip abductor muscles induced variations in all joint contact force components during walking (Figure 2). Marked sensitivity of hip and knee contact forces was predicted at the instants of maximum force magnitude (Table 1). Particularly, CV = 18.3% and 19.4% was found respectively for hip and knee force magnitude in their first force peak, while it was less marked at the ankle. The induced variations in all knee load components were slightly larger than hip load components (Table 1).

In the first force peak, the hip and knee contact force components tended to increase, except for the lateral hip component and the anterior knee component (Figure 3): the maximum mean differences in joint force magnitudes were 20% at the hip (50th percentile = 4%) and 55% at the knee (50th percentile = 9%). Conversely, the second peak hip forces decreased, whereas knee forces increased (Figure 3): the maximum mean differences in joint force magnitudes were -12% at the hip (50th percentile = -4%) and 50% at the knee (50th percentile = 14%). In general, knee force components differed more compared to the hip force components. The peak ankle forces tended to increase with less marked effect (maximum mean difference = 6%)

The correlation analysis results are reported in Table 2. Overall, the weakness of gluteus medius compartments, particularly that of GMedA, was most correlated to the joint contact forces. Conversely, the weakness of the other abductor compartments was less correlated, and GMinA and GMinM did not show any significant correlations with the output variables.

Table 1 - Variation in the perturbed joint contact forces induced by the abductor muscle weakness during the Monte Carlo simulations: descriptive statistics parameters (mean, std and CV) at the peaks of hip, knee and ankle joint force magnitude expressed in BW. Force components are: antero-posterior (Fx), proximo-distal (Fy), medio-lateral (Fz) and magnitude (F).

1st Peak	Hip				Knee			
Force Component	***Fx***	***Fy***	***Fz***	**F**	***Fx***	***Fy***	***Fz***	**F**
Mean (BW)	*0.27*	*-4.11*	*0.88*	4.21	*0.77*	*-2.66*	*-0.11*	2.78
Std (BW)	*0.20*	*0.74*	*0.26*	0.77	*0.26*	*0.49*	*0.06*	0.54
CV	*73.4%*	*18.0%*	*29.7%*	18.3%	*34.0%*	*18.3%*	*54.7%*	19.4%
2nd Peak	**Hip**				**Knee**			
Force Component	***Fx***	***Fy***	***Fz***	**F**	***Fx***	***Fy***	***Fz***	**F**
Mean (BW)	*-2.35*	*-3.94*	*0.59*	4.64	*-1.14*	*-3.88*	*-0.13*	4.05
Std (BW)	*0.36*	*0.35*	*0.13*	0.45	*0.20*	*0.45*	*0.06*	0.49
CV	*15.3%*	*8.9%*	*21.9%*	9.7%	*17.3%*	*11.7%*	*47.9%*	12.0%
Peak	**Ankle**							
Force Component	***Fx***	***Fy***	***Fz***	**F**				
Mean (BW)	*-1.80*	*-4.00*	*-0.26*	4.40				
Std (BW)	*0.18*	*0.21*	*0.05*	0.23				
CV	*9.9%*	*5.2%*	*20.1%*	5.2%				

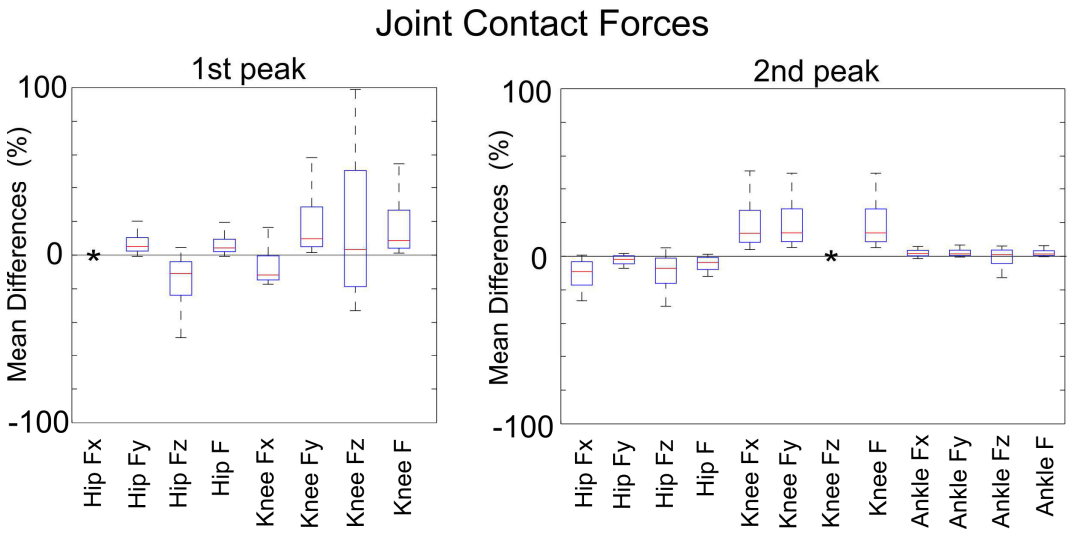

Figure 3 - Deviations in the perturbed joint contact forces from the baseline simulations. Box plots of the relative mean differences (%) between the results of the perturbed simulations and the baseline simulation, averaged over five subjects. (*) neglected since the baseline absolute values were below 0.1 BW (see Figure 2). The box plots represent the statistical distribution of the dependent variables: red horizontal bar is 50th percentile (median), upper and lower edges are 75th and 25th percentiles, and upper and lower bars are maximum and minimum values. Red crosses are outliers, if any. Force components are: antero-posterior (Fx), proximo-distal (Fy), medio-lateral (Fz) and magnitude (F)

Table 2 - Correlation analysis of input and output variables at the instants of peaks of joint contact force magnitudes. The table shows the statistically significant (p < 104) coefficients (r) between muscle weakness of individual hip abductors (columns) and the joint contact force components (rows). Positive correlation implies that the weaker the muscle, the higher the output quantity (taken with sign).

1st force peak of Joint Contact Magnitudes								
		GMedA	GMedM	GMedP	GMinA	GMinM	GMinP	TFL
Joint Contact Forces	Hip Fx (+Ant)	0.69	0.42	-	-	-	-	-
	Hip Fy (+Prox)	-0.4	-	-	-	-	-0.3	-0.44
	Hip Fz (+Lat)	-	-0.44	-0.6	-	-	-0.4	-
	Hip F	0.46	-	-	-	-	0.27	0.42
	Knee Fx (+Ant)	0.56	0.36	-	-	-	-	-
	Knee Fy (+Prox)	-0.65	-0.39	-	-	-	-	-
	Knee Fz (+Lat)	-0.59	-	-	-	-	-	0.7
	Knee F	0.64	0.36	-	-	-	-	-

2nd force peak of Joint Contact Magnitudes								
		GMedA	GMedM	GMedP	GMinA	GMinM	GMinP	TFL
Joint Contact Forces	Hip Fx (+Ant)	0.79	0.45	-	-	-	-	-0.28
	Hip Fy (+Prox)	0.84	0.37	-	-	-	-	-0.4
	Hip Fz (+Lat)	-	-0.35	-0.64	-	-	-0.42	-
	Hip F	-0.81	-0.43	-	-	-	-	0.33
	Knee Fx (+Ant)	-0.64	-0.47	-0.34	-	-	-	-
	Knee Fy (+Prox)	-0.62	-0.47	-0.36	-	-	-	-
	Knee Fz (+Lat)	-0.68	-0.45	-0.31	-	-	-	0.28
	Knee F	0.62	0.47	0.36	-	-	-	-
	Ankle Fx (+Ant)	0.28	-	-	-	-	-	0.29
	Ankle Fy (+Prox)	-	-	-	-	-	-	-
	Ankle Fz (+Lat)	0.58	0.35	-	-	-	-	-
	Ankle F	-	-	-	-	-	-	-

Discussion

Weak hip abductor muscles can induce joint overloading and hence the risk of disease progression in osteoarthritis subjects. To our knowledge, this is the first study investigating how the weakness of hip abductor muscles is related to lower-limb joint contact forces. We adopted a probabilistic modelling approach performing a Monte-Carlo analysis, to evaluate the sensitivity of the joint contact force components to perturbation of the force-generating capacity of the ipsilateral abductor muscle compartments during normal walking. We perturbed the maximum isometric force of the abductor muscles using an efficient strategy (Latin Hypercube Sampling) that enabled to uniformly sample the range of reduced maximum force-generating capacity of the abductors, in order to simulate a wide spectrum of muscle dysfunction. In the perturbed simulations, the baseline

kinematics was forced to be tracked but was allowed to change in case the dynamic equilibrium was not satisfied. The analysis was mainly focused on the gait instants of maximum total joint contact forces, particularly relevant in the context of detecting overloading risk.

The perturbed simulations revealed how the muscular system was able to compensate for weakness of the hip abductor muscles, under the assumption of optimal conditions of motor control strategy in the calculation of the optimal muscle excitations (Thelen and Anderson, 2006). That is, the normal gait kinematics could be successfully tracked after changes in compensatory muscle excitations (Figure 4). Indeed, among the perturbed simulations in the peaks of joint contact force magnitudes, the deviations in joint angles from the baseline simulations did not exceed one degree, with few exceptions of unsuccessful kinematics tracking (1.5% of the perturbed simulations) regarding some joint degrees of freedom (Figure 4). These cases were, however, excluded from statistical analyses.

We found that the weakness of hip abductor muscles affected joint contact forces during normal walking, particularly at the hip and knee joints, leading to an overall increase of joint loading (Figure 2). At the first force peak, the hip force magnitude tended to increase (50th percentile mean difference = 4%), with an increase in the distal and medial components (Figure 3). Conversely, at the second peak, the hip force magnitude tended to decrease (50th percentile mean difference = -4%), due to a decrease in all force components. The effect on the knee was even more pronounced (Figure 3): at both force peaks, the knee force magnitude tended to increase with a more marked effect on the second peak (50th percentile mean difference = 14%). All knee force components, except for the anterior component at the first peak, tended to increase.

The concurrent increase in the first hip and knee force peaks was due to the synergistic action of flexor and extensor muscles of the hip and knee joints (Figure 5). This might be explained by the marked compensatory action of the anterior and middle compartments of gluteus maximus, compensating for the weak abductors. As a result, their action as hip extensors increased, requiring an increase in the hip flexor force induced by the rectus femoris to restore muscular

balance at the hip joint in the sagittal plane. The knee extensor action of the rectus femoris induced a compensatory increase of the knee flexors. During the second force peak, the abductor muscle weakness led to a decrease in hip contact force and an increase in knee contact force. The hip abductor weakness was mainly compensated by a decrease in iliopsoas force, and to restore normal hip flexor moment balance, the rectus femoris activity increased. However, to maintain balance at the knee, a compensatory increase in biceps femoris and gastrocnemius forces was predicted (Figure 5). This decreased the loading of the hip, but simultaneously induced a marked overloading of the knee. These observed compensatory changes in muscle forces, underlying the changes in joint contact forces, are in agreement with previous findings on muscle compensation strategy for muscle weakness (van der Krogt et al., 2012), calculated using the same generic model (Delp et al., 1990).

The correlation analysis (Table 2) revealed that gluteus medius, and particularly the anterior compartment, constituted a key factor in the hip and knee loading conditions, while gluteus minimus had a marginal role. Weakness of anterior gluteus medius significantly correlated with all hip and knee forces (except for the lateral hip component), playing a main role in the patterns of the perturbed joint contact forces.

This is the first study evaluating the influence of weak hip abductor muscles on joint loading with a probabilistic approach, therefore a direct comparison of the results with the literature was not possible. However, the observed muscle compensation strategies due to the abductor weakness, are in agreement with the findings presented in van der Krogt et al., 2012, where same patterns of muscle forces are shown for weak abductor compensation. As such, this agreement indirectly confirms the reliability of the variations in joint contact forces, since they are directly related to the muscle forces acting on the corresponding joints. In general, the variations in hip contact forces were in contrast with the unchanged hip forces due to halved abductor force-generating capacity found in Lenaerts et al., 2008. However, different models and simulation approaches were used.

There are limitations affecting the results presented in this study. First, the gait analysis data used to perform the gait simulations were measured on healthy

young subjects, who may not be representative of a population with risk for osteoarthritis. However, to separate the effects, the purpose was to investigate how and to what extent hip abductor weakness could affect joint loads without altering normal gait. Second, the state-of-the-art generic musculoskeletal model (Delp et al., 1990) includes a 1 degree-of-freedom planar joint at the knee (Yamaguchi and Zajac, 1989), which may represent an oversimplification when analyzing the calculated components of knee contact forces. Future studies should investigate the use of more complex knee models to confirm the results here presented.

Our results denote the importance of normal abduction function in preventing hip and knee joint overloading, with possible implications in osteoarthritis subjects. The weakness of gluteus medius, particularly the anterior compartment, may increase the risk for disease progression. We found a more marked risk of joint overloading at the knee, that highlights how weak hip abductor muscles represent a relevant action mechanism contributing to progression of osteoarthritis at the knee joint, even more than the hip. This insight strengthens the relevance of strength training protocols for the gluteus medius, with particular focus on the anterior compartment.

In conclusion, this study used a probabilistic modelling approach to give insights into how the weakness of hip abductor muscles affects joint contact forces during walking, while tracking normal gait. In general, we found that the muscular system was able to compensate for abductor weakness. Lower-limb joint contact forces were affected, and risk of overloading was found at the hip and knee, with more marked implication of the latter. The loading conditions were found to be mostly sensitive to gluteus medius weakness, particularly the anterior compartment, focusing the attention of future research on loading condition analysis with clinical data and strength training programs.

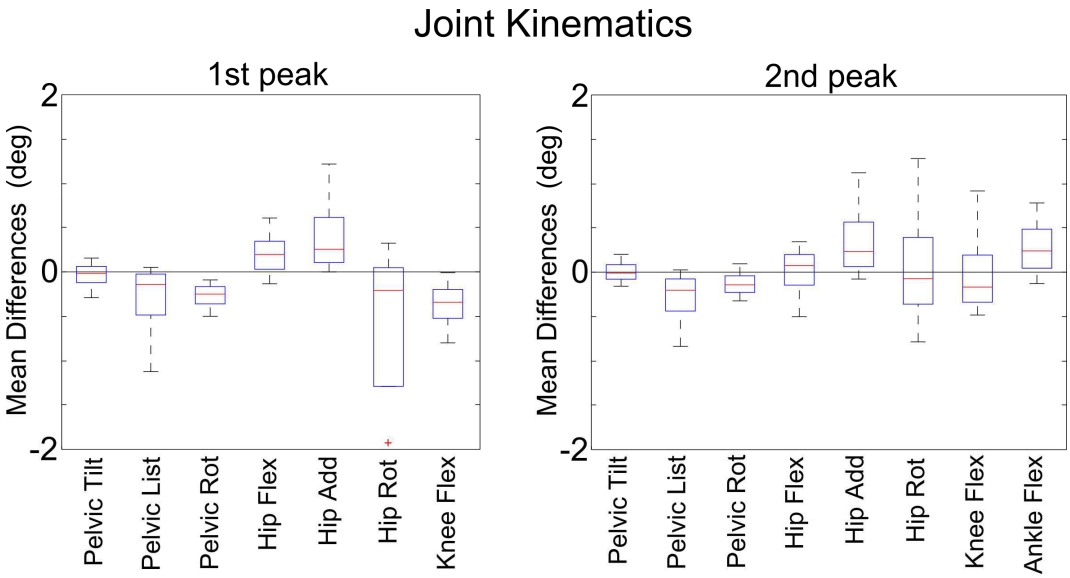

Figure 4 - Deviations in joint kinematics from the baseline simulations. Box plots of the mean differences (deg) between the results of the perturbed simulations and the baseline simulation, averaged over five subjects. The box plots represent the statistical distribution of the dependent variables: red horizontal bar is 50th percentile (median), upper and lower edges are 75th and 25th percentiles, and upper and lower bars are maximum and minimum values. Red crosses are outliers, if any. Differences not exceeding one degree are negligible

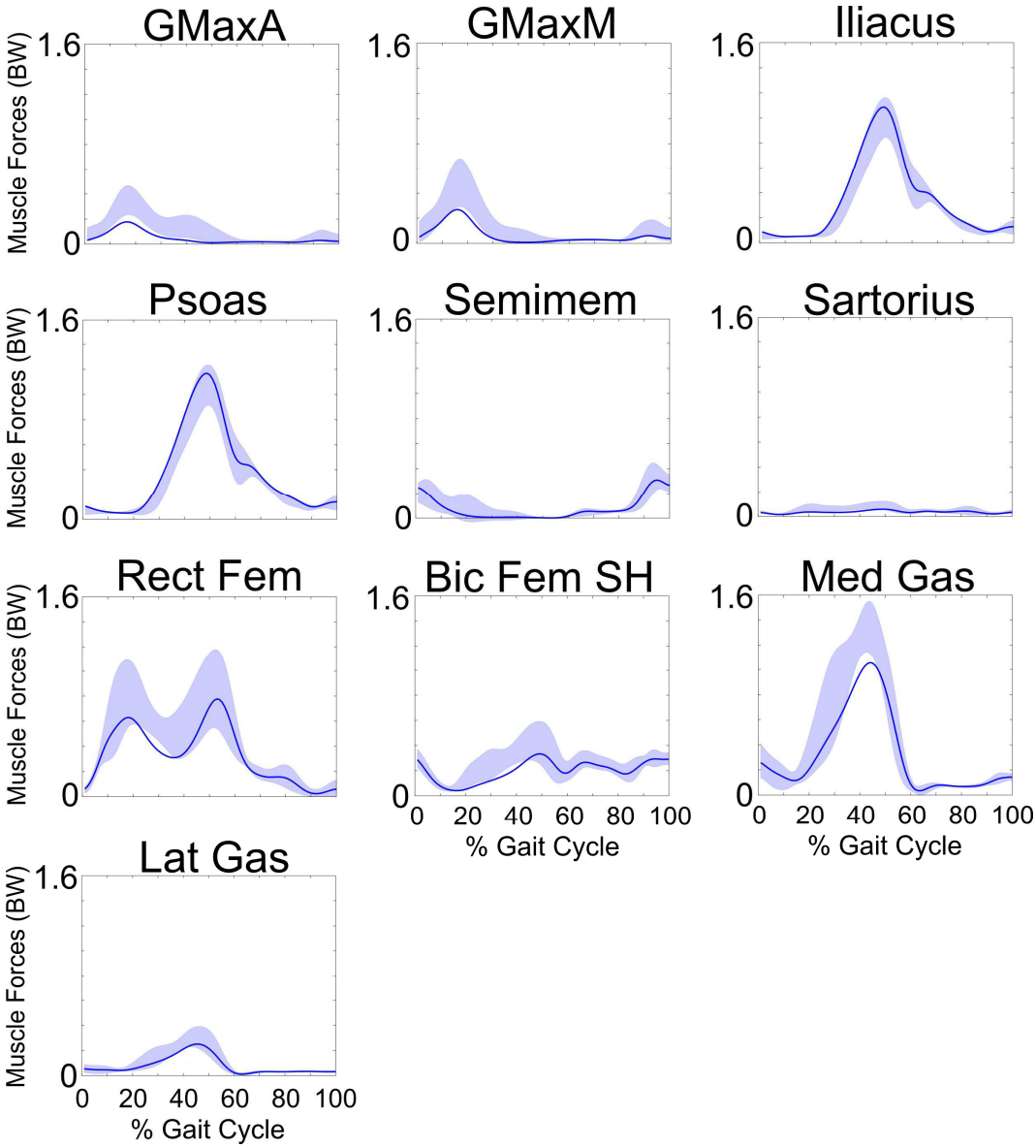

Figure 5 - Variations in major muscle forces (BW) induced by perturbing the maximum force-generating capacity of the hip abductor muscles in the simulated gait cycle. The curves show the standard deviations of the perturbed simulations (shaded area), run within the Monte Carlo analysis, compared to the baseline simulation (solid line). The values were averaged over five subjects. Abbreviations: Gluteus Maximus Anterior (GMaxA), Gluteus Maximus Middle (GMaxM), Iliacus (Iliacus), Psoas (Psoas), Semimembranosus (Semimem), Sartorius (Sartorius), Rectus Femoris (Rect Fem), Biceps Femoris Short Head (Bic Fem SH), Medial Gastrocnemius (Med Gas), Lateral Gatrocnemius (Lat Gas)

Conflict of interest statement

None of the authors had financial or personal conflict of interest that could inappropriately influence this study.

Acknowledgements

This study was supported by the NMS Physiome project (grant 248189) funded by the European Union. The authors gratefully thank Christophe Meyer (University Hospital Pellenberg, Belgium) for the gait analysis data and Davide Monari (K.U. Leuven, Belgium) for the productive discussions on implementation of the modelling framework.

Appendix

Supplementary data

Table A1. Baseline values of maximum isometric forces of hip abductor muscles

Maximum Isometric Forces of hip abductor muscles (N)						
GMedA	GMedM	GMedP	GMinA	GMinM	GMinP	TFL
819	573	653	270	285	323	233

Table A2. Stochastic input variables uniformly sampled with the latin hypercube strategy, used in the corresponding perturbed models

	Maximum Isometric Forces of hip abductor muscles (N)						
	GMedA	GMedM	GMedP	GMinA	GMinM	GMinP	TFL
Set 1	742.0	12.5	566.7	35.3	239.9	181.5	185.8
Set 2	475.4	122.1	117.2	258.4	158.0	183.5	114.8
Set 3	470.4	547.8	131.9	247.1	124.4	127.6	50.2
Set 4	254.2	30.0	106.2	170.5	109.6	290.3	26.4
Set 5	566.6	351.4	255.7	212.5	112.4	278.3	90.3
Set 6	155.2	452.8	637.7	156.8	271.3	262.3	35.0
Set 7	207.7	521.8	118.7	21.8	89.3	9.1	208.5
Set 8	546.5	353.7	408.0	199.8	245.6	188.7	9.4
Set 9	651.3	41.2	417.7	12.1	121.5	69.4	0.9
Set 10	688.1	69.9	299.3	225.6	123.1	319.1	157.7
Set 11	142.7	222.9	151.7	174.7	0.4	285.6	78.5
Set 12	192.6	297.1	154.6	234.9	15.3	36.0	119.2
Set 13	196.7	139.0	543.9	185.6	188.5	135.1	183.6

Set 14	534.5	437.7	356.5	264.0	134.0	240.9	224.1
Set 15	459.5	387.2	92.3	96.1	132.7	149.0	195.9
Set 16	163.2	285.9	156.8	100.9	75.4	113.7	194.5
Set 17	301.3	214.2	99.5	255.8	26.6	65.9	167.7
Set 18	418.0	182.9	459.3	71.7	277.3	216.5	209.7
Set 19	807.6	116.8	584.1	216.6	13.3	316.1	143.7
Set 20	229.5	253.7	262.5	155.5	228.6	21.1	195.5
Set 21	284.0	251.2	288.0	196.1	138.5	240.3	49.6
Set 22	241.5	518.8	632.0	180.1	143.4	185.1	24.3
Set 23	123.5	67.5	251.1	5.1	234.8	297.0	123.2
Set 24	377.0	111.2	129.7	107.1	220.8	283.2	203.6
Set 25	439.5	326.9	312.9	122.7	204.1	4.6	31.1
Set 26	181.2	553.0	426.8	14.0	129.4	33.8	139.6
Set 27	795.5	339.7	423.0	16.7	154.8	118.3	198.8
Set 28	498.0	102.8	341.1	242.0	96.1	202.9	151.3
Set 29	410.9	569.4	377.2	260.7	69.5	252.5	151.6
Set 30	486.6	336.9	206.1	113.4	161.5	307.8	130.4
Set 31	246.9	178.8	452.1	144.8	248.7	292.9	222.6
Set 32	814.8	466.2	225.5	239.5	68.2	63.0	209.2
Set 33	203.6	84.2	20.8	60.8	98.6	48.6	116.4
Set 34	712.3	407.7	94.8	23.5	136.7	126.3	56.7
Set 35	61.0	308.8	456.3	228.1	254.7	137.7	64.4
Set 36	311.9	88.5	327.6	49.8	72.3	31.0	31.7
Set 37	541.8	446.1	5.6	5.6	156.0	99.5	65.8
Set 38	494.2	414.5	1.1	182.9	35.5	150.8	59.8
Set 39	729.1	322.5	572.4	27.2	238.8	2.3	135.3
Set 40	667.3	147.5	280.6	179.3	259.2	121.9	88.5
Set 41	673.9	200.3	123.2	205.8	71.1	73.8	42.8
Set 42	739.6	494.9	577.2	39.6	218.3	107.8	143.2
Set 43	480.1	129.5	180.7	124.2	193.4	105.9	190.8
Set 44	815.7	169.0	183.3	3.2	27.6	238.7	172.7
Set 45	19.7	183.6	253.5	65.7	5.8	265.2	128.5
Set 46	174.1	281.5	513.3	167.3	263.0	243.9	18.8
Set 47	587.9	10.1	468.0	110.0	40.3	311.6	155.4
Set 48	472.4	559.9	538.7	187.4	201.3	275.3	80.3
Set 49	513.1	400.4	164.5	91.6	140.5	288.9	67.7
Set 50	594.8	256.5	433.0	188.7	141.6	55.2	52.7
Set 51	146.3	97.5	506.3	9.3	118.1	142.1	168.6
Set 52	361.7	571.4	310.2	55.1	185.3	93.6	46.0
Set 53	701.7	161.8	485.0	260.5	180.7	87.3	124.7
Set 54	707.8	19.4	488.4	115.2	65.2	187.3	10.8
Set 55	454.1	76.0	89.9	181.9	171.3	218.5	54.9
Set 56	427.9	301.9	461.1	50.6	184.6	195.8	192.9
Set 57	413.8	270.2	436.5	202.9	38.8	167.1	18.1

Set 58	531.0	526.0	493.7	47.9	211.8	56.7	226.5
Set 59	489.0	397.2	579.6	177.5	58.0	51.8	4.3
Set 60	281.6	266.5	9.7	234.3	86.9	50.7	92.3
Set 61	697.2	243.4	237.8	26.8	237.0	25.6	184.6
Set 62	768.8	324.1	59.7	118.1	241.6	198.3	161.2
Set 63	432.0	215.1	595.9	6.9	49.2	201.6	54.4
Set 64	386.2	378.8	335.8	75.8	165.9	192.1	39.4
Set 65	745.7	91.4	619.2	21.2	273.5	298.6	41.4
Set 66	614.4	434.7	193.9	245.4	231.8	84.6	206.9
Set 67	677.5	368.6	139.8	126.1	33.1	27.6	201.8
Set 68	638.3	562.5	611.4	84.2	221.3	104.4	189.0
Set 69	671.0	62.6	652.2	146.6	190.8	42.9	169.3
Set 70	48.1	106.8	274.5	25.4	233.5	169.6	111.7
Set 71	803.3	363.5	38.3	67.6	95.3	19.5	87.3
Set 72	85.0	95.5	72.6	133.5	226.6	207.2	89.1
Set 73	733.8	27.2	521.8	149.7	42.1	253.6	57.9
Set 74	408.5	312.9	446.4	56.5	90.3	45.6	162.0
Set 75	356.6	496.5	225.0	215.8	151.4	98.0	96.7
Set 76	600.5	103.4	438.9	240.8	100.4	58.7	197.7
Set 77	523.4	484.5	17.4	85.6	115.3	83.6	148.2
Set 78	93.2	208.2	442.3	78.2	20.5	133.6	85.2
Set 79	128.5	393.4	28.0	32.5	276.3	189.5	171.7
Set 80	403.5	423.5	265.6	104.3	93.9	159.0	47.9
Set 81	465.4	5.6	412.5	190.7	280.6	277.1	63.0
Set 82	389.7	539.4	562.6	112.0	223.5	94.3	124.0
Set 83	611.9	448.4	641.1	210.8	230.6	305.6	199.5
Set 84	399.1	113.2	336.5	218.8	257.6	110.5	62.2
Set 85	680.1	309.7	58.1	232.2	177.7	273.7	22.1
Set 86	375.6	132.9	216.4	228.3	270.3	41.0	212.7
Set 87	435.1	44.1	149.4	217.6	224.8	226.9	158.9
Set 88	70.6	358.5	146.5	201.8	170.6	48.3	98.4
Set 89	27.1	244.1	282.1	67.3	52.9	220.1	222.1
Set 90	423.6	342.1	125.9	116.9	11.8	211.6	146.9
Set 91	106.2	558.2	517.6	141.6	54.8	67.3	116.7
Set 92	556.7	492.1	379.8	98.5	56.7	232.6	91.0
Set 93	210.8	140.7	196.7	17.6	163.6	91.5	145.2
Set 94	537.3	469.8	103.3	238.5	267.8	229.5	83.2
Set 95	761.9	428.3	46.8	214.3	79.9	225.4	112.0
Set 96	327.1	160.0	292.5	173.7	209.9	214.1	174.8
Set 97	644.7	217.8	13.6	99.3	103.2	261.3	13.2
Set 98	383.0	470.7	176.9	165.2	197.6	237.2	52.2
Set 99	339.8	259.3	364.8	252.4	256.3	86.7	149.5
Set 100	23.2	230.7	491.0	169.0	215.7	234.6	232.9
Set 101	89.4	532.7	540.1	220.6	277.9	157.0	188.3

Set 102	136.0	15.2	187.6	136.5	206.4	204.0	101.7
Set 103	518.8	372.3	522.8	160.2	150.7	12.9	29.2
Set 104	444.2	515.5	87.3	79.0	264.5	108.5	163.3
Set 105	171.3	537.1	570.3	89.0	24.1	164.9	230.1
Set 106	771.5	544.1	84.5	45.7	282.6	266.8	191.3
Set 107	3.0	347.2	591.2	207.0	110.6	142.1	118.3
Set 108	799.9	226.9	615.0	265.5	2.9	193.2	136.3
Set 109	275.6	502.2	272.7	51.4	181.8	124.8	130.5
Set 110	287.7	463.7	601.9	94.3	84.6	13.4	1.3
Set 111	309.4	135.6	504.3	12.2	8.3	77.2	95.1
Set 112	52.9	333.7	213.4	69.5	243.1	80.3	69.4
Set 113	244.8	123.3	396.6	209.6	169.3	171.7	105.7
Set 114	221.5	201.6	399.2	207.9	45.9	102.6	16.6
Set 115	527.6	527.7	161.5	194.0	47.2	301.0	204.0
Set 116	13.0	64.6	62.1	37.2	260.3	136.9	215.6
Set 117	657.1	47.5	551.1	58.8	118.7	222.6	47.1
Set 118	344.0	298.5	430.6	158.3	106.5	271.6	174.1
Set 119	761.3	292.0	260.8	108.2	73.3	299.2	6.8
Set 120	686.1	392.1	450.4	93.0	191.2	14.6	153.9
Set 121	585.1	440.7	321.9	250.9	235.7	124.2	76.4
Set 122	692.2	79.1	34.5	204.7	127.8	271.0	127.9
Set 123	352.2	175.2	384.1	134.9	203.3	280.8	66.5
Set 124	54.2	118.0	621.1	266.6	261.6	160.7	217.0
Set 125	250.5	174.6	233.0	142.6	104.8	264.5	39.7
Set 126	62.0	279.6	346.8	130.7	132.0	210.1	110.3
Set 127	179.8	144.6	228.8	253.5	16.3	7.9	228.7
Set 128	784.6	56.1	199.3	267.4	194.2	258.3	12.0
Set 129	367.5	382.0	113.6	184.0	149.0	304.3	121.0
Set 130	291.6	565.5	512.2	154.6	198.9	312.1	219.7
Set 131	321.7	33.5	314.4	150.0	213.6	303.1	61.4
Set 132	131.4	331.1	303.3	164.6	82.6	164.4	213.5
Set 133	634.0	2.8	475.0	63.8	164.9	117.3	228.0
Set 134	502.6	318.1	70.1	30.1	153.4	75.6	72.4
Set 135	191.9	483.7	209.4	172.0	58.9	37.9	84.1
Set 136	621.9	51.3	135.5	80.8	125.5	208.5	59.0
Set 137	4.6	7.5	645.2	223.3	65.6	154.0	214.9
Set 138	218.8	194.3	76.2	125.1	19.3	72.5	33.0
Set 139	34.6	500.0	350.2	140.2	227.7	96.3	179.6
Set 140	757.0	265.5	471.7	254.9	4.6	169.5	225.3
Set 141	578.0	372.6	371.1	236.4	268.2	60.6	71.6
Set 142	791.9	544.6	629.7	82.3	145.7	248.0	231.5
Set 143	334.4	54.3	419.3	1.0	107.2	268.1	160.2
Set 144	305.0	195.6	586.8	163.3	51.1	139.2	44.6
Set 145	166.2	225.6	590.8	243.8	9.0	39.6	103.8

Set 146	188.1	59.0	330.6	193.0	77.7	22.8	211.2
Set 147	572.3	425.3	368.2	82.5	176.4	153.2	181.7
Set 148	355.8	163.5	530.8	42.9	148.1	112.4	15.5
Set 149	109.8	451.5	546.3	106.5	281.0	227.8	36.8
Set 150	68.6	246.4	191.5	195.3	63.9	308.6	82.2
Set 151	39.2	506.2	464.5	231.6	173.6	69.9	75.6
Set 152	753.3	402.0	142.4	47.1	167.2	146.0	165.6
Set 153	119.2	459.4	647.5	118.8	28.7	17.2	43.9
Set 154	573.5	411.0	43.4	71.1	32.0	130.9	7.9
Set 155	448.4	238.7	625.4	38.7	37.5	130.6	8.9
Set 156	661.4	364.8	241.5	222.7	138.0	155.5	5.4
Set 157	43.7	128.4	354.8	73.8	199.6	291.3	22.7
Set 158	725.2	552.6	501.4	44.5	17.8	179.5	178.8
Set 159	80.4	418.3	51.4	62.8	130.1	1.0	107.9
Set 160	101.9	357.6	345.4	248.7	52.7	5.2	99.7
Set 161	787.1	432.5	634.0	53.1	195.5	29.3	132.2
Set 162	776.5	204.7	478.6	16.1	251.2	320.9	186.8
Set 163	781.2	315.5	480.3	75.5	274.9	322.1	33.8
Set 164	563.5	304.6	374.2	112.4	284.3	25.9	134.3
Set 165	298.5	234.4	497.0	198.6	2.4	175.1	146.3
Set 166	261.5	150.8	599.5	89.7	44.8	115.7	133.0
Set 167	589.9	35.9	389.2	132.2	76.4	78.1	96.5
Set 168	94.4	286.6	167.3	56.9	113.4	18.8	140.9
Set 169	116.4	157.1	31.4	269.5	43.9	161.9	25.5
Set 170	458.4	272.6	404.2	225.1	250.4	101.1	171.1
Set 171	723.9	476.6	294.5	256.8	208.0	205.9	156.9
Set 172	10.8	188.0	552.0	190.3	115.5	313.8	153.4
Set 173	213.7	237.2	172.0	103.9	36.1	119.6	138.6
Set 174	397.2	377.0	40.3	143.5	144.0	199.7	205.6
Set 175	151.3	534.4	11.6	176.0	244.9	231.2	221.2
Set 176	77.1	25.4	268.3	2.0	82.8	245.9	218.8
Set 177	341.3	345.0	219.5	151.6	101.5	63.1	20.2
Set 178	263.2	443.4	410.8	101.6	174.5	250.3	121.3
Set 179	640.3	190.9	607.7	262.2	60.6	223.9	164.3
Set 180	608.3	276.2	391.8	10.4	247.6	294.5	176.4
Set 181	157.5	93.8	53.8	40.9	61.6	35.1	200.4
Set 182	228.1	489.1	323.6	138.3	31.0	287.1	27.3
Set 183	369.6	21.2	66.6	29.2	98.2	147.4	182.3
Set 184	605.3	457.6	319.5	35.0	214.1	173.4	141.7
Set 185	505.0	292.7	110.4	246.0	252.7	242.9	28.6
Set 186	650.4	169.1	204.4	87.3	208.5	53.8	113.6
Set 187	236.0	81.0	559.1	230.0	78.9	11.2	103.6
Set 188	628.1	480.3	385.8	161.0	187.5	259.5	177.2
Set 189	623.3	511.2	359.8	168.6	120.6	176.9	3.4

Set 190	269.9	518.3	80.6	32.2	178.4	82.0	70.6
Set 191	716.9	152.1	285.6	95.1	22.3	144.2	77.1
Set 192	316.2	37.6	607.0	128.9	24.5	194.0	38.0
Set 193	509.9	261.2	175.9	127.0	182.7	90.0	73.8
Set 194	329.9	386.0	25.7	197.4	10.2	250.8	108.6
Set 195	112.8	72.8	304.7	135.4	158.9	179.0	106.1
Set 196	551.6	211.9	533.8	121.4	160.1	215.1	14.1
Set 197	714.5	417.1	247.5	60.7	91.3	282.4	94.1
Set 198	558.9	474.7	556.7	148.4	217.4	317.2	126.7
Set 199	29.4	406.4	528.4	152.8	88.3	44.6	80.5
Set 200	271.1	509.5	244.7	19.0	265.2	255.5	100.7

References

Amaro, A., Amado, F., Duarte, J.A., Appell, H.J., 2007. Gluteus medius muscle atrophy is related to contralateral and ipsilateral hip joint osteoarthritis. International Journal of Sports Medicine 28(12):1035-9.

Beaulieu, M.L., Lamontagne, M., Beaulé, P.E., 2010. Lower limb biomechanics during gait do not return to normal following total hip arthroplasty. Gait & Posture 32(2):269-73.

Chang, A., Hayes, K., Dunlop, D., Song, J., Hurwitz, D., Cahue, S., Sharma, L., 2005. Hip abduction moment and protection against medial tibiofemoral osteoarthritis progression. Arthritis and Rheumatism 52(11):3515-9.

Costa, R.A., de Oliveira, L.M., Hiroko Watanabe, S., Jones, A., Natour, J., 2010. Isokinetic assessment of the hip muscles in patients with osteoarthritis of the knee. Clinics 65(12):1253-1259.

Davis, R.B., Õunpuu, S., Tyburski, D., Gage, J.R., 1991. A gait analysis data collection and reduction technique. Human Movement Science 10(5):575-587.

Delp, S.L., Anderson, F.C., Arnold, A.S., Loan, P., Habib, A., John, C.T., Guendelman, E., Thelen, D.G., 2007. OpenSim: open-source software to create and analyze dynamic simulations of movement. IEEE Transactions on Biomedical Engineering 54, 1940–1950.

Delp, S.L., Loan, J.P., Hoy, M.G., Zajac, F.E., Topp, E.L., Rosen, J.M., 1990. An interactive graphics-based model of the lower extremity to study orthopaedic surgical procedures. IEEE Transactions on Biomedical Engineering 37(8):757-67.

Erdemir, A., McLean, S., Herzog, W., van den Bogert, A.J., 2007. Model-based estimation of muscle forces exerted during movements. Clinical Biomechanics (Bristol, Avon) 22(2):131-154.

Felson, D.T., 2004. Obesity and vocational and avocational overload of the joint as risk factors for osteoarthritis. Journal of Rheumatology 31(70):2-5.

Hinman, R.S., Hunt, M.A., Creaby, M.W., Wrigley, T.V., McManus, F.J., Bennell, K.L., 2010. Hip muscle weakness in individuals with medial knee osteoarthritis. Arthritis Care & Research 62(8):1190-3.

Jandrić, S., 1997. Muscle parameters in coxarthrosis. Medicinski pregled 50(7-8):301-4.

Lafeber, F.P.J.G., Intema, F., Van Roermund, P.M., Marijnissen, A.C.A., 2006. Unloading joints to treat osteoarthritis, including joint distraction. Current opinion in rheumatology 18(5):519-25.

Lenaerts, G., De Groote, F., Demeulenaere, B., Mulier, M., Van der Perre, G., Spaepen, A., Jonkers, I., 2008. Subject-specific hip geometry affects predicted hip joint contact forces during gait. Journal of Biomechanics 41(6):1243-1252.

Lenaerts, G., Mulier, M., Spaepen, A., Van der Perre, G., Jonkers, I., 2009. Aberrant pelvis and hip kinematics impair hip loading before and after total hip replacement. Gait & Posture 30(3):296-302.

Madsen, M.S., Ritter, M.A., Morris, H.H., Meding, J.B., Berend, M.E., Faris, P.M., Vardaxis, V.G., 2004. The effect of total hip arthroplasty surgical approach on gait. Journal of Orthopaedic Research 22(1):44-50.

Mündermann, A., O' Dyrby, C., Andriacchi, T.P., 2005. Secondary gait changes in patients with medial compartment knee osteoarthritis: increased load at the ankle, knee, and hip during walking. Arthritis and Rheumatism 52(9):2835-44.

Pandy, M.G, Andriacchi., T.P., 2010. Muscle and joint function in human locomotion. Annual Review of Biomedical Engineering 12:401-433.

Piva, S.R., Teixeira, P.E.P., Almeida, G.J.M., Gil, A.B., DiGioia III, A.M., Levison, T.J., Kelley Fitzgerald, G., 2011. Contribution of hip abductor strength to physical function in patients with total knee arthroplasty. Physical Therapy 91(2):225-33.

Steele, K.M., DeMers M.S., Schwartz, M.H., Delp, S.L., 2011. Compressive tibiofemoral force during crouch gait. Gait & Posture 35(4):556-60.

Taddei, F., Martelli, S., Valente, G., Benedetti, M.G., Leardini, A., Manfrini, M., Viceconti, M., 2012. Femoral loads during gait in a patient with massive skeletal reconstruction. Clinical Biomechanics (Bristol, Avon) 27(3):273-80.

Thelen, D.G., Anderson, F.C., 2006. Using computed muscle control to generate forward dynamic simulations of human walking from experimental data. Journal of Biomechanics 39(6):1107-1115.

van der Krogt, M.M., Delp, S.L., Schwartz, M.H., 2012. How robust is human gait to muscle weakness? Gait & Posture 36(1):113-9.

Wilson, W., van Burken, C., van Donkelaar, C., Buma, P., van Rietbergen, B., Huiskes, R., 2006. Causes of Mechanically Induced Collagen Damage in Articular Cartilage. Journal of Orthopaedic Research 2:220-228.

Woltring, H.J., 1986. A Fortran package for generalized, cross-validatory spline smoothing and differentiation. Advances in Engineering Software 8(2):104-113.

Wu, J.Z., Herzog W., Epstein, M., 2000. Joint contact mechanics in the early stages of osteoarthritis. Medical Engineering & Physics 22(1):1-12.

Yamaguchi, G.T., Zajac, F.E., 1989. A planar model of the knee joint to characterize the knee extensor mechanism. Journal of Biomechanics 22(1):1-10.

PART III

Sensitivity of model predictions to kinematic parameters

Chapter 6

Sensitivity of a subject-specific musculoskeletal model to the uncertainties on joint axes location

Chapter 7

Sensitivity of a subject-specific musculoskeletal model to joint kinematics calculated with different methods

Chapter 6

Sensitivity of a subject-specific musculoskeletal model to the uncertainties on the joint axes location

Saulo Martelli[1], Giordano Valente[2,3], Marco Viceconti[4], Fulvia Taddei[1]

[1] Department of Mechanical Engineering, University of Melbourne, Australia
[2] Laboratorio di Tecnologia Medica, Istituto Ortopedico Rizzoli, Bologna, Italy
[3] Department of Industrial Enginnering, University of Bologna, Italy
[4] Department of Mechanical Engineering, University of Sheffield, United Kingdom

Journal article under review at Human Movement Science, 2012

Author contributions

S. Martelli designed and managed the project, wrote the paper, assisted with model developments and post-processing of results

G. Valente developed the models, performed the simulations of gait, post-processed the results, created the figures, assisted with project design and writing the paper

M. Viceconti obtained funding, assisted with project design and writing the paper

F. Taddei obtained funding, assisted with project design, model developments and writing the paper

Abstract

Subject-specific musculoskeletal models have become key tools in the clinical decision making process. However, the sensitivity of the calculated solution to the unavoidable errors committed deriving the model parameters from the available information is not fully understood. The aim of this study was to calculate the sensitivity of all the kinematics and kinetics variables to the inter-examiner uncertainty in the identification of the lower limb joint models. The study was based on the computer-tomography (CT) of the entire lower-limb from a single donor and the motion capture from a body-matched volunteer. The hip, the knee and the ankle joint models were defined following the International Society of Biomechanics (ISB) recommendations. Using a software interface, five expert anatomists identified on the donor's images the necessary bony locations five times with a three day time interval. A detailed subject-specific musculoskeletal model was taken from an earlier study, and re-formulated to define the joint axes by input the necessary bony locations. Gait simulations were run using OpenSim within a Monte Carlo stochastic scheme, where the locations of the bony landmarks were varied randomly according to the estimated distributions. Trends for the joint angles, moments, and the muscle and joint forces did not substantially change after parameter perturbations. The highest variations were: (a) 11 degrees for the joint angles, (b) 1 %BWxH for the joint moments, (c) 0.33 BW for the muscle forces and, (d) 0.30 BW for the joint forces. In conclusion, the identification of the joint axes from clinical images is a robust procedure for human movement modelling and simulation.

Keywords

Musculoskeletal model; hip load variation; muscle force sensitivity; joint axes uncertainty; gait simulations

Introduction

In the last decade, musculoskeletal models have evolved from exclusively research tools to clinical methods used in the decision-making process (Jonkers et al., 2008). In this new context, subject-specific models, typically generated from heterogeneous data such as clinical images, published atlases and direct anthropometrical measurements, are key factors in the calculation of reliable mechanical variables (Lenaerts et al., 2008, 2009; Scheys et al., 2008; Valente et al., 2012). For example, subject-specific models were found to be key factors for an accurate calculation of muscle lever arms (Lenaerts et al., 2008; Valente et al., 2012), skeletal forces (Lenaerts et al., 2008), bone stresses (Jonkers et al., 2008), and for properly addressing the related clinical implications (Steele et al., 2011; Taddei et al., 2012). However, the error committed in extracting the model parameters from the available clinical information affects the calculated variables in a way that need to be investigated.

The model identification process involves several and fairly complex operations (Scheys et al., 2009; Taddei et al., 2012). The skeletal geometry is often extracted from clinical images with an error in the order of two pixels (Testi et al., 2001). The inertial parameters can be derived from simple anatomical measurements using regression equation with not less than a 21.3% error on one or more parameters (Durkin & Dowling, 2006). The muscle attachment locations can be automatically estimated from Magnetic Resonance Images (MRI) with an average error of 6.1 mm (Scheys et al., 2009). The hip joint center location can be determined using a functional method from simple recordings of the hip motion or, as a possible alternative, using regression equations from simple measurements that can be easily taken on the patient skin. The functional method was able to estimate the hip joint center with an average error of 13 mm, whilst regression equations showed a higher average error up to 30 mm (Leardini et al., 1999). The joint axes of the knee and the ankle can be defined using the location of prominent bony landmarks lying on each respective joint axis (Grood & Suntay, 1983; Wu et al., 2002). To this purpose, a computer-based procedure, the so-called Virtual Palpation procedure, has been recently proposed to locate all the necessary bony

landmarks on the available clinical images with an uncertainty up to 3 mm (Taddei et al., 2007). Whatever the adopted identification process is, the errors committed clearly alter the calculated variables in a way that is not known a-priori.

Several authors investigated the sensitivity of calculated skeletal forces to changes of the model parameters. Changes of the muscle physiological cross section area (PCSA) within the physiological range led to 11% variation of the hip force (Brand, Pedersen, & Friederich, 1986) and up to more than 100% variation of the calculated muscle forces (Brand et al., 1986; Herzog, 1992). Xiao and Higginson, 2010 perturbed selected muscle parameters (i.e., the number of muscle lines of action, the maximum isometric force, the optimal fiber length and the tendon slack length) by a ±10% factor, showing variations in the calculated muscle forces up to 12.8 times the magnitude of the imposed parameter perturbations. Scaling a general pelvis model on personalised anthropometric information can induce an up to 3 cm misallocation of the hip and a consequent shift of the calculated hip force in the order of 0.5 times body weight (BW) (Lenaerts et al., 2009). To date, no studies reported the sensitivity of the calculated muscle and joint forces to the error committed in defining the lower-limb joint axes from clinical images.

The aim of this study is to estimate the sensitivity of the calculated muscle and joint forces associated with inter-examiner uncertainty in locating the relevant skeletal landmarks (Grood & Suntay, 1983; Wu et al., 2002). To this aim, the uncertainty on the landmark positions was assessed and its effect on the calculated skeletal forces estimated by means of a subject-specific musculoskeletal model of the lower limbs, performed with a Monte Carlo stochastic scheme.

Materials and Methods

The study was based on a large CT dataset from a single donor and the motion data from a body-matched volunteer. Five expert anatomists identified the necessary bony landmarks using the Virtual Palpation procedure (Taddei et al., 2007), providing the necessary measurements for the estimation of the probability density distribution of the landmark locations. A musculoskeletal model was taken from an earlier study (Martelli et al., 2011), and reformulated in a

parametrical way to define the articular joints from the necessary landmark locations. A Monte Carlo stochastic scheme was used to generate an adequate set of joint models from the estimated distributions. A standard software pipeline (OpenSim (Delp et al., 2007), www.simtk.org) was used to calculate the body kinematics, the joint moments and the muscle and joint forces for a selected stride. Results were post-processed to expose the variations of calculated parameters.

The CT dataset and the motion data

The CT dataset was taken from an 81-year-old donor (female, 167 cm height and 63 kg weight) during an earlier study (Viceconti, Clapworthy, & Van Sint Jan, 2008). The dataset was recorded with a clinical scanning machine (manufacturer: Siemens Medical Solutions USA, Inc., model: Sensation 64) using common physical parameters (tube voltage: 120 kVp, tube current: 270 mA). The dataset included the entire lower limbs, from the entire pelvis down to the entire feet. The pixel size was 0.9765 mm while the spacing was 1 mm.

The body motion was recorded from a body-matched volunteer (female, 25 years old, 165 cm height and 57 kg weight) following the gait analysis protocol proposed by Leardini et al., (2007), which provided 3D motion (Vicon Motion Capture, Oxford UK) of the lower limb segments (sampling rate 100Hz) and the ground reaction forces at both feet (sampling rate 2000Hz). A single trial of walking at normal speed was selected for this study; recordings contained in order the stance and swing phase for the right leg, while, for the left leg, the sequence was opposite containing the swing phase first and the stance phase last.

Both the CT dataset and the motion data are are freely available for download at www.physiomespace.com (Viceconti et al., 2008).

Estimation of the joint centers and axes

The joint centers and axes were defined according to the International Society of Biomechanics (ISB) (Wu et al., 2002) using the location of relevant bony landmarks. The bony locations necessary to identify the hip, the knee, and the ankle model were the hip center (HC), the lateral epicondyle (LE), the medial epicondyle (ME), the lateral malleolus (LM), and the medial malleolus (MM).

The HC location was estimated as the sphere that best fitted the femoral head surface, through a multimodal visualization approach allowing a combined 3D visualization of the CT volume and the skeletal surface (Taddei et al., 2007). The femoral epicondyles and the tibio-fibular malleoli were located by picking the selected location on the skeletal surface extracted from the CT images. Five expert anatomists located the full set of bony locations on both legs using a dedicated software environment (NMSBuilder[1]). Each anatomist repeated all the measurements three times with a time interval of three days.

The parametric musculoskeletal model

The base musculoskeletal model is extensively described in an earlier work (Martelli et al., 2011). The biomechanical model was defined as a 7-segment, 10 degree-of-freedom (DOFs) articulated system, actuated by 82 muscle-tendon units. Three ideal joints articulated each leg: a ball-and-socket (3 DOFs) at the hip and a hinge (1 DOF) at both the knee and the ankle. A well-established muscular model of the lower extremity (Delp et al., 1990) was manually registered on the subject-specific anatomy by an expert anatomist. In the earlier study (Martelli et al., 2011), the model was validated showing a good agreement between the calculated muscle and hip forces with, respectively, the available EMG recording and published measurements of hip force (Figure 1). In the present study, the model was re-created in a parametric form using an in-house routine (MATLAB©, The Mathworks Inc., USA) to allow the definition of the joint axes from the necessary landmark locations. Specifically, the knee axis was defined from ME and LE locations, assuming the knee axis passing through the two bony locations and the knee center as the midpoint between the two (Grood & Suntay, 1983). Similarly, the ankle axis was defined from MM and LM locations, assuming the ankle axis passing through the two bony locations and the ankle center as the midpoint between the two (Wu et al., 2002).

[1] https://www.biomedtown.org/biomed_town/nmsphysiome/reception/alpha/

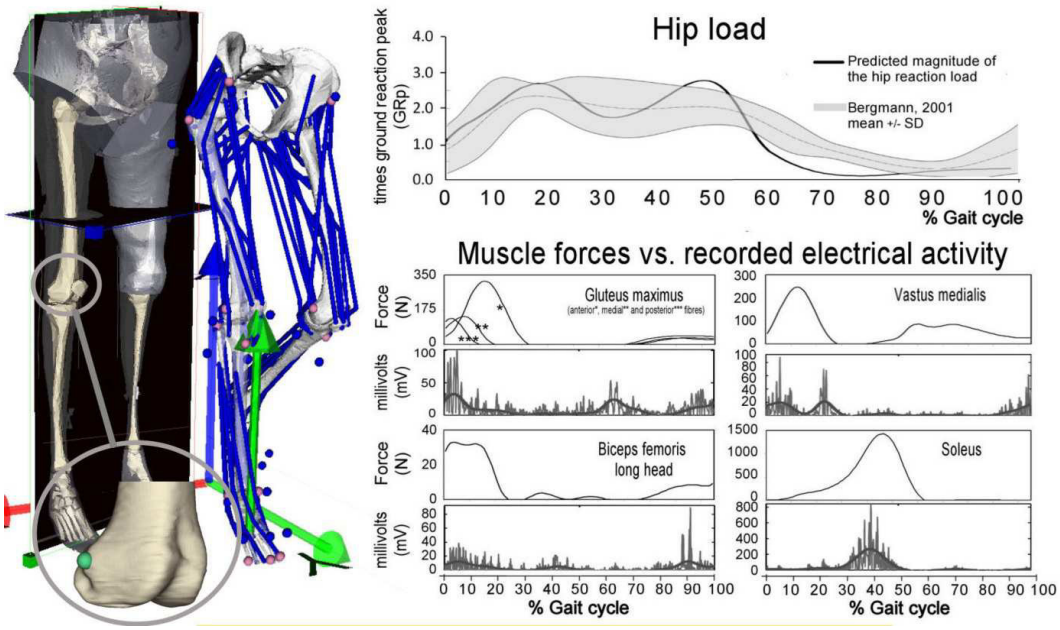

Figure 1 - The comparison of calculated hip and muscle forces with published measurements and the available electromyography is taken from an earlier study (right) (Martelli et al., 2011). On the left, the CT volume and superimposed the extracted skeletal and skin geometries, a highlight of the identified lateral epicondyle (LE) and the OpenSim model during an intermediate frame of gait

The Probabilistic Design

The AP and the CC coordinates of the femoral epicondyles and the tibio-fibular malleoli were defined as normally distributed variables. The mean position and the standard deviation of the femoral epicondyles were assigned the mean position and the variance from the estimated epicondyles. The mean position and the standard deviation of the tibio-fibular malleoli were assigned the mean position and the variance from the estimated malleoli. The hip joint center, the medio-lateral position of the femoral epicondyles, and the medio-lateral position of the tibio-fibular malleoli were assigned deterministic values, equal to the mean identified locations. A Latin Hypercube Sampling technique (LHS), which is a more efficient form of a Monte Carlo simulation method, was applied using Matlab© (The Mathworks Inc., USA). The algorithm was used to randomly generate an appropriate set of bony locations, known as the "sampling points" hereinafter, which were distributed in space according to the probability

distribution estimated from the five anatomists' measurements. The number of the necessary sampling points was determined by checking convergence of all the input and output variables. Convergence was assumed when the inclusion of an additional sampling point induced changes of the standard deviation <2% and of the mean value <0.2%.

The calculation of the skeletal kinematics, kinetics, and the muscle and joint forces

The musculoskeletal model was input with each sampling point, and the gait cycle was simulated using a standard pipeline, including inverse kinematics, inverse dynamics, static optimization and JointReaction analysis (Delp et al., 2007). The time histories of all the kinematics, the kinetics, and the muscle and joint forces were calculated and normalized in terms of percentage of gait cycle. Calculated forces were normalized in terms of body weight (BW) whilst calculated moments were normalised in terms of percentage of body weight times subject height (%BW*H). The muscle forces were grouped according to their main function (Table 1). To superimpose the time histories for the right and the left leg, the left swing phase was artificially moved before the left stance. Variations of the calculated distributions were presented for the joint kinematics, moments, and calculated forces. All the analyses were performed using Matlab© (The Mathworks Inc., USA).

Table 1 - The modelled muscles grouped according to their main function

Hip Abductors	Hip Adductors	Hip Extensors	Hip Flexors	Hip Rotators
Gluteus Medius	Adductor Brevis	Biceps Femoris Long Head	Iliacus	Gemellus
Gluteus Minimus	Adductor Longus	Gluteus Maximus	Psoas	Pectineus
Tensor Fascia Latae	Adductor Magnus	Semimembranosus	Rectus Femoris	Pyriform
	Gracilis	Semitendinosus	Sartorius	Quadratus Femoris
Knee Extensors	**Knee Flexors**	**Ankle Dorsiflexors**	**Ankle Plantarflexors**	
Rectus Femoris	Biceps Femoris Long Head	Extensor Digitorum	Flexor Digitorum	
Vastus Intermedius	Biceps Femoris Short Head	Extensor Hallucis	Flexor Hallucis	
Vastus Lateralis	Gastrocnemius	Peroneus Tertius	Gastrocnemius	
Vastus Medialis	Semimembranosus	Tibialis Anterior	Peroneus Brevis	
	Semitendinosus		Peroneus Longus	
			Soleus	
			Tibialis Posterior	

Results

Estimation of the joint centers and axes

The standard deviation of the hip center coordinates were lower than 0.4 mm. The standard deviation of the antero-posterior and the cranio-caudal coordinates of the femoral epicondyles were 2.0 mm and 1.4 mm respectively. The standard deviation of the antero-posterior and the cranio-caudal coordinates of the tibio-fibular malleoli were 1.1 mm and 1.5 mm respectively.

Convergence analysis

For all the investigated input and output variables, 400 runs were sufficient to reach an asymptotic plateau ensuring convergence. Figure 2 shows the two variables that required the full set of runs to reach convergence (i.e. the ankle and the knee peak contact force).

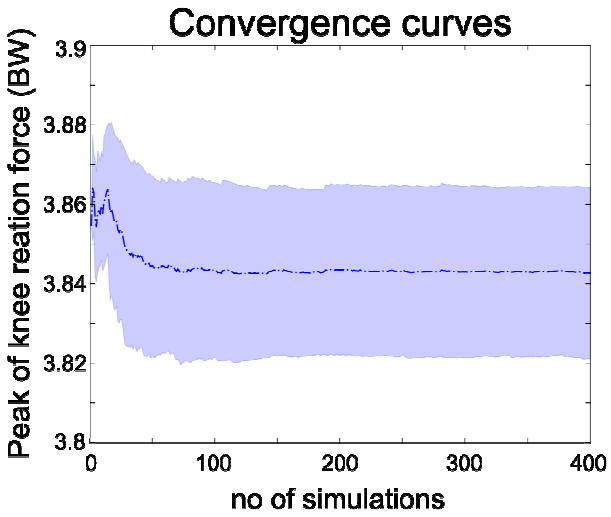

Figure 2 - Convergence curves of the joint reaction forces at the knee (BW). Mean and SD are below the convergence threshold (2%)

Uncertainties on joint kinematics, joint moments, and joint and muscle forces

The variation of all the kinematics and kinetics variables showed similar patterns for both legs. Throughout stride, all the joint angles never exceeded 5.4 degree variation with the only exception for the hip rotation angle, which reached 11

degree variation during mid swing (Figure 3). The variation of the hip moments never exceeded 0.5 %BWxH for either the adduction, the flexion and the rotation axis, with peak variations predicted during the stance-to-swing and swing-to-stance transition phases. The variation of the knee moment was up to 1 %BWxH, calculated during late stance, whilst the variation of the ankle moment was up to 0.72 %BWxH calculated, again, during late stance (Figure 4).

Patterns for the principal muscle groups and the joint forces were consistent for both legs, either in terms of magnitude and timing (Figure 5), showing the tendency for moderately higher variations during early and late stance, synchronously with peak variations of the joint moments (Figure 6). The highest variation of muscle forces was 0.33 BW, calculated during early stance for the ankle plantarflexors. The peaks of the force variations at the joints were 0.26 BW at the hip, 0.16 BW at the knee, and 0.33 BW at the ankle.

Expressing the force variation calculated for each muscle group and joint as a percentage of the peak force calculated for the same muscle group or joint, force variations for the joints never exceeded the 9% of the peak force whilst the force variations for the muscle groups reached the 114% of the peak force, the force variation calculated for the hip flexors during late stance.

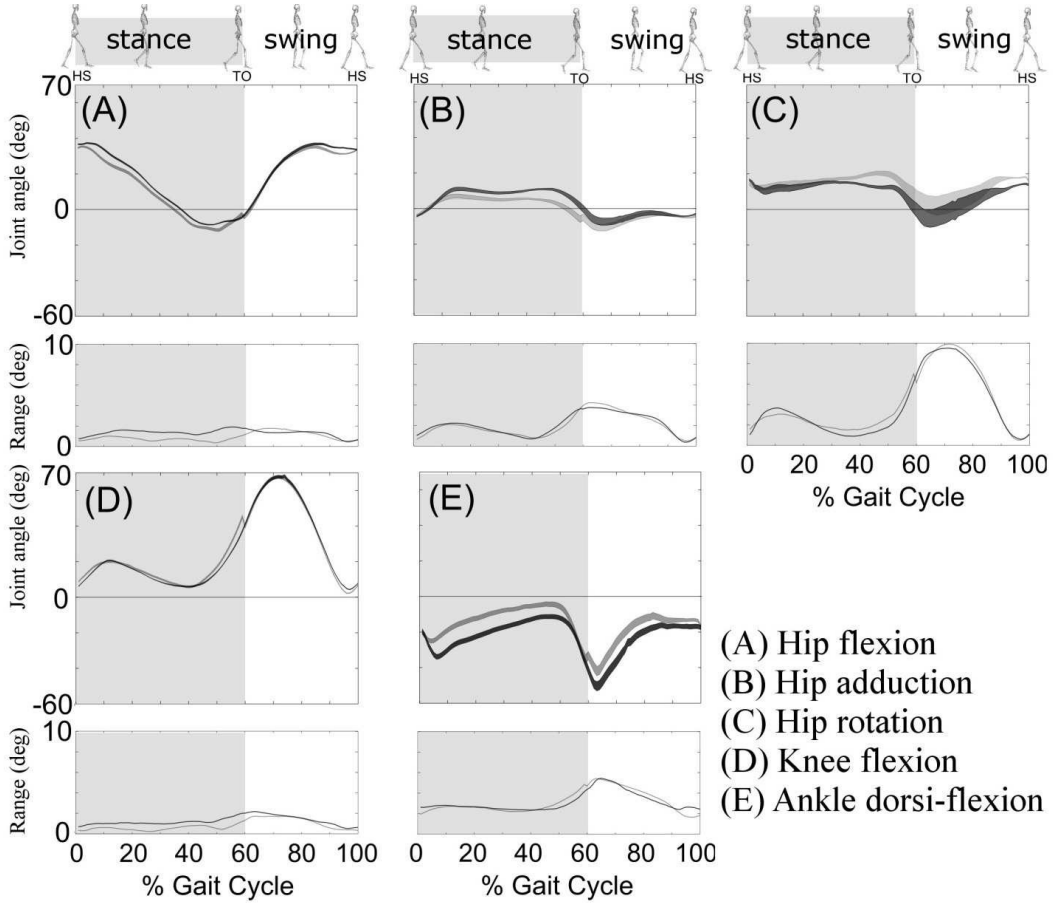

Figure 3 - The variation bands (top) for the joint angles (degrees) and the range of the respective calculated values (bottom). In dark grey are represented the joint angles for the right leg while in light grey are represented the joint angles for the left leg. The stance and the swing phase subdivided by the heel strike (HS) and toe off (TO) instants are also indicated

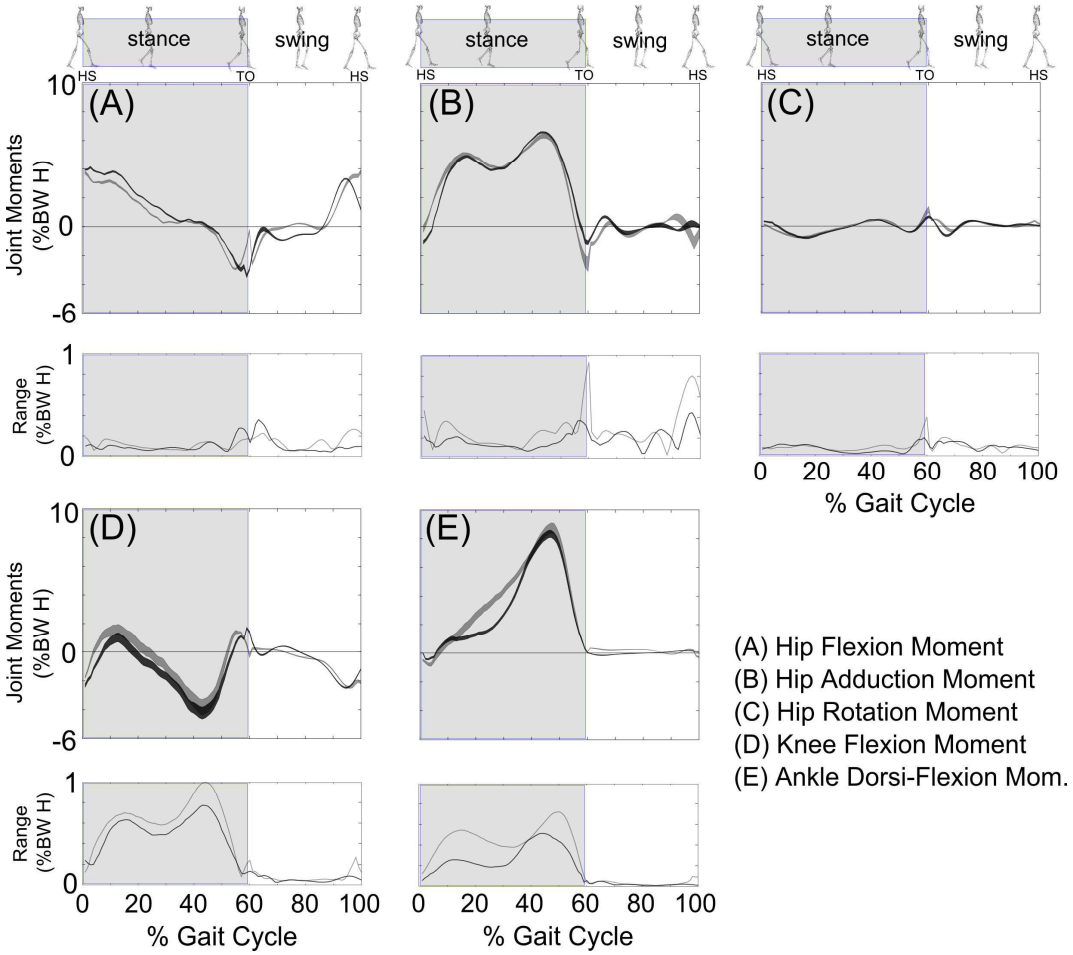

Figure 4 - The variation bands (top) for the joint moments and the range of the respective calculated values (bottom). In dark grey are represented the joint moments for the right leg while in light grey are represented the joint moments for the left leg. The calculated values are normalised as a percentage of the body weight (BW) times the subject high (H). The different phases of the stride are indicated as in Figure 3

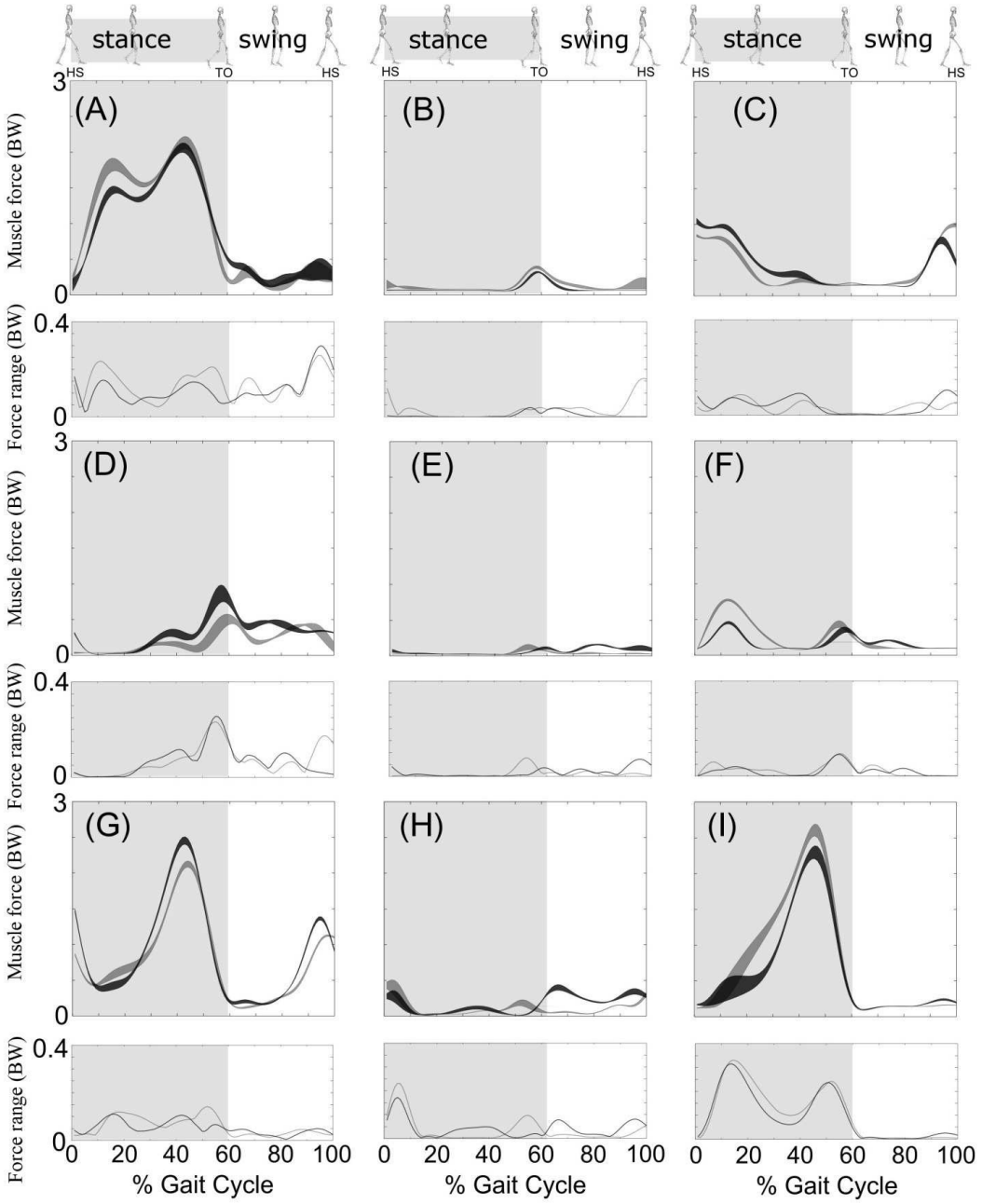

Figure 5 - The variation bands (top) for the muscle forces and the range of the respective calculated values (bottom). In a consecutive order, the graphs represent (A) the hip abductors, (B) the hip adductors, (C) the hip extensors, (D) the hip flexors, (E) the hip extensors, (F) the knee extensors, (G) the knee flexors, (H) the ankle dorsiflexors and (I) the ankle plantarflexors. In dark grey are represented the muscle forces calculated for the right leg while in light grey are represented the muscle forces calculated for the left leg. The calculated values are normalised as a percentage of the body weight (BW). The different phases of the stride are indicated as in Figure 3.

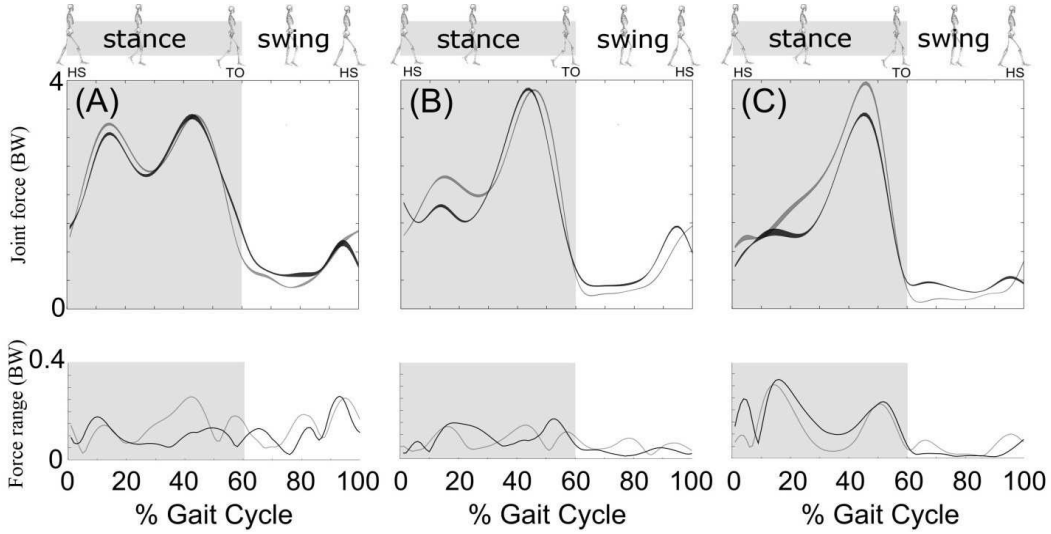

Figure 6 - The variation bands (top) for the hip (A), the knee (B) and the ankle force (C) as well as trends for the calculated range (bottom). In dark grey are represented the joint forces for the right leg while in light grey are represented the joint forces for the left leg. The calculated values are normalised as a percentage of the body weight (BW). The different phases of the stride are indicated as in Figure 3

Discussion

Modelling the patient musculoskeletal system has become important in the clinical decision-making process (Jonkers et al., 2008), stimulating the emergence of methodologies to identify the model parameters from the available clinical information. However, the effect on the calculated variables of the unavoidable errors committed during the model identification process is not fully elucidated. The aim of the study was to estimate the variability of the calculated muscle and joint forces due to the inter-examiner uncertainty in locating the necessary bony locations.

Variations in the bony landmark locations induced generally small variations of all the investigated variables, not substantially altering the calculated patterns. Indeed, the calculated variations of the joint angles were in average 2.3 degrees, and never exceeded the 11 degrees calculated for the hip rotation angle. Variations of the joint moments never exceeded the 11 % of the peak moment. Grouping muscle and joint forces together, variations never exceeded the 0.33 BW, a value that represents the 8-10% of the peak joint forces, which ranged from 3.44 BW at the hip to 4.04 BW at the ankle. This uncertainty level is consistent with

applications for human motion modelling and simulations such as investigations into bone stresses and the related clinical implications (Jonkers et al., 2008). However, the sensitivity of forces calculated for each single muscle was much higher with force variations reaching the same order of magnitude of the median calculated force. Therefore, conclusions taken on calculations of the muscle force magnitude should be considered cautiously.

The presented results compare well with published reports of intermediate findings. An earlier study (Taddei et al., 2007) reported an up to 2.3 mm inter-examiner variability in the location of the necessary bony landmarks, in good agreement with present findings. The joint kinematics showed an up to 11 degree variation, in good agreement with the 8 degree inter-examiner uncertainty reported by Della Croce et al. (1999). In their study, however, the authors used different optimization algorithms to calculate the instantaneous pose of each body segment from that used in this study. The much higher variation of muscle forces (up to 114%) than that of joint forces (9%) over their median value compares well with earlier studies (Brand et al., 1986; Herzog, 1992). Brand et al. (1986) showed two to eight time variations in muscle forces and an up to 11% variation of the hip force by using different sets of the muscle physiological cross section area from different subjects. Herzog (1992) showed up to 100% variations of the calculated muscle forces resulting from perturbations of the muscle parameters within physiological boundaries.

This study has some limitations that may have affected the presented results. First, assuming the hip center and the medio-lateral components of both the femoral epicondyles and the tibio-fibular malleoli as deterministic variables, might have led to smaller variations of all the calculated variables. This, however, allowed a drastic reduction of the number of simulations necessary to reach convergence. Moreover, the uncertainty on the estimation of the hip center is very small and the medio-lateral component of the femoral epicondyles and tibial malleoli has little effect on the knee and ankle axis orientations, suggesting that these parameters are of secondary importance. Second, the results have been generated using one anatomical dataset. It is possible that the inclusion of additional subjects may lead

to larger variations of all the investigated variables; more research is necessary to solve this limitation.

Despite the aforementioned limitations, the present findings provide the first quantitative comprehensive evaluation of the sensitivity of all the calculated lower-limb kinematics and kinetics variables to the inter-examiner uncertainty in defining the joint axes. By providing a better understanding of the reliability of the computed solution, these results could be helpful for those interested in human movement modelling and simulation, and contribute to a better informed decision-making process in clinical contexts.

In summary, the identification of the lower-limb joint axes through the location of prominent bony locations from CT images is a robust procedure to generate musculoskeletal models. Indeed, the sensitivity of the kinematics, the joint moments, and the joint forces to the joint axes uncertainty is moderate. However, conclusions based on calculated muscle forces should be interpreted with caution due to their higher sensitivity to joint axes uncertainties.

Conflicts of interest

None

Ackowledgements

This study was co-funded by the EC-funded projects NMSPhysiome (FP7 #24818965) and VPHOP (Grant #223865). We thank Irene Brambilla for the contribution to the preliminary analysis.

References

Brand, R. A., Pedersen, D. R., & Friederich, J. A. (1986). The sensitivity of muscle force predictions to changes in physiologic cross-sectional area. *Journal of biomechanics*, *19*(8), 589–596.

Della Croce, U., Cappozzo, A., & Kerrigan, D. C. (1999). Pelvis and lower limb anatomical landmark calibration precision and its propagation to bone

geometry and joint angles. *Medical & biological engineering & computing*, *37*(2), 155–161.

Delp, S. L., Anderson, F. C., Arnold, A. S., Loan, P., Habib, A., John, C. T., … Thelen, D. G. (2007). OpenSim: open-source software to create and analyze dynamic simulations of movement. *IEEE Transactions on Biomedical Engineering*, *54*(11), 1940–1950.

Delp, S. L., Loan, J. P., Hoy, M. G., Zajac, F. E., Topp, E. L., & Rosen, J. M. (1990). An interactive graphics-based model of the lower extremity to study orthopaedic surgical procedures. *IEEE Transactions on Biomedical Engineering*, *37*(8), 757–767.

Durkin, J. L., & Dowling, J. J. (2006). Body segment parameter estimation of the human lower leg using an elliptical model with validation from DEXA. *Annals of biomedical engineering*, *34*(9), 1483–1493.

Grood, E. S., & Suntay, W. J. (1983). A joint coordinate system for the clinical description of three-dimensional motions: application to the knee. *Journal of biomechanical engineering*, *105*(2), 136–44.

Herzog, W. (1992). Sensitivity of muscle force estimations to changes in muscle input parameters using nonlinear optimization approaches. *Journal of biomechanical engineering*, *114*(2), 267–268.

Jonkers, I., Lenaerts, G., Mulier, M., Van der Perre, G., & Jaecques, S. (2008). Relation between subject-specific hip joint loading, stress distribution in the proximal femur and bone mineral density changes after total hip replacement. *Journal of Biomechanics*, *41*(16), 3405–3413.

Leardini, A, Sawacha, Z., Paolini, G., Ingrosso, S., Nativo, R., & Benedetti, M. G. (2007). A new anatomically based protocol for gait analysis in children. *Gait Posture*, *26*, 560–71.

Leardini, Alberto, Cappozzo, A., Catani, F., Toksvig-Larsen, S., Petitto, A., Sforza, V., … Giannini, S. (1999). Validation of a functional method for the estimation of hip joint centre location. *Journal of biomechanics*, *32*(1), 99–103.

Lenaerts, G., Bartels, W., Gelaude, F., Mulier, M., Spaepen, A., Van der Perre, G., & Jonkers, I. (2009). Subject-specific hip geometry and hip joint centre location affects calculated contact forces at the hip during gait. *Journal of Biomechanics*, *42*(9), 1246–1251.

Lenaerts, G., De Groote, F., Demeulenaere, B., Mulier, M., Van der Perre, G., Spaepen, A., & Jonkers, I. (2008). Subject-specific hip geometry affects predicted hip joint contact forces during gait. *Journal of biomechanics*, *41*(6), 1243–1252.

Martelli, S., Taddei, F., Cappello, A., Van Sint Jan, S., Leardini, A., & Viceconti, M. (2011). Effect of sub-optimal neuromotor control on the hip joint load during level walking. *Journal of Biomechanics*, *44*(9), 1716–1721.

Scheys, L., Loeckx, D., Spaepen, A., Suetens, P., & Jonkers, I. (2009). Atlas-based non-rigid image registration to automatically define line-of-action muscle models: a validation study. *Journal of biomechanics*, *42*(5), 565–72.

Scheys, L., Van Campenhout, A., Spaepen, A., Suetens, P., & Jonkers, I. (2008). Personalized MR-based musculoskeletal models compared to rescaled generic models in the presence of increased femoral anteversion: effect on hip moment arm lengths. *Gait Posture*, *28*(3), 358–365.

Taddei, F., Ansaloni, M., Testi, D., & Viceconti, M. (2007). Virtual palpation of skeletal landmarks with multimodal display interfaces. *Medical informatics and the Internet in medicine*, *32*(3), 191–8.

Taddei, F., Martelli, S., Valente, G., Leardini, A., Benedetti, M. G., Manfrini, M., & Viceconti, M. (2012). Femoral loads during gait in a patient with massive

skeletal reconstruction. *Clinical biomechanics (Bristol, Avon)*, *27*(3), 273–280.

Testi, D., Zannoni, C., Cappello, A., & Viceconti, M. (2001). Border-tracing algorithm implementation for the femoral geometry reconstruction. *Computer Methods and Programs in Biomedicine*, *65*(3), 175–82.

Valente, G., Martelli, S., Taddei, F., Farinella, G., & Viceconti, M. (2012). Muscle discretization affects the loading transferred to bones in lowerlimb musculoskeletal models. *Proceedings of the Institution of Mechanical Engineers, Part H: Journal of Engineering in Medicine*, *226*(2), 161–9.

Viceconti, M., Clapworthy, G., & Van Sint Jan, S. (2008). The Virtual Physiological Human - a European initiative for in silico human modelling - A European Initiative for in silico Human Modelling. *The journal of physiological sciences*, *58*(7), 441–6.

Wu, G., Siegler, S., Allard, P., Kirtley, C., Leardini, A., Rosenbaum, D., … Stokes, I. (2002). ISB recommendation on definitions of joint coordinate system of various joints for the reporting of human joint motion--part I: ankle, hip, and spine. International Society of Biomechanics. *Journal of biomechanics*, *35*(4), 543–548.

Chapter 7

Sensitivity of a subject-specific musculoskeletal model to joint kinematics calculated with different methods

Giordano Valente[1,2], Lorenzo Pitto[1], Maria Cristina Bisi[3], Rita Stagni[3], Luca Cristofolini[2], Fulvia Taddei[1]

[1] Laboratorio di Tecnologia Medica, Istituto Ortopedico Rizzoli, Bologna, Italy

[2] Department of Industrial Engineering, University of Bologna, Italy

[3] Department of Electric, Electronic and Information Engineering, University of Bologna, Italy

Unpublished work submitted to the 24th Congress of the International Society of Biomechanics (ISB), Brazil, 2013

Author contributions

G. Valente assisted with project design and management, developed the models, performed the simulations of motion, interpreted the results

L. Pitto segmented the imaging data, post-processed the gait data, developed the models, performed the simulations of gait

M.C. Bisi and R. Stagni collected the gait data, assisted with imaging data collection

L. Cristofolini assisted with project management and imaging data collection

F. Taddei obtained funding, assisted with project management and modeling development

Abstract

Joint kinematics affects calculated skeletal forces using musculoskeletal models. However, the influence of different inverse kinematics outputs on calculated muscle and joint forces has not been assessed yet. Most research focused on the use of marker trajectories from single calibration as input to global optimization problems for the calculation of joint kinematics.

This study evaluates the sensitivity of a subject-specific musculoskeletal model predictions to different global optimization solutions to calculate joint kinematics during motion, including landmark trajectories reconstructed with different methods, and variable weightings of landmark errors in the global optimization problem. Results show small differences in both kinematics and dynamics simulation outputs, denoting the important influence of joint constraints in the intrinsic formulation of the global optimization problem. The study is being extended to variable weightings of whole lower-limb markers, to more complex joints and to other motor tasks.

Introduction

A deep knowledge of the physiological loading conditions on the skeletal system during human movements may have significant clinical implications, contributing in the improvement of clinical treatments in several orthopedics and neurological contexts. Musculoskeletal models, in conjunction with inverse and forward dynamics methods, have been increasingly adopted to predict muscle and joint contact forces and answer several research questions [1]. A key difficulty related to the gap between musculoskeletal modeling and clinical practice is represented by the lack of a thorough validation of model predictions. Therefore, an accurate knowledge of model sensitivity to the several parameters and hypotheses involved, improves the clinical confidence in the model predictions.

Joint kinematics can be calculated from the reconstructed trajectories of markers attached to the skin surface through motion analysis methods. Since soft tissue artifact (STA) is recognized as the most critical source of error in motion analysis, several compensation methods were proposed, particularly global optimization (GO) [2] and double calibration (DC) [3]. Results on calculated joint kinematics

using different methods show significant variability [4], which particularly depends on the assumptions of joint constraints imposed to perform the GO.

In skeletal force analyses using musculoskeletal models, the first step of an inverse problem solution usually involves an inverse kinematics problem to calculate joint angles from marker trajectories, solving for the minimization of the weighted sum of squared distances (i.e. errors) between measured and model-determined marker positions (GO).

Most researchers have used, as input for GO, landmark trajectories from single calibrations (SC), and no studies were found that adopted appropriate weightings of marker errors to minimize STA, i.e. kinematics-dependent weights reflecting their reliability. Calculated joint kinematics affects inverse dynamics solutions, propagating to muscle and joint contact force calculations, but their sensitivity has not been studied yet.

Since landmark trajectories reconstructed from DC are less affected by STA [3,4], the aim of this study is to assess, using a subject-specific musculoskeletal model of the lower limbs, 1) how joint kinematics calculated with GO using as inputs the reconstructed trajectories of skeletal landmarks from DC differ from those using landmarks from SC [5] and from SC including variable weightings of marker errors optimized to reduce STA, and 2) how these different kinematics affect the prediction of muscle and joint contact forces using an inverse dynamics and static optimization approach.

Methods

A 7 segment, 10 degree of freedom articulated system of the lower limbs, actuated by 82 musculotendon units, was created from MR images of a healthy subject. The rigid body properties were derived from the MR volumes. Each hip was modeled as a ball-and-socket joint, each knee and ankle as a hinge, according to the ISB recommendations [6]. The musculotendon paths were modeled registering the origin, insertion and via-points of an available dataset [7] onto the subject-specific geometry, and musculotendon dynamics parameters were derived from MR volumes.

Marker trajectories (BTS Smart-D optoelectronic system with a 29 marker CAST protocol [5]), ground reaction forces and muscle activities of the subject were recorded during normal walking. Positions of anatomical landmarks were reconstructed using SC (with standing pose calibration) and DC (calibrations in standing and seated on a chair poses).

Three GO problems were solved, minimizing the weighted sum of squared errors between measured and model-determined landmark positions, to calculate joint kinematics during the stance phase of walking, running Inverse Kinematics simulations with the following inputs:

1) SC: Landmark trajectories reconstructed from SC, all weights of landmark errors set to 1.
2) SC optimized: Landmark trajectories reconstructed from SC, weights of thigh landmark errors optimized, considering STA characteristics [8], such that could linearly vary during motion between 0 and 1 within the physiological range of knee flexion (unreliable positions at maximum flexion; reliable at 0°).
3) DC: Landmark trajectories reconstructed from DC, all weights of landmark errors set to 1.

The calculated sets of joint kinematics were then used as inputs for Inverse Dynamics, Static Optimization and JointReaction analysis simulations in OpenSim [9], to calculate the corresponding sets of net joint moments, muscle forces and joint contact forces. Results using the two SC methods (method 1 end method 2) were compared against those using the DC method (method 3).

Results and Discussion

In the stance phase of a gait cycle, the calculated joint kinematics with method 1 showed maximum differences of 4 degrees, found in the knee flexion (Figure 1). The values obtained with method 2 slightly differed from method 1 (few tenths of degree), denoting how variable weightings of landmark errors in the thigh does not have a major effect in the calculation of joint kinematics using GO. The corresponding dynamic simulation solutions showed maximum differences of 0.2 BW in muscle forces, found in soleus and gastrocnemius, and 0.3 BW in joint contact forces, found in the knee (Figure 2). Results obtained with method 2

reflect slight differences compared to method 1, confirming a minor effect on dynamic results.

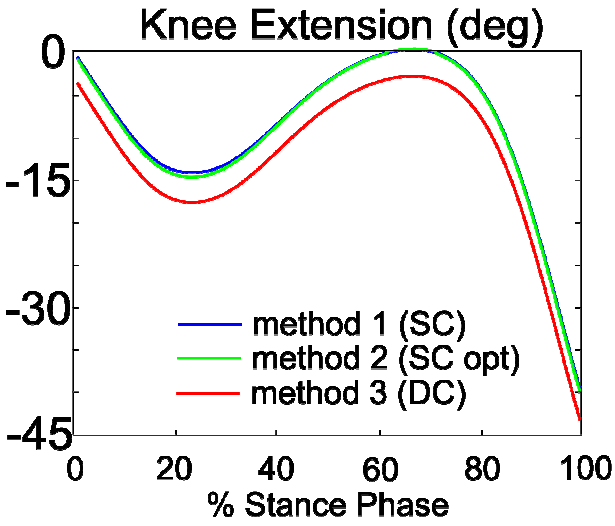

Figure 1 - Knee flexion angle calculated during stance of a walking trial with the 3 described methods

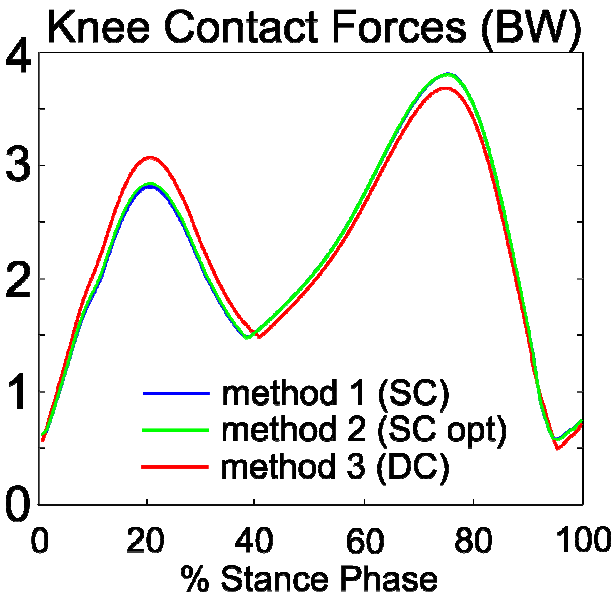

Figure 2 - Magnitude of knee contact force calculated during stance of a walking trials using joint kinematics obtained with the 3 described methods

Conclusion

This study aims at evaluating how joint kinematics calculated with different methods affect skeletal load predictions by a subject-specific musculoskeletal model. Assuming that landmark trajectories reconstructed from DC, never used in published musculoskeletal simulations, are less affected by STA than other presented methods, we compared commonly used GO outputs using landmark trajectories from SC (method 1 and method 2) with those from DC (method 3), to then evaluate the effect on dynamic simulations. The differences between the methods were not marked (particularly between method 1 and method 2), denoting the influence of joint constraints in the intrinsic formulation of global optimization, and highlighting the relevance of accurate lower-limb joint models. For further investigation, the study is being extended to variable weightings of landmark errors for the whole lower limb, to more complex models of lower-limb joints and to simulations of other motor tasks (stair climbing, chair rising).

Acknowledgements

This study is supported by the NMS Physiome project (grant 248189) funded by the European Union.

References

1. Pandy M.G., and Andriacchi T.P., Muscle and joint function in human locomotion, Annu Rev Biomed Eng, 12:401-33, 2010.
2. Lu T.W., and O'Connor J.J., Bone position estimation from skin marker co-ordinates using global optimisation with joint constraints, J Biomech. 32:129-34, 1999.
3. Cappello A., et al., Soft Tissue Artifact Compensation in Knee Kinematics by Double Anatomical Landmark Calibration: Performance of a Novel Method During Selected Motor Tasks, IEEE Trans Biomed Eng, 52:992-8, 2005.
4. Stagni R., et al., Double calibration vs. global optimisation: performance and effectiveness for clinical application. Gait Posture. 29:119-22, 2009.

5. Cappozzo A., et al., Position and orientation in space of bones during movement: anatomical frame definition and determination, Clin Biomech. 10:171-8, 1995.
6. Wu G., et al., ISB recommendation on definitions of joint coordinate system of various joints for the reporting of human joint motion--part I: ankle, hip, and spine. International Society of Biomechanics, J Biomech. 35:543-48, 2002.
7. Delp S.L., et al., An interactive graphics-based model of the lower extremity to study orthopaedic surgical procedures, IEEE Trans Biomed Eng. 37:757-67, 1990.
8. Stagni R., et al., Quantification of soft tissue artefact in motion analysis by combining 3D fluoroscopy and stereophotogrammetry: a study on two subjects, Clin Biomech. 20:320-9, 2005
9. Delp S.L., et al., OpenSim: open-source software to create and analyze dynamic simulations of movement, IEEE Trans Biomed Eng. 54:1940-50, 2007.

PART IV

Tool development for subject-specific modeling and simulation

---

Chapter 8

NMSBuilder:

software for creating subject-specific musculoskeletal models

Chapter 8

NMSBuilder: software for creating subject-specific musculoskeletal models

Giordano Valente[1], Saulo Martelli[1], Stefano Perticoni[2], Debora Testi[2], Fulvia Taddei[1], Marco Viceconti[1,3]

[1] Laboratorio di Tecnologia Medica, Istituto Ortopedico Rizzoli, Bologna, Italy

[2] BioComputing Competence Center, SCS s.r.l., Italy

[3] Department of Mechanical Engineering, University of Sheffield, United Kingdom

Author contributions

G. Valente (*co-Investigator*) designed and tested the software operations, produced test data, verified the implemented algorithms

S. Martelli (*co-Investigator*) designed the preliminary software operations and produced test data

S. Perticoni (*co-Investigator*) developed and implemented the software operations

D. Testi (*Principal Investigator*) obtained funding and assisted with software development

F. Taddei (*Principal Investigator*) obtained funding and assisted with the design of the software operations

M. Viceconti (*Project Coordinator*) obtained funding and coordinated the project

Introduction

This chapter summarizes one of the objectives being achieved within the NeuroMusculoSkeletal (NMS) Physiome project: the development of a software for subject-specific musculoskeletal modeling (NMSBuilder) as tool integration of the two largest research projects focused on personalized, predictive, and integrative musculoskeletal medicine, i.e., the Osteoporotic Virtual Physiological Human (VPHOP) funded by the European Union, and the Center for Physics-based Simulation of Biological Structures (SIMBIOS) funded by the USA National Institute of Health.

The development and the use of NMSBuilder have represented key features in the achievements of the research aims of the present thesis. Particularly, NMSBuilder represents an efficient framework, in the form of an open-source and user-friendly Graphical User Interface (GUI), to process biomedical data, define the features of musculoskeletal multibody systems, create and analyze OpenSim models and simulations. Material related to the NMSBuilder development is freely available for download from a dedicated internet page[1]. This includes software installers, user manual, test data and getting-started tutorials, which will be periodically updated with new software versions and additional material until the end of the project.

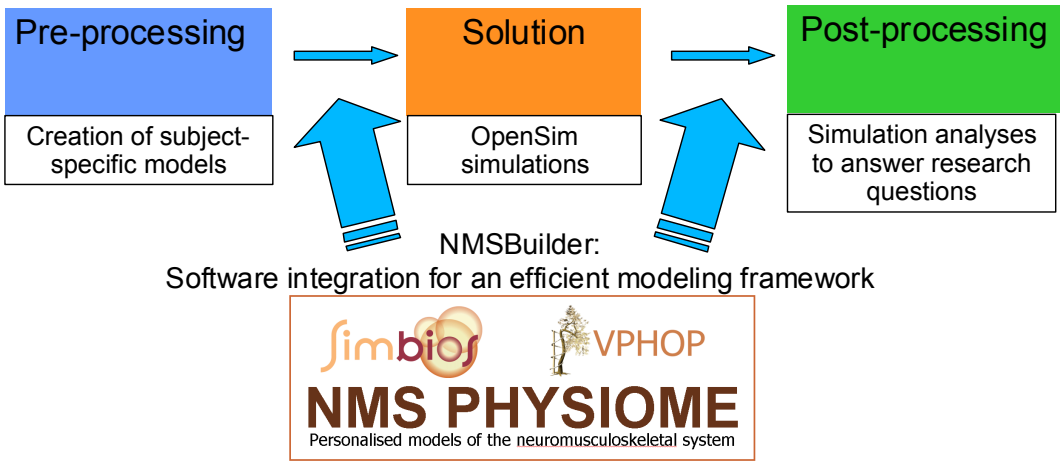

Figure 1 - NMSBuilder as an efficient framework for subject-specific musculoskeletal modeling and simulation

[1] https://www.biomedtown.org/biomed_town/nmsphysiome/reception/alpha/

The NMS Physiome project: concept and aims

The *Tools to develop the NeuroMusculoSkeletal Physiome: VPHOP-SIMBIOS cooperation* (project acronym: NMS Physiome) is a project funded by the European Union under the Seventh Framework Programme with grant agreement no. 248189 for small or medium-scale focused research projects[2]. The project has the duration of 42 months from January 2010 to June 2013, and the consortium, made of six beneficiary institutions, particularly involves the Rizzoli Orthopedic Institute (IOR), which also coordinates VPHOP[3], and Stanford University (SFU), which also coordinates SIMBIOS[4]. The project is based on the concept of development new Information and Communication Technology (ICT) that makes personalized, predictive, and integrative musculoskeletal medicine possible. With this project, the consortium intended to establish a more organic cooperation between VPHOP and SIMBIOS, structured around three objectives:

a) Integrate the project communities *Simtk*[5] and *Biomed Town*[6]
b) Integrate the project tools, i.e., the neuromusculoskeletal software being developed by the two consortia, ensuring interoperability among software, data formats, ontologies
c) Work collaboratively on grand challenges of efficient multiscale modeling of the musculoskeletal system, creation of accurate subject-specific models from clinically available data, development of modeling methods to cope with the probabilistic nature of the neuromotor function

The integration of *Simtk.org* and *Biomed Town* is creating a large global Internet community for integrative research, both in terms of number of members and of number of resources these members will access through it. They will be able to access the extensive collection of data, programs, and services that these two communities already provide, plus all those that are being developed both separately and collaboratively. If serious integrative research is possible only

[2] http://www.nmsphysiome.eu/
[3] http://www.vphop.eu/
[4] http://simbios.stanford.edu/
[5] https://simtk.org/xml/index.xml
[6] https://www.biomedtown.org/

through team science on a grand scale, this new virtual community will provide the ideal environment for it.

A similar reasoning applies to the integration of the software tools. A synergistic outcome from this activity is expected, since it will provide for the first time a complete workflow for multiscale musculoskeletal modeling, thus being much more than the sum of its parts. But the biggest progress beyond the state of the art is expected to come from the research components of this project. If there will be the possibility of solving the body-organ multiscale model of the neuromusculoskeletal system with sufficient speed, while accounting for all inter- and intra-subject sources of variability, not only fundamental research will be impacted, but also a solution for a number of clinically relevant problems will be provided, such as predicting the risk of fracture in osteoporotic patients, understanding the post-stroke neuromuscular compensation mechanisms, and improving assessments of disease severity for pediatric cerebral palsy and other similar diseases and conditions.

The whole project is organized in five work packages (WP) as follows:

WP1: Project management, dissemination and exploitation

WP2: Community services integration

WP3: Software tools integration

WP4: Probabilistic body-organ modeling

WP5: Technology assessment framework

IOR is particularly involved, from technical and scientific points of view, in WP3 and WP4. WP3 aims at integrating the *Multimodal Application Framework* (MAF)-based software NMSBuilder, with the SIMBIOS solvers OpenSim[7] and FEBio. WP4 aims at developing a probabilistic body-organ modeling environment, allowing to run probabilistic simulations using the OpenSim Application Programming Interface (API)[8] through the development of algorithms and a probabilistic simulator prototype using MATLAB and Octave. To achieve those WP aims, a common development plan was created to provide specifications on what are the parameters necessary to create a subject-specific

[7] https://simtk.org/home/opensim

[8] https://simtk.org/api_docs/opensim/api_docs/

musculoskeletal model and run deterministic and stochastic simulations of motion.

The software tools integration (WP3) is currently completed and the NMSBuilder software has been publicly released. The following sections summarize the integration strategy and the capabilities of the integrated software, with focus on the framework to create subject-specific musculoskeletal models for OpenSim.

Integration strategy

The main activities aimed at integrating NMSBuilder with the OpenSim API in order to provide a complete tool chain to process biomedical data, create multibody models of the musculoskeletal system, perform and analyze dynamic simulations of movement. The considered applications are:

- NMSBuilder, MAF-based pre-processing application, which allows to build subject-specific models from the biomedical data;
- OpenSim, multibody dynamics solver particularly suitable for musculoskeletal systems;

Multimod Application Framework

The Multimod Application Framework (MAF)[9] is an open-source freely available framework for the rapid development of applications based on the Visualisation ToolKit (VTK)[10] and other specialised libraries. It is implemented in C++ and provides high-level components that can be easily combined to develop a vertical application in different areas of scientific visualization (Figure 1). MAF core has been further extended by an additional software layer, called MAFMedical, which contains all components that are specific to the biomedical application domain.

A generic MAFMedical application, such the one implemented during the NMS Physiome project, is defined by choosing the needed elements from the framework, and by eventually specializing them. It is also possible to develop

[9] https://www.biomedtown.org/biomed_town/MAF/

[10] http://www.vtk.org/

ad-hoc components that are only necessary to the application itself, and to plug-in additional 3rd parties libraries.

However, there are four types of components that form any MAF-based application:

- Virtual Medical Entities (VMEs), which are the data objects
- Views, providing interactive visualization of the VMEs
- Operations, which create new VMEs or modify existing ones. Special operations are the Importers that let the user import and convert into VME data structure almost any biomedical dataset, and the Exporters that can convert the VME into files formatted according to the most common standards
- Interface Elements, generic GUI components that define the user interface of the application

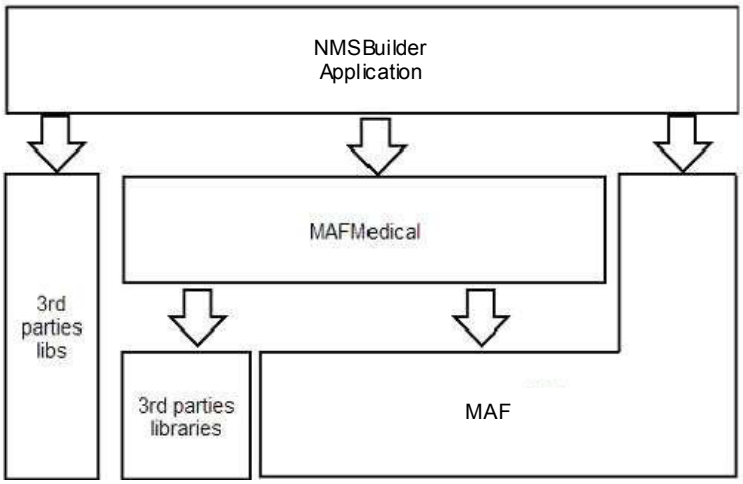

Figure 1 - MAF architecture

NMSBuilder application

NMSBuilder has the basic structure of any MAF application (Figure 2), which comprehends a well-defined GUI environment composed by a main Working Area, a lateral Control Bar showing the VME hierarchical structure, a Log Bar for the system messages, and the main menu (Menu Bar) with at least five items:

- File: this item contains all the commands related to input/output operations; the basic features are open/save/new commands to

respectively load, store, or initialize a new msf (MAF Storage Format) session file

- Edit: this item contains the commands to cut/copy/paste/delete any VME from the tree. There are also the undo/redo commands
- View: this item contains the list of the available views. It is also possible to select which of the other bars (Control Bar, Log Bar, Tool Bar and Time Bar) have to appear in the principal window
- Operations: this item contains a list of available operations within the application; if an operation cannot be run with the selected VME as input, the operation name appears in grey
- Tools: it defines a list of available settings for any MAF application

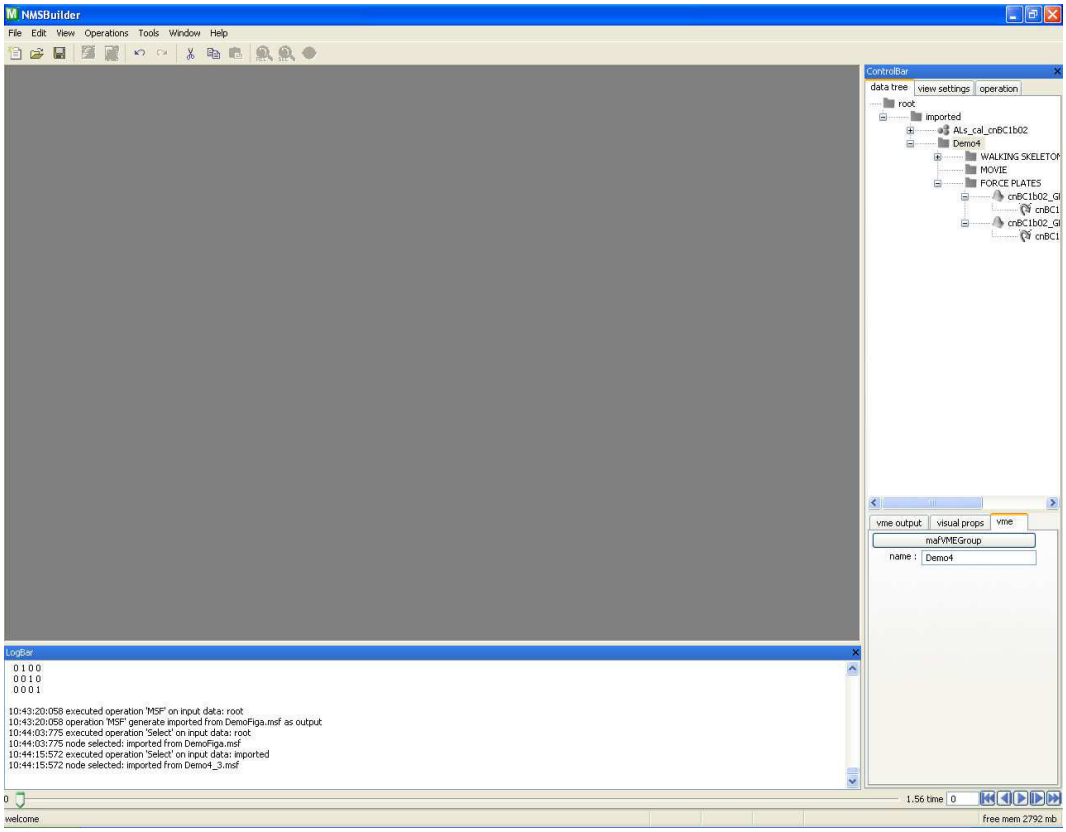

Figure 2 – NMSBuilder: MAF-based application GUI

The first version of NMSBuilder was developed plugging as first step a series of importers, operations and views coming from the MAF-based application previously developed within the VPHOP project. This application was the

starting point for the implementation and integration in the NMS Physiome project.

OpenSim

OpenSim[11] is a freely available, user extensible software system that lets users develop models of musculoskeletal structures and create dynamic simulations of movement. The software provides a platform on which the biomechanical community can build a library of simulations that can be exchanged, tested, analyzed, and improved through multi-institutional collaboration. The core software is written in C++, and the GUI is written in Java. OpenSim plug-in technology makes it possible to develop customized controllers, analyses, contact models, and muscle models among other things. These plugins can be shared without the need to alter or compile source code. Open-source, third party tools are used for some basic functionality, including the Xerces Parser from the Apache Foundation for reading and writing XML files[12] and VTK for visualization. The use of plug-in technology allows computational components such as integrators and optimizers to be updated as appropriate without extensive restructuring. OpenSim provides a GUI (Figure 2) that allows access to many of the software features and with which users can analyze existing models and simulations and develop new ones. For example, the user can import motion analysis data, scale a computer model of the musculoskeletal system, perform inverse dynamics analyses, and plot results all from the graphical interface.

OpenSim version 1.0 was first introduced at the Conference of the American Society of Biomechanics in 2007, and from version 2.0, an Application Programming Interface (API) has been added, allowing researchers to access and customize OpenSim core functionality.

[11] https://simtk.org/home/opensim

[12] http://xerces.apache.org/xerces-c/

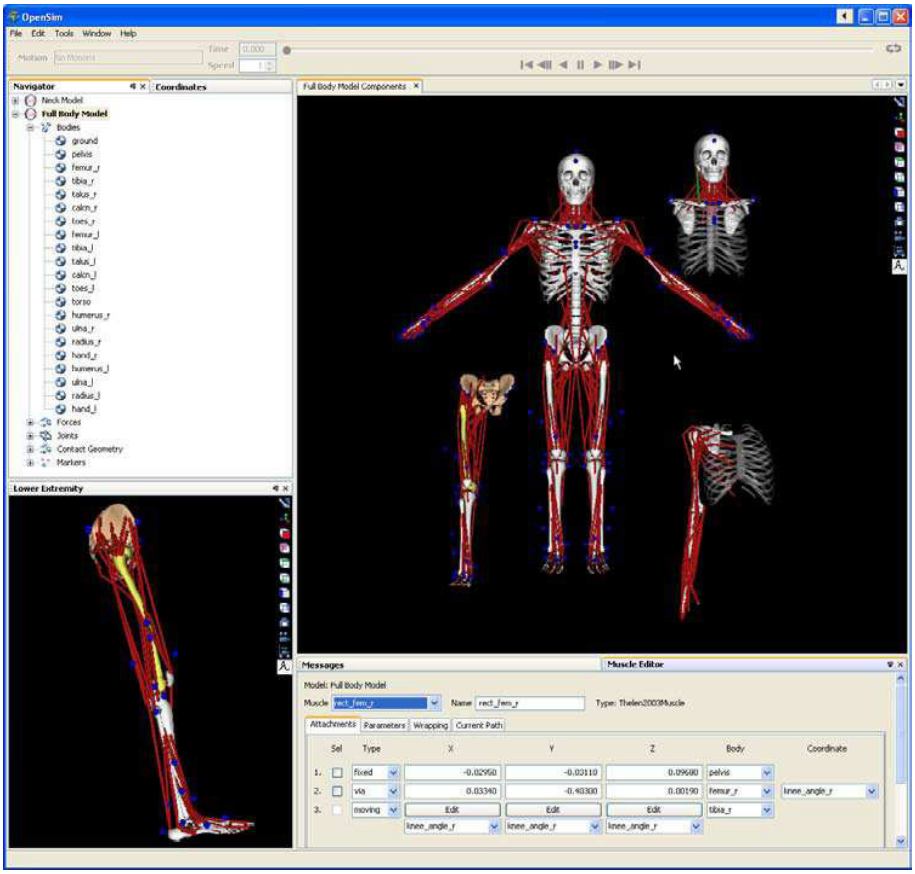

Figure 3 - Screenshot from OpenSim GUI. Models of different musculoskeletal structures, including the lower extremity, upper extremity and neck, can be loaded, viewed and analyzed. Muscles are shown as red lines; virtual markers are shown as blue spheres.

Development plan

The two software tools are highly complementary in their functionalities: NMSBuilder can act as data pre-processor (there are no modelling and simulation features in MAF) for the OpenSim simulation tools (where the pre-processing capabilities from medical data are limited). Moreover, the presence of the OpenSim API makes it possible to call and run the dynamic simulations in the background without running the OpenSim GUI.

The core problem was to allow in MAF an efficient generation of a complete musculoskeletal model, run an OpenSim simulation and store the results in a convenient way for a future use.

A musculoskeletal model is made of a multibody system connected by positional constraints (i.e. the joints), and actuated by several musculotendon units (i.e. the actuators), each connected to two (or three) different body parts (see Introduction of the thesis). Each body part represents a segment of the body (e.g. a foot) assumed rigid. The dynamical definition of a body part consists of a coordinate reference system (CRS) and the inertial properties.

The positional constraints that define the kinematics chain of the body parts are the joints. Each joint is represented by two CRS (the *i* and the *j* joint frames hereinafter) that are rigidly connected to one of the two parts that the joint is linking. In OpenSim, the body has no degrees of freedom (DOFs) until a joint is defined; the joint constraints have a specific meaning to limit the degrees of freedom permitted by the joints. The joint specifies the degrees of freedom between two bodies: considering simple and ideal joints such as hinge or ball-and-socket joints, the type of the joint defines which DOFs are constrained.

The muscles bundles are often modelled as poly-lines connecting two attachment points that are rigidly connected to the two body parts supposed to be moved by the muscles. The muscle bundle path, often complex, can be approximated by a poly-line assigning one or more intermediate points (via-points hereinafter), each of them rigidly connected to a selected body part. In this case both the muscle attachment points and the via-points move rigidly fixed to the selected body part.

A more sophisticated method to define the instantaneous path of a muscle bundle is the wrapping around a parametric surface. In this case a parametric surface (i.e. a sphere, a cylinder or an ellipsoid) is defined rigidly connected to a selected body part, mimicking the constraints acting on the muscle bundle during motion. As a result the muscle attachment points are the only muscle locations that move rigidly connected to the each body part. The mechanical action exerted by a muscle at the two attachment sites is evaluated through normalized equations (which are built in OpenSim) and a number of parameters that, for each muscle bundles, identify the correct equation.

Once the model and a target motion are available, it is possible to run a musculoskeletal simulations, e.g., inverse kinematics, inverse, dynamics, static optimization,...

MAF was not thought to be a musculoskeletal simulation environment, thus no dedicated objects are currently available to define a model structure and its components: bodies, joints and muscles. Nevertheless most of their basic components are already supported by MAF (Table 1).

Table 1 – Parts of a musculoskeletal model and their basic parameters and types. *X* indicates the data types supported by MAF.

Parts of a musculoskeletal model	Parameters	Type of data	Supported by MAF
Bodies	mass	scalar	X
	centre of mass	vector	X
	inertial matrix	matrix	X
Joints	frame i	matrix	X
	frame j	matrix	X
	positional constraints	function	-
Muscles	poly-line	matrix	X
	force-length-velocity relationship	function	-

With above mentioned limitations, the definition of a musculoskeletal model in MAF was only partially possible. The basic idea for the integration strategy was that the user, a modeller, could use NMSBuilder for doing some of the pre-processing of the biomedical data and could then be able to complete the model creation process, interface with OpenSim to launch the solution and store the results for visualization.

Software tools integration

The integration was performed by including into NMSBuilder the features to properly convert the MAF-based data objects into the OpenSim format, and create and launch in an easy way the scripts to configure and run the OpenSim simulations. The information are passed to the OpenSim simulation engine using the API. After the simulation is run, the results operations are stored in NMSBuilder for post-processing and visualization purposes.

In terms of file format conversion, an importer/exporter for/to the VTP format for surfaces is necessary in NMSBuilder. No other file formats issues have been identified in the technical analysis.

Then, the integration relies on the integration within NMSBuilder of a automatic procedure (i.e., a *wizard*) and a text editor allowing the user to write in a user-friendly manner the simulation models and scripts to be passed to the OpenSim API. In agreement with the eXtreme Programming (XP) approach (Figure 4) in use for the development management, NMSBuilder provides the user a friendly interface, which can map into OpenSim API commands the NMSBuilder data structure and information. The text editor has been fundamental in the designing and testing phases, and it has been left only for expert users.

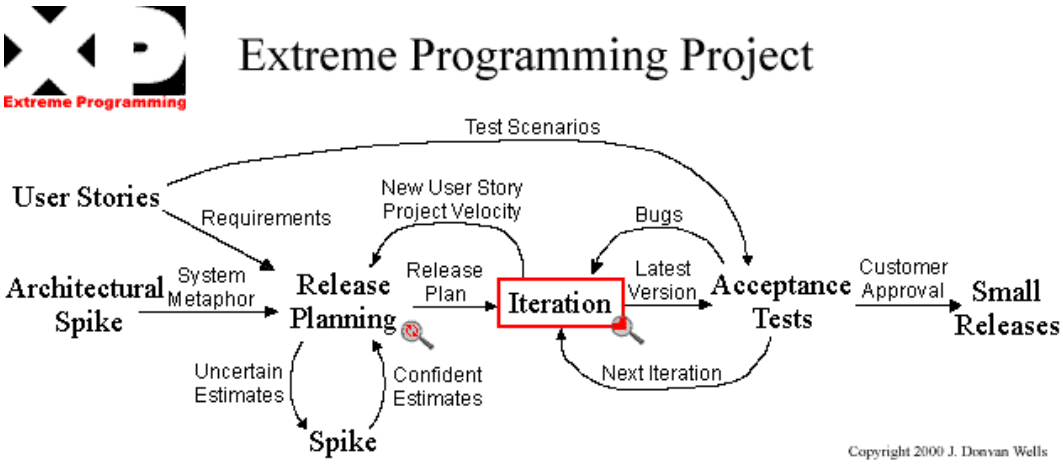

Figure 4 – Flow chart of the XP agile development method, adopted in the software tools integration. Investigators of the Rizzoli Orthopedic Institute acted as application expert designing the requirements and testing the periodic releases of the software

From the analysis described above, a number of components were identified to be developed as specialization of MAF basic features (VMEs, Views and Operations). The scheme in Figure 5 presents the integration approach for MAF and OpenSim.

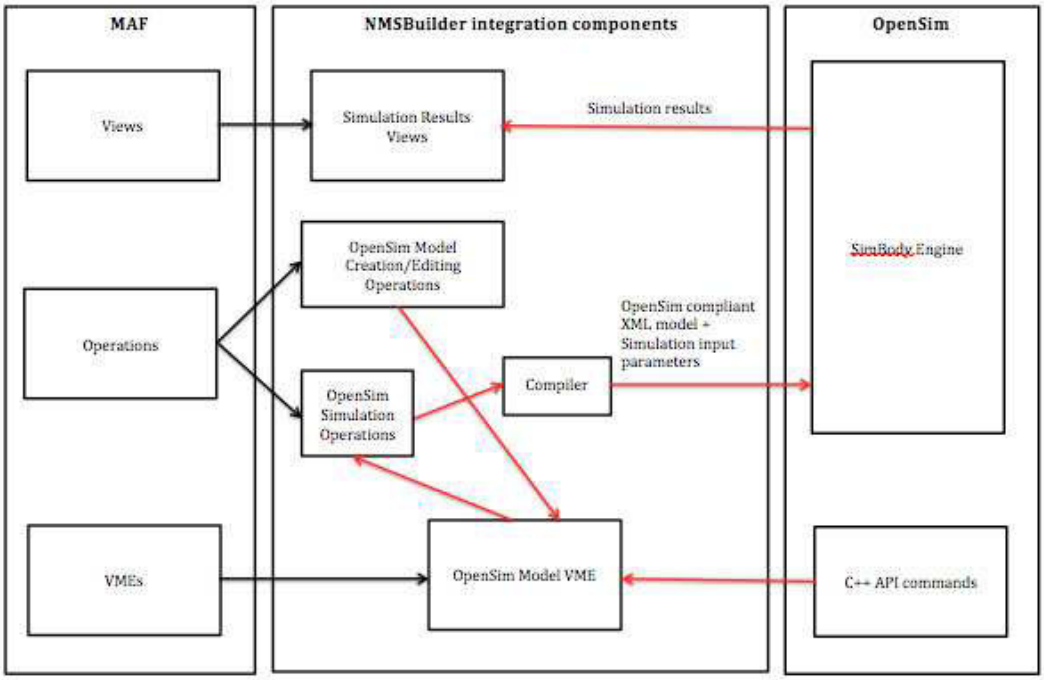

Figure 5 – Schematic representation of the components involved in the MAF-OpenSim integration. Specialized components from MAF are represented in black, the communication flow in red

In particular, on the left side of Figure 5 the general components of the MAF framework are presented as described in the initial sections, while on the right side the components of OpenSim involved in the integration are listed.

In the central part of the scheme the specialized components (developed during NMS Physiome project) to achieve the integration are represented. They consist of:

- new VME which represents a general OpenSim model (C++ commands of the API) to be used as a template for the construction on the patient-specific OpenSim model and simulation
- three specialized operations to edit the template model, define the simulation to be run, and compile the C++ commands of the API to generate the OpenSim model
- specialized views for the post-processing and visualisation of the simulation results.

The red arrows in Figure 5 represent the flow of information among the modules.

In summary, NMSBuilder provides a model template, which can be automatically edited to include the patient specific information provided by the data in the NMSBuilder data tree. The model is composed by commands from the OpenSim API in C++. When completed, a specialized operation will run the model by calling a compiler which will generate the .osim model file to be then opened into the OpenSim user interface, or will launch the OpenSim simulation which will call directly the SimBody Engine. The results can be stored into NMSBuilder, which will provide specialized visualization tools.

NMSBuilder integrated software

All details on the software operations are described in the user manual, together with tutorials and test data, at the dedicated Biomed Town page[13].

A launch webinar of NMSBuilder has been held, demonstrating the efficient framework for subject-specific musculoskeletal modeling with a case study. A recording of the webinar is freely available from a dedicated Stanford University page[14].

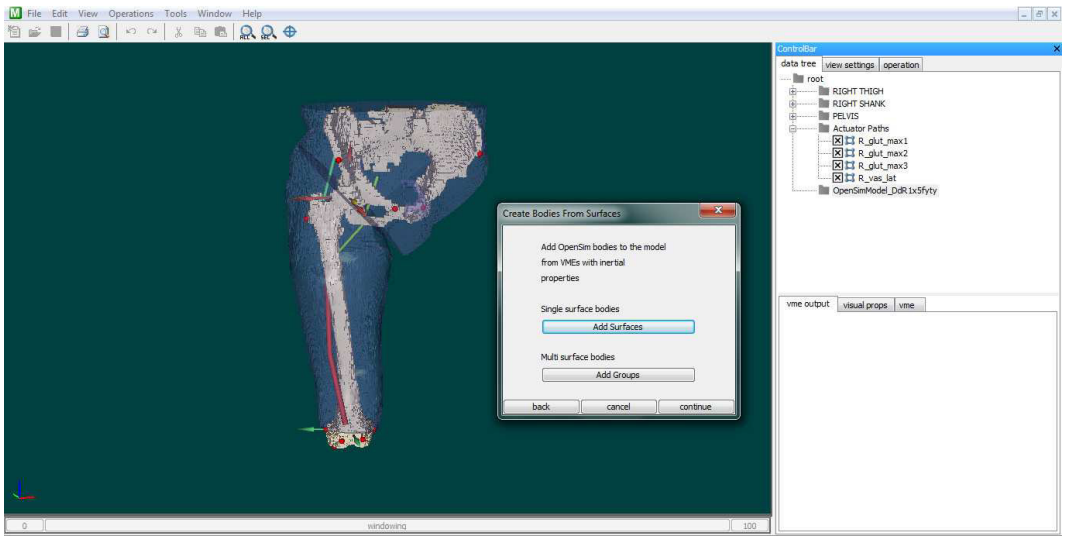

Figure 5 – Screenshot of the NMSBuilder GUI during the guided procedure of creation of an OpenSim musculoskeletal model

[13] https://www.biomedtown.org/biomed_town/nmsphysiome/reception/alpha/

[14] http://www.stanford.edu/group/opensim/support/event_details.html?id=55&title=Webinar-NMSBuilder-Software-for-Creating-Patient-Specific-OpenSim-Models

General Discussion

An accurate knowledge of the physiological loading conditions on the skeletal system during human movements may have significant clinical implications in several orthopedic and neurological contexts. However, the determination of skeletal loading conditions in vivo and their relationship to the health of bone and cartilage tissues, still represent an open question. Computational modeling of the musculoskeletal system is the only practicable method providing a valuable approach to muscle and joint loading analyses in vivo. Significant advances in computer technology and the development of computationally efficient simulation algorithms are driving musculoskeletal models towards important challenges in clinical scenarios. The lack of a thorough validation of model predictions represents a crucial shortcoming limiting the translation process of computational methods into the orthopedic and neurological

practice. Alternatively, sensitivity analyses are increasingly performed to evaluate the uncertainty of model outputs. However, there is a still a need for understanding how several modeling parameters affects skeletal load predictions, and a complete scenario of critical parameters has not been assessed yet. In addition, a growing concern about the accuracy of scaled-generic models is focusing the attention on subject-specific modeling, particularly when pathological musculoskeletal conditions need to be studied. Nevertheless, subject-specific data cannot be always collected in the research and clinical practice, and there is a lack of valuable methods and frameworks for building models and incorporating them in simulations of motion, still preventing the system to be practical, user friendly and effort effective.

The overall aim of the present PhD thesis was to introduce improvements to the state-of-the-art musculoskeletal modeling for the prediction of physiological skeletal loads (i.e. muscle and joint forces) during motion. In particular, a threefold goal was articulated as follows: (i) develop state-of-the art subject-specific models and perform clinical and methodological analyses of skeletal loads predictions; (ii) analyze the sensitivity of model predictions to relevant musculotendon model parameters and kinematic uncertainties; (iii) design an efficient software framework integrating and simplifying the effort-intensive phases of subject-specific modeling pre-processing.

The goals were achieved with a four-part research project, whose strengths and added value are discussed as follows.

The first part allowed to underline the relevance of subject-specific musculoskeletal modeling to determine physiological skeletal loads during gait, with a clinical and a methodological application. In the clinical application (Chapter 1), full CT images of a pediatric oncology case and gait analysis measurements, allowed a high level of subject-specific detail to be included to understand if and to which extent the biomechanical conditions were altered due to reconstruction surgery. This led to conclude that small kinematic asymmetries between the operated and the contralateral legs were amplified in the femoral forces, with significant differences in the skeletal loads between legs. In the other application (Chapter 2), differences in skeletal load predictions between scaled-

generic and MRI-based models were found, although in presence of non-pathological conditions. This corroborated the choice of full subject-specific modeling for the analyses of pathological conditions.

The second and the third part of the thesis allowed to characterize the sensitivity of skeletal load predictions to major musculotendon parameters and kinematic uncertainties, and to develop robust probabilistic methods applied for methodological and clinical purposes. The definition of musculotendon architecture in a model, i.e. number and position of actuators, was found to significantly affect the skeletal load predictions on a subject-specific basis (Chapter 3 and Chapter 4). On the other hand, in a subject-specific model identification process, once clinical images were available and the uncertainty in virtually locating the relevant anatomical landmarks was known, the skeletal load predictions were not significantly affected by the uncertainty in the identification of lower-limb joint axes determined by the landmark locations (Chapter 6). In addition, different joint kinematics calculated solving a global optimization problem did not significantly affect skeletal load predictions (Chapter 7). A robust probabilistic approach (i.e., Monte-Carlo method with Latin Hypercube Sampling strategy) was applied to perform sensitivity analyses. On the one hand, it allowed to perform a clinical study to analyze the sensitivity of joint contact forces to the force-generating capacity of hip abductor muscles (Chapter 5). The predicted joint loads were found significantly affected by muscle weakness, and they were most sensitive to gluteus medius, particularly the anterior compartment. On the other hand, the same probabilistic method was adopted for methodological purposes (Chapter 6), to appropriately sample the anatomical landmark positions due to the uncertainty in their identification.

The fourth part of the thesis allowed to create an efficient framework for subject-specific modeling and simulation, which is practical, user friendly and effort effective. The operations for an open-source software were designed and tested, and the developed software (NMSBuilder) was made freely accessible to the biomechanical community (Chapter 8). Specific operations have been designed to integrate the capabilities of biomedical data pre-processing modeling with the OpenSim solver tools. The result is a useful platform to efficiently create

and analyze subject-specific models from different biomedical data. NMSBuilder, in its ongoing versions, has been used as support to create all the subject-specific models presented in this thesis, representing an essential tool in the conduction of this research. Furthermore, the identification of the lower-limb joint axes through the location of anatomical skeletal landmarks from CT images, was performed in NMSBuilder and considered a robust procedure to generate musculoskeletal models (Chapter 6).

The present research is affected by some limitations. First, the developed subject-specific models included a one degree of freedom hinge joint to model the mechanics of both knees and ankles, as adopted in several published models [1,2]. As discussed throughout the thesis, these joint mechanics models may oversimplify the description of knee and ankle joint kinematics. In particular, a marked influence of joint constraints in the intrinsic formulation of global optimization (to obtain the inverse kinematics solution) was observed (Chapter 7). This highlights the relevance of accurate lower-limb joint models. In addition, previous research showed how different joint models significantly affect muscle and joint contact force predictions [3–5]. Second, in most subject-specific analyses here presented, neither musculotendon dynamics nor excitation-contraction dynamics were implemented in the musculotendon actuator models. Implementation of muscle force-length-velocity relationships implies the definition of specific musculotendon parameters (i.e., tendon slack length, optimal fiber length, pennation angle), which are impossible to measure from clinical images. Therefore, they need to be derived from other dataset or calculated through optimization [1]. The only attempt was made in the first model (Chapter 1), where those parameters were estimated through optimization [6], and the hybrid Computed Muscle Control algorithm [7] was used to predict muscle forces accounting for musculotendon dynamics. In the other models, pure static optimization was adopted, without accounting for force-length-velocity properties. This has been shown not to significantly affect muscle force predictions for walking [8], but it may be for other motor tasks. Third, all models developed and used in the present research included musculotendon actuator paths modeled with series of line segments and intermediate via-points accounting for muscle

wrapping around bones and other structures, as generally performed in musculoskeletal modeling [9–11]. This simplification limits the ability of models to accurately represent the paths of muscles with complex geometry and assumes that moment arms are equivalent for all fibers within a muscle compartment. Important research has been performed to incorporate more accurate and complex MRI-based models of musculotendon geometry into multibody musculoskeletal models [12–14]. However, these approaches were too effort-intensive and costly, and the influence on predicted skeletal loads has not been assessed yet.

From the discussion of these limitations, consequent recommendations improving this research regard: (i) implementation of more complex knee and ankle joint models, to describe the corresponding joint kinematics more accurately and understand the influence on skeletal load predictions; (ii) use of probabilistic methods to assess an overall scenario of the crucial model parameters affecting the skeletal load predictions; (iii) development of efficient methods to include a more accurate description of musculotendon paths, based on more sophisticated muscle wrapping modeling, and understand the influence on skeletal load predictions.

Since the crucial aim of musculoskeletal modeling is to successfully translate models and methods into the clinical practice, it is obvious that better methods for measuring, modeling, simulating, and analyzing movement will lead to a more advanced understanding of skeletal loading conditions in vivo, getting closer to sufficient model reliability for the clinics. The present PhD research, with the discussed limitations, introduced improvements to the state-of-the-art musculoskeletal modeling for the prediction of physiological skeletal loads during motion. Certain advances in computer technology and new efficient methods enabling to model musculoskeletal anatomy accurately on a subject-specific basis, will guide musculoskeletal modeling towards a clinical decision-making tool for a personalized, predictive, and integrative musculoskeletal medicine.

References

[1] Pandy M. G., and Andriacchi T. P., 2010, "Muscle and joint function in human locomotion," Annu Rev Biomed Eng, **12**, pp. 401-433.

[2] Erdemir A., McLean S., Herzog W., and van den Bogert A. J., 2007, "Model-based estimation of muscle forces exerted during movements," Clin Biomech (Bristol, Avon), **22**(2), pp. 131-154.

[3] Dumas R., Chèze L., and Verriest J.-P., 2007, "Adjustments to McConville et al. and Young et al. body segment inertial parameters.," Journal of biomechanics, **40**(3), pp. 543-53.

[4] Sandholm A., Schwartz C., Pronost N., Zee M., Voigt M., and Thalmann D., 2011, "Evaluation of a geometry-based knee joint compared to a planar knee joint," The Visual Computer, **1**.

[5] Glitsch U., and Baumann W., 1997, "The three-dimensional determination of internal loads in the lower extremity," J Biomech, **30**(11-12), pp. 1123-1131.

[6] Garner B. a., and Pandy M. G., 2003, "Estimation of Musculotendon Properties in the Human Upper Limb," Annals of Biomedical Engineering, **31**(2), pp. 207-220.

[7] Thelen D. G., and Anderson F. C., 2006, "Using computed muscle control to generate forward dynamic simulations of human walking from experimental data," J Biomech, **39**(6), pp. 1107-1115.

[8] Anderson F. C., and Pandy M. G., 2001, "Static and dynamic optimization solutions for gait are practically equivalent," J Biomech, **34**(2), pp. 153-161.

[9] Delp S. L., Loan J. P., Hoy M. G., Zajac F. E., Topp E. L., and Rosen J. M., 1990, "An interactive graphics-based model of the lower extremity to study orthopaedic surgical procedures.," IEEE transactions on bio-medical engineering, **37**(8), pp. 757-67.

[10] Heller M. O., Bergmann G., Deuretzbacher G., Dürselen L., Pohl M., Claes L., Haas N. P., and Duda G. N., 2001, "Musculo-skeletal loading conditions at the hip during walking and stair climbing," Journal of Biomechanics, **34**(7), pp. 883-893.

[11] Klein Horsman M. D., Koopman H. F. J. M., van der Helm F. C. T., Prose L. P., and Veeger H. E. J., 2007, "Morphological muscle and joint parameters for musculoskeletal modelling of the lower extremity," Clinical Biomechanics, **22**(2), pp. 239-247.

[12] Arnold a S., Salinas S., Asakawa D. J., and Delp S. L., 2000, "Accuracy of muscle moment arms estimated from MRI-based musculoskeletal models of the lower extremity.," Computer aided surgery : official journal of the International Society for Computer Aided Surgery, **5**(2), pp. 108-19.

[13] Blemker S. S., and Delp S. L., 2005, "Three-Dimensional Representation of Complex Muscle Architectures and Geometries," Annals of Biomedical Engineering, **33**(5), pp. 661-673.

[14] Blemker S. S., Asakawa D. S., Gold G. E., and Delp S. L., 2007, "Image-based musculoskeletal modeling: applications, advances, and future opportunities.," Journal of magnetic resonance imaging : JMRI, **25**(2), pp. 441-51.

Scientific Publications

Articles in International Journals

Martelli S., Valente G., Viceconti M., Taddei F. Sensitivity of a subject-specific musculoskeletal model to the uncertainties on the joint axes location. Human Movement Science, 2012, under review

Valente G., Taddei F., Jonkers I. Influence of weak hip abductor muscles on joint contact forces during normal walking: a probabilistic modelling analysis. Journal of Biomechanics, 2012, under review

Valente G., Martelli S., Taddei F., Farinella G., Viceconti M. Muscle discretization affects the loading transferred to bones in lower-limb musculoskeletal models. Proc. IMechE, Part H: J. Engineering in Medicine, 2012, 226(2): 161-70

Taddei F., Martelli S., Valente G., Leardini A., Benedetti M.G., Manfrini M., Viceconti M. Femoral loads during gait in a patient with massive skeletal reconstruction. Clinical Biomechanics, 2012, 27(3): 273-80

Proceedings of International Conferences

Valente G., Martelli S., Taddei F., Viceconti M. Sensitivity of skeletal load predictions to the uncertainties of the lower-limb joint parameters. Proceedings of the 18th Congress of the European Society of Biomechanics, Lisbon, Portugal, July 1-4, 2012

Valente G., Martelli S., Taddei F. Influence of lower-limb muscle discretization on the prediction of skeletal loads. Proceedings of the 10th Symposium on Computational Methods in Biomechanics and Biomedical Engineering, Berlin, Germany, April 11-14, 2012, ISBN: 978-0-9562121-5-3

Valente G., Martelli S., Taddei F., Farinella G., Viceconti M. Modelling the lower limb muscles in musculoskeletal models: a discretisation method. Proceedings of the 23rd Congress of the International Society of Biomechanics, Brussels, Belgium, July 3-7, 2011

Valente G., Martelli S., Brambilla I., Taddei F., Viceconti M. Sensitivity of the skeletal loads of the lower limbs to the uncertainties of kinematics parameters. Proceedings of the 13th International Symposium on Computer Simulation in Biomechanics, Leuven, Belgium, June 30th – July 2nd, 2011

Martelli S., Taddei F., Valente G., Leardini A., Benedetti M.G., Viceconti M., Manfrini M. Femoral loads during walking following limb-salvage surgery: a case study. Proceedings of the International Conference of the Czech Society of Biomechanics, Sychrov, Czech Republic, October 4-6, 2010, ISBN: 978-80-7372-648-5

Taddei F., Valente G., Martelli S., Leardini A., Benedetti M.G., Viceconti M., Manfrini M. Data Fusion for Modelling in Paediatric Oncology. Proceedings of the Symposium on Analysis and simulation of human

motion (IUTAM), Leuven, Belgium, September 13-15, 2010, ISBN: 978-94-6018-247-1

Valente G., Martelli S., Taddei F., Farinella G., Van Sint Jan S., Viceconti M. The mechanical effect of the lower limb muscles on the skeletal system: a modelling perspective. Proceedings of the Symposium on Analysis and simulation of human motion Symposium (IUTAM), Leuven, Belgium, September 13-15, 2010, ISBN: 978-94-6018-247-1

Taddei F., Valente G., Martelli S., Leardini A., Benedetti M.G., Viceconti M., Manfrini M. Analysis of the lower limb mechanics during level walking after a massive skeletal reconstruction: a case study. Proceedings of the 17th Congress of the European Society of Biomechanics, Edinburgh, UK, July 5-8, 2010

Valente G., Martelli S., Taddei F., Farinella G., Van Sint Jan S., Viceconti M. Modelling the mechanical effect of the muscular system of the lower limb. Proceedings of the 17th Congress of the European Society of Biomechanics, Edinburgh, UK, July 5-8, 2010

Martelli S., Valente G., Taddei F., Leardini A., Viceconti M. Intra-subject variability of femoral neck strains during walking: a case study. Proceedings of the 4th International Congress on Computational Bioengineering, Bertinoro, Italy, September 16-18, 2009

Proceedings of National Conferences

Valente G., Martelli S., Taddei F., Leardini A., Benedetti M.G., Viceconti M., Manfrini M. Biomechanical analysis of the lower limbs during level walking for a case of massive skeletal reconstruction. Proceedings of the 2nd National Congress of Bioengineering (GNB), Torino, Italy, July 8-10, 2010

About the author

Giordano Valente received his B.S. and M.S. in Mechanical Engineering from the University of L'Aquila, Italy, in 2004 and 2007 respectively. His Master thesis regarded the development of a multibody-dynamics model of the human spine for orthotic applications.

He joined the LTM group at the Rizzoli Orthopedic Institute in 2008 to collaborate as research engineer in the development of modeling methods of the lower-limb musculoskeletal system, and as application expert in the development of dedicated biomedical software.

In 2010 he was enrolled in the Ph.D. program of the Bioengineering school at the University of Bologna, Italy, working on a project funded by the Rizzoli Orthopedic Institute. During his Ph.D., the main research interests regarded the development of subject-specific musculoskeletal models of the lower limbs for the prediction of skeletal loads, and sensitivity analyses of model predictions with

probabilistic methods. He has been involved as co-investigator in the NMS Physiome project, funded by the European Union, as application expert in charge to design software operations within the development of a toolkit for personalized musculoskeletal modeling and simulation.

Giordano is currently a Senior Research Fellow at the Rizzoli Orthopedic Institute, carrying on with the musculoskeletal modeling research towards further challenges.